

12-1-2015

Optimization of the Development Process for Air Sampling Filter Standards

Rajah Marie Mena
University of Nevada, Las Vegas

Follow this and additional works at: <https://digitalscholarship.unlv.edu/thesesdissertations>



Part of the [Environmental Sciences Commons](#), and the [Physics Commons](#)

Repository Citation

Mena, Rajah Marie, "Optimization of the Development Process for Air Sampling Filter Standards" (2015). *UNLV Theses, Dissertations, Professional Papers, and Capstones*. 2561.
<http://dx.doi.org/10.34917/8220141>

This Thesis is protected by copyright and/or related rights. It has been brought to you by Digital Scholarship@UNLV with permission from the rights-holder(s). You are free to use this Thesis in any way that is permitted by the copyright and related rights legislation that applies to your use. For other uses you need to obtain permission from the rights-holder(s) directly, unless additional rights are indicated by a Creative Commons license in the record and/or on the work itself.

This Thesis has been accepted for inclusion in UNLV Theses, Dissertations, Professional Papers, and Capstones by an authorized administrator of Digital Scholarship@UNLV. For more information, please contact digitalscholarship@unlv.edu.

OPTIMIZATION OF THE DEVELOPMENT PROCESS FOR AIR SAMPLING FILTER STANDARDS

By

RaJah Marie Mena

Bachelor of Science
University of Nevada, Las Vegas
2006

A thesis submitted in partial fulfillment
of the requirements for the

Master of Science – Health Physics

Department of Health Physics and Diagnostic Sciences
School of Allied Health Sciences
Division of Health Sciences
The Graduate College

University of Nevada, Las Vegas
December 2015



Thesis Approval

The Graduate College
The University of Nevada, Las Vegas

April 24, 2015

This thesis prepared by

RaJah Mena

entitled

Optimization of the Development Process for Air Sampling Filter Standards

is approved in partial fulfillment of the requirements for the degree of

Master of Science – Health Physics
School of Dental Medicine

Ralf Sudowe, Ph.D.
Examination Committee Chair

Kathryn Hausbeck Korgan, Ph.D.
Graduate College Interim Dean

Steen Madsen, Ph.D.
Examination Committee Member

Carson Riland, Ph.D.
Examination Committee Member

Vernon Hodge, Ph.D.
Graduate College Faculty Representative

Abstract

Optimization of the Development Process for Air Sampling Filter Standards

By

RaJah Mena

Dr. Ralf Sudowe, Advisory Committee Chair
Assistant Professor of Health Physics and Radiochemistry
University of Nevada, Las Vegas

Air monitoring is an important analysis technique in health physics. However, creating standards which can be used to calibrate detectors used in the analysis of the filters deployed for air monitoring can be challenging. The activity of a standard should be well understood, this includes understanding how the location within the filter affects the final surface emission rate. The purpose of this research is to determine the parameters which most affect uncertainty in an air filter standard and optimize these parameters such that calibrations made with them most accurately reflect the true activity contained inside. A deposition pattern was chosen from literature to provide the best approximation of uniform deposition of material across the filter. Samples sets were created varying the type of radionuclide, amount of activity (high activity at 6.4 – 306 Bq/filter and one low activity 0.05 – 6.2 Bq/filter, and filter type. For samples analyzed for gamma or beta contaminants, the standards created with this procedure were deemed sufficient. Additional work is needed to reduce errors to ensure this is a viable procedure especially for alpha contaminants.

Acknowledgements

To God: Thank you for letting me experience all of the love and support of the people below and for the strength and perseverance to make it through to this point.

To my sweet husband George, I promised you like 8 years ago I'd finish my master's really quick and we'd be on our way to California. I guess it's taken a bit longer than I anticipated. Thank you for sticking with me through all of this any way. Thank you for watching the kids while I worked on data for hours. Thank you for patiently waiting for all of this silliness to end so you could get your wife back. But, most of all, thank you for being the rock of our family and holding it down when I needed you most. I love you so manys.

To my kids: Gabby, Eli, and George for doing your chores, walking quietly around the office door, trying not to drive George crazy, and the million and one other little things you did to help me get through this. I love you guys!

To my parents: Look! I'm finally done! And no, this is not for a PhD.

To my GLVCC Family: thanks to all of you for your love, support and friendship through this process. Thanks for listening to me drone on and on about things you'll never need to know about just because it interests me.

To my RSL Family: Thank so much to Wendolyn, Jeremy, Avery, Uncle Bob, Don, Colin, Linda, Rich, Papa John, Rusty, Piotr, Ashlee, Teri, Tanu, Steve Luke, and Bill for all of your support over the years. Thanks for helping learn instrumentation, answering silly math questions, proofing my documents, listening to me complain, drawing millions of whiteboard sketches of spectra, and just genuinely loving me through all of this.

To My Committee:

Ralf, thank you for sticking with me all these years. I know you must have wondered a million times if we'd ever get here and I'm so glad that we have.

Carson, you're more like a dad than a committee member. I have started and ended this journey with you and have you to thank for so many things. Thank you for showing me (a decade ago now...wow) what health physics is really about and for all of the countless hours of working problems with me through undergrad and grad school. Thanks for seeking me out for a job because I would have never met my awesome RSL family without you. Thanks for always having my back and helping me to see the world (literally and figuratively). I will love you forever.

Steen and Dr. Hodge, thank you so much for agreeing to support me in this project. Thank you for answering all of my silly emails and for your feedback in the early days.

To My Helpers: Thanks so much to Balazs Bene, I most certainly could not have come anywhere close to finishing without you. Thank you for taking an interest in the work and progress of a total stranger but fellow student. You stepped in when I really needed a friend at school and I will be forever grateful.

Thank you Athena Gallardo for helping with the autoradiography section and for all of the fun conversations in the dark while we waited. Thanks also to Jason Richards and Lucas Boron-Brenner for pitch hitting when Balazs was away – you guys are lifesavers.

Lastly, National Security Technologies...for paying for this degree and allowing me to be school loan free!

Table of Contents

Abstract.....	iii
Acknowledgements.....	iv
List of Tables	vii
List of Figures	viii
Chapter 1 - Introduction	1
Chapter 2 – Literature Review	11
Chapter 3 – Materials and Methods.....	14
Chapter 4 – Results and Discussion	27
Chapter 5 – Error Sources	87
Chapter 6 – Conclusion	91
Chapter 7 – Future Work	92
Bibliography	93
Curriculum Vitae	94

List of Tables

Table 1 - Filter media used in experiments with radioactive materials.....	20
Table 2 - Sample inventory	22
Table 3 - Activity concentrations of low and high activity standard solutions	22
Table 4 - Data collected for various droplet volumes and filter media.	29
Table 5 - Summary of the peak to total area ratios between all filters.	36

List of Figures

Figure 1 Auto-radiograph of 47-mm, soaked filter standard. (McFarland)	9
Figure 2 - Pattern B was the final pattern put forth by the research group. All material is confined within the active counting area and each deposition point had an average diameter of about 5 ± 1 mm (Ceccatelli, De Felice and Fazio).	12
Figure 3 - Pattern A was the initial pattern attempted by researchers. Material was deposited in the center of 19 hexagons in concentric circles from center. The hexagon sides extended to the edge of the filter (Ceccatelli, De Felice and Fazio).	12
Figure 4 - Machining a circle into a Plexiglass sheet.....	15
Figure 5 - Pattern affixed to the plastic sheet to machine holes for future pipetting.....	15
Figure 6 - The completed pipetting apparatus	16
Figure 7 - Pipetting dye onto filter matrix	17
Figure 8 - Filter media completely dry in cell culture dishes. Note the unique spread of the dye across the membrane filter in the upper right corner of the image.....	18
Figure 9 - The PIPS detector position was not parallel to the filter.....	23
Figure 10 - The same beading effect was observed in the plastic simulant as in glass fiber filter paper.	27
Figure 11 - An image capture using the optical microscope camera from a glass fiber filter with a $5 \mu\text{L}$ droplet.....	28
Figure 12 - Average diameter [μL] and droplet volume area compared using paper filters.....	29
Figure 13 - Average area [μm^2] and droplet volume are compared using paper filters.....	30
Figure 14 - Comparison of droplet diameter size between plastic simulants and glass fiber filter paper. The $10 \mu\text{L}$ droplets were within the margin of error for both filter matrices.....	31
Figure 15 - Comparison of the relative average droplet area between plastic simulants and glass fiber filter paper. As seen in the diameter comparisons, the areas measured for each were within the margin of error for all matrices for a given droplet volume.	31
Figure 16 - 1 hour exposure of a series of filter paper media. (1) Hi-Q FP2063-20 high activity Am-241 using $15 \mu\text{L}$ droplets (2) Hi-Q FP2061-47 high activity Am-241 using $15 \mu\text{L}$ droplets (3) Millipore Fluoropore high activity Am-241 using $15 \mu\text{L}$ droplets (4) Hi-Q FP2063-20 high activity Am-241 using $10 \mu\text{L}$ droplets (5) Hi-Q FP2061-47 high activity Am-241 using $10 \mu\text{L}$ droplets (6) Millipore Fluoropore high activity Am-241 using $10 \mu\text{L}$ droplets (7) Pall 60301 high activity Am-241 using $10 \mu\text{L}$ droplets..	32
Figure 17 - 1 hour exposure of a series of filter paper media. (1) Hi-Q FP2063-20 high activity Am-241 using $5 \mu\text{L}$ droplets (2) Hi-Q FP2061-47 high activity Am-241 using $5 \mu\text{L}$ droplets (3) Pall 60301 high activity Am-241 using $5 \mu\text{L}$ droplets (4) Hi-Q FP2063-20 high activity Am-241 using $10 \mu\text{L}$ droplets (5) Reverse side of Hi-Q FP2063-20 high activity Am-241 using $15 \mu\text{L}$ droplets (6) Reverse side of Hi-Q 2061-47 high activity Am-241 using $15 \mu\text{L}$ droplets.....	33
Figure 18 - An example of a spectrum resulting from a glass fiber filter (Hi-Q 2063-20) treated with the high activity Am-241 solution.	34
Figure 19 - The same spectrum with the smoothing algorithm applied.	35

Figure 20- This high activity Am-241 spectrum has been smoothed to show two distinct areas of activity.	37
Figure 21 - Smoothed low activity glass fiber filter Am-241 spectrum.....	38
Figure 22 - Measured activity in Hi-Q 2063-20 filters treated with high activity solution of Am-241.	39
Figure 23 -Measured activity in Hi-Q 2063-20 filters treated with low activity solution of Am-241.40	
Figure 24 -Measured activity in Hi-Q 2061-47 filters treated with high activity solution of Am-241.	41
Figure 25 -Measured activity in Hi-Q 2061-47 filters treated with low activity solution of Am-241.42	
Figure 26 -FWHM measured in Hi-Q 2063-20 filters treated with high activity solution of Am-241.43	
Figure 27-FWHM measured in Hi-Q 2063-20 filters treated with low activity solution of Am-241.44	
Figure 28-FWHM measured in Hi-Q 2061-47 filters treated with high activity solution of Am-241.45	
Figure 29 - FWHM measured in Hi-Q 2061-47 filters treated with low activity solution of Am-241.46	
Figure 30 - Measured activity in Pall 60301 filters treated with high activity solution of Am-241.47	
Figure 31 - Measured activity in Pall 60301 filters treated with low activity solution of Am-241.48	
Figure 32 - Measured activity in Millipore Fluopore (FSL) filters treated with high activity solution of Am-241	49
Figure 33 - Measured activity in Millipore Fluoropore (FSL) filters treated with low activity solution of Am-241	50
Figure 34 - FWHM measured in Pall 60301 filters treated with high activity solution of Am-241.51	
Figure 35 - FWHM measured in Pall 60301 filters treated with low activity solution of Am-241. 52	
Figure 36 - FWHM measured in Millipore Fluopore (FSL) filters treated with high activity solution of Am-241.	53
Figure 37 - FWHM measured in Millipore Fluopore (FSL) filters treated with low activity solution of Am-241.	53
Figure 38 - Percent difference in calculated activity versus theoretical activity for all samples treated with high activity solution of Am-241.....	55
Figure 39 - Percent difference in calculated activity versus theoretical activity for all samples treated with low activity solution of Am-241.	56
Figure 40 - Resolution of the Cs-137 662 keV peak for all samples treated with the high activity standard solution.	57
Figure 41 - Resolution of the Cs-137 662 keV peak for all samples treated with the low activity standard solution.	58
Figure 42 - FWHM for Hi-Q 2063-20 filters treated with high activity Cs-137 solution. Error bars are indicative of the standard deviation for all three samples created for each filter set.	59
Figure 43 - FWHM for Hi-Q 2061-47 filters treated with high activity Cs-137 solution. Error bars are indicative of the standard deviation for all three samples created for each filter set.	60
Figure 44 - FWHM for Pall 60301 filters treated with high activity Cs-137 solution. Error bars are indicative of the standard deviation for all three samples created for each filter set.	61
Figure 45 - FWHM for Millipore Fluoropore (FSL) filters treated with high activity Cs-137 solution. Error bars are indicative of the standard deviation for all three samples created for each filter set.	62

Figure 46 - FWHM for Hi-Q 2063-20 filters treated with low activity Cs-137 solution. Error bars are indicative of the standard deviation for all three samples created for each filter set.	63
Figure 47 - FWHM for Hi-Q 2061-47 filters treated with low activity Cs-137 solution. Error bars are indicative of the standard deviation for all three samples created for each filter set.	64
Figure 48 - FWHM for Pall 60301 filters treated with low activity Cs-137 solution. Error bars are indicative of the standard deviation for all three samples created for each filter set.	65
Figure 49 - FWHM for Millipore Fluoropore (FSL) filters treated with low activity Cs-137 solution. Error bars are indicative of the standard deviation for all three samples created for each filter set. ...	66
Figure 50 - Measured activity for Cs-137 high activity for Hi-Q 2063-20 samples with standard deviation	67
Figure 51 - Measured activity for Cs-137 low activity for Hi-Q 2063-20 samples with standard deviation	68
Figure 52 - Measured activity for Cs-137 high activity for Hi-Q 2061-47 samples with standard deviation	69
Figure 53 - Measured activity for Cs-137 low activity for Hi-Q 2061-47 samples with standard deviation	70
Figure 54- Measured activity for Cs-137 high activity for Pall 60301 samples with standard deviation	71
Figure 55- Measured activity for Cs-137 low activity for Pall 60301 samples with standard deviation	72
Figure 56- Measured activity for Cs-137 high activity for Millipore Fluoropore (FSL) samples with standard deviation	73
Figure 57 - Measured activity for Cs-137 low activity for Millipore Fluoropore (FSL) samples with standard deviation	74
Figure 58 - The percent difference in the measured activity of all high activity samples versus their expected value.	75
Figure 59 - The percent difference in the measured activity of all low activity samples versus their expected value.	75
Figure 60 – Hi-Q 2063-20 High Activity Sr-90 Samples with Standard Deviation Calculated	76
Figure 61 - Hi-Q 2063-20 High Activity Sr-90 Samples with Theoretical Activity.....	77
Figure 62 - Hi-Q 2063-20 Low Activity Sr-90 Samples with Standard Deviation Calculated.....	77
Figure 63 - Hi-Q 2063-20 Low Activity Sr-90 Samples with Theoretical Activity	78
Figure 64 - Hi-Q 2061-47 Sr-90 High Activity Samples with Standard Deviation Calculated.....	78
Figure 65 - Hi-Q 2061-47 Sr-90 High Activity Samples with Theoretical Activity.....	79
Figure 66 - Hi-Q 2061-47 Sr-90 Low Activity Samples with Standard Deviation Calculated.....	79
Figure 67 - Hi-Q 2061-47 Sr-90 Low Activity Samples with Theoretical Activity	80
Figure 68 - Pall 60301 Sr-90 High Activity Samples with Standard Deviation Calculated.....	80
Figure 69 - Pall 60301 Sr-90 High Activity Samples with Theoretical Activity	81
Figure 70 - Pall 60301 Sr-90 Low Activity Samples with Standard Deviation Calculated	81
Figure 71 - Pall 60301 Sr-90 Low Activity Samples with Theoretical Activity	82
Figure 72 – Millipore Fluoropore Sr-90 High Activity Samples with Standard Deviation Calculated	82
Figure 73 – Millipore Fluoropore Sr-90 High Activity Samples with Theoretical Activity	83

Figure 74 - Millipore Fluoropore Sr-90 Low Activity Samples with Standard Deviation Calculated	83
Figure 75 - Millipore Fluoropore Sr-90 Low Activity Samples with Theoretical Activity	84
Figure 76 - Spectrum of planchet used to mount a FSL low activity filter treated with Cs-137....	89

Chapter 1 Introduction

Background

Sampling air for radioactive particulates is an important technique when performing assessments for environmental studies, occupational radiation protection, and emergency response. Along with external monitoring, data from air sampling instrumentation provides critical information about the potential dose that may be incurred by persons working or living in an area. In the event that radiological material is dispersed into the air, whether intentionally or by accident, the material may be available for inhalation by humans. Depending upon the material this pathway can pose a danger to those in the immediate area. Dose from suspended radiological particulates may also pose a legal threat for companies who employ radiological workers or if those particulates have migrated into an area inhabited by the general public.

When considering dose by inhalation, radionuclides that decay by alpha emission are often the nuclides of interest, as they pose the greatest internal dose hazard. Measuring the activity in air containing mainly alpha emitting radionuclides is difficult, as these radiations are not easily detected with handheld instrumentation. Furthermore, not every particle that can be detected is considered respirable nor can the volume of air measured be assumed. The determination of the respirable particle size varies between organizations and regulating documents. However, a commonly accepted upper threshold for respirable particle size is 10 μm (Mishima and Pinkston). This infers that particles above 10 μm do not provide a significant contribution to internal dose from inhalation and should not be collected. Inclusion of non-respirable particles in the analysis of a filter sample can lead to an overestimation of

inhalation dose. Therefore, a sampling of the particulates in air must be performed using a filter that adequately collects the particles of interest, namely those smaller than 10 μm . Similarly, in certain applications, the air must be samples at a specific rate and height, which mimics the air intake of an average person to reduce errors introduced by factors such as altitude specific air concentration, breakthrough, and inappropriate assumptions of activity levels.

Once the sample is collected, it must be analyzed using techniques that are applicable to the radiation type of interest. Typical analysis techniques include liquid scintillation counting, alpha spectroscopy, gamma spectroscopy, and low-level gross alpha/beta counting using gas proportional detection. The analysis method chosen will depend upon the nuclide of interest (more importantly, the major decay mode of the nuclide), time constrictions, the current state of the sample (to include the presence of other nuclides or contaminants) and whether an identification of the nuclides in the sample is required. Each technique has a specific purpose, but not all are applicable for each sample type.

The simplest analysis to perform is gamma spectroscopy, provided that the system is already in place. Gamma spectroscopy can be performed using instruments with various types of detector media, however, the most common currently used detector media are sodium iodide with thallium doping (NaI(Tl)) and high purity germanium (HPGe) crystals. Systems using NaI(Tl) do not require any special cooling and can be used within minutes of activation. A reasonable spectrum can be obtained using these systems, with average resolution of a 3" x 3" crystal being 7.5 - 8.5% at the 662 keV peak of cesium-137 (Cabot). Systems using HPGe crystals require cooling via either liquid nitrogen or a sterling engine, which can take up to

twelve hours to complete. The benefit of using an HPGe system is the significantly improved energy resolution possible. The standard resolution is $< 1.0\%$, which means that peaks in the cobalt-60 range (1332 keV) can typically be resolved within 3 keV in an 8000-channel spectrum. Filter samples analyzed with NaI(Tl) and HPGe systems require no preparations other than contamination control (placing the sample in a holder or plastic bag) and an initial calibration in the appropriate geometry.

Another relatively simple analysis is gross alpha/beta counting. The sample may or may not require initial pretreatment prior to counting. This is most important for alpha counting given the possible losses in the total number of counts due to self-attenuation and dust loading. Samples are placed into gas flow proportional counters on planchets and trays appropriately sized for the filters and are counted for a given amount of time. Gas flow proportional counters are useful in situations where the nuclide type is known or nuclide identification is not required and a rough order of magnitude calculation is required. These counting results are often simply go-no go indications. However, the detection efficiency of proportional counters is better than that attainable with gamma spectroscopy.

Samples analyzed by liquid scintillation and alpha spectroscopy can be the most time consuming and challenging to prepare. In either case, it may be required to ash and/or dissolve the filter and its contents (Burnett and Burchfield). Dissolution of filters calls for the use of extremely corrosive mixtures of nitric, hydrofluoric, and hydrochloric acids which pose safety hazards when handled in the laboratory. However, more filter samples types can be analyzed this way, since not all filter paper is ashless. Consistency in utilizing this technique will universally reduce the number of variables in the study, thereby reducing the uncertainty in the

results. Once the filters are dissolved, additional techniques will need to be employed to remove impurities from the resulting solution (Shaw) such as chemical separation by column chromatography or solvent extraction. Dissolution will destroy the integrity of the sample, which could present chain of custody issues for samples processed under contract. Liquid scintillation may be performed at this point for radionuclides emitting beta particles. The radioactive material can also be deposited onto a planchet using an applicable technique such as electrodeposition, microprecipitation or micro-pipetting for spectroscopy. Sample preparation can take hours up to days to complete.

Low-level alpha spectroscopy can be performed using silicon based detectors under vacuum. In the ideal case the solution has been deposited onto the planchet in a layer thin enough that there is almost no self-attenuation of the alpha particles. This ensures that there is very little material on the planchet to count. The resultant spectrum has an energy resolution of about 20 - 40 keV, which is reasonable for peaks that lie in the 3 - 8 MeV range. However, in some situations this may require that specific chemical separations be performed to remove nuclides with energies too close to the energies of interest to deconvolute the spectrum.

When direct measurements of the filter are taken, the instruments must be calibrated for the medium and geometry of the filter. To accomplish this, standards have been developed by various vendors to simulate measurement conditions that could be expected from a filter of that type. Such standards can consist of either a filter or an electroplated radiation source.

Of the two standard types, the filter is the most representative, however it is also the most difficult to manufacture consistently with minimal error. Aqueous solutions of radiological material and an acid are regularly used to create these standards. The radioactive

material must cover the filter in a reproducible and well characterized manner. However, the physical properties of fiber and membrane based filters encourage the uncontrolled spreading of radiological material (Ceccatelli, De Felice and Fazio). The effects of improper preparation can be great and are dependent on the radiation type of interest. When working with alpha particles, for example, peaks in the alpha spectrum may be broadened, shifted, or absent due to self-attenuation or attenuation by the filter medium itself. Measurements of gamma and beta emitters may be affected due to counts lost in the inactive filter area.

Research is required to optimize the parameters that contribute to incorrect measurements. This research project will investigate the appropriate amount of solution to be deposited and best concentration of radioactive material in the standard HCl and HNO₃ solvents. Additionally, the effect of the manner in which the material is placed on the filter will be examined. How the material spreads in common filter types and potential for material losses will also be studied.

Sampling

Air sampling is performed in several different industries for various purposes. Generally, the purpose is to determine the quantity of some material or contaminant in the air for the purpose of ensuring the safety of people in and around some area. In the field of health physics, air sampling is usually performed to determine the possible risk to humans from inhalation of radioactive materials. Safety professionals may be concerned with indoor air quality due to radon or materials being handled in a fume hood. Sampling equipment may be deployed outdoors, attached to workers lapels, secured in a facility, or operated manually by an individual. A safety professional chooses equipment, software, and filter media based on several factors.

Analysis of areas expected to contain low levels of radioactivity may dictate the use of a sample pump with a high air collection velocity, increasing the volume of air passing through the filter media and thereby increasing the amount of activity which may be deposited on its face. However, in the case of emergency response, low volume air sample pumps (collection velocities near 1 cubic foot per minute) are used to simulate the average breathing rate of humans and are typically placed with the filter head about 1.5 m from the ground. The same types of pumps and set up may also be deployed in non-emergency analysis.

Collection

Technicians typically collect samples at the field location using simple tools. The sampler collection head (housing where filter media are placed during the collection period) may be removed from the motor casing or stay in place while the end cap is removed to expose the filter media. Using gloved hands, the end cap may be detached by unscrewing from the collection head or releasing securing clips. The filter media then are removed with tweezers and placed into either an anti-static envelope or plastic storage bag. Large filters may be folded before placing them into storage containers. The storage containers may be transferred to a collection site to be triaged for eventual laboratory disposition. Considering this process, it is important to note the opportunities for damage to the filter media. Filters used for environmental purposes must be rugged enough to withstand typical field handling, yet thin enough to resist dust loading.

Filter Types

Filters, for the purposes of environmental air sampling, can be classified into two groups: depth filters and surface loading filters (AirSamplingCrse), describing how the material is to be deposited as air passes through them. Each filter medium has qualities which make it suitable for certain purposes and unsuitable for others. For example, in situations where it is expected that radioactive materials may be contained in water vapor, then a hydrophilic filter may be chosen. However, if the filter is to be analyzed for alpha contamination using alpha spectrometry, then the burial losses introduced as materials are pulled deep into the filter may not be acceptable.

Depth filters may include those such as glass fiber and cellulose filters. They are made up of layers of fibers positioned to form an irregular network (Hoover). The result is generally a durable and thick cotton-like material. These are ideal for situations where technicians are required to make a filter change in adverse weather conditions or are handling the filters with gloved hands. These filters can handle higher air velocities, such as with a standard high volume sample pump pulling 40 cubic feet/minute (cfm) of air for reasonable sampling periods (such as an 8-hour shift) with minimal breakthrough.

The most common types of surface filters are membrane filters. The filters are made from various types of materials including esters and polyethylene (Hoover). Membrane filters tend to be less durable and do not tolerate much handling. Membrane filters are intended to collect material at their surface which makes them ideal for collecting air samples in an area suspected or known to contain airborne alpha contamination. Many lapel (personal or breathing zone) air

samplers use membrane filters. Their short run time, low air flow (about 1 cfm), and minimal handling make membrane filters a sensible choice for this purpose.

Creating Filter Standards

The ideal filter standard is one in which the material best represents the characteristics of a filter used in practice. The filter should have an even distribution of radioactive materials across its surface. The activity of the radionuclide(s) used should be well understood, meaning the uncertainty and potential for losses should also be known. It is common for standards to be created using a liquid solution of water, acid, and the radionuclide(s) of interest.

Filter standards can be made in many ways. Some standards are created by soaking the filter medium in a solution of radioactive materials. The filter is dried by evaporation or gentle heating and is sometimes sealed with a polyester tape. This method is not necessarily advised as radioactive materials tend to collect on the edges of the filter paper creating a ring of higher concentration as can be seen in Figure 1 (McFarland). This poses an issue for analyses performed using detectors with a small diameter with respect to the size of the filter. In this case, those counts would be lost and the potential for low-energy tailing in the resulting alpha spectrum increases.

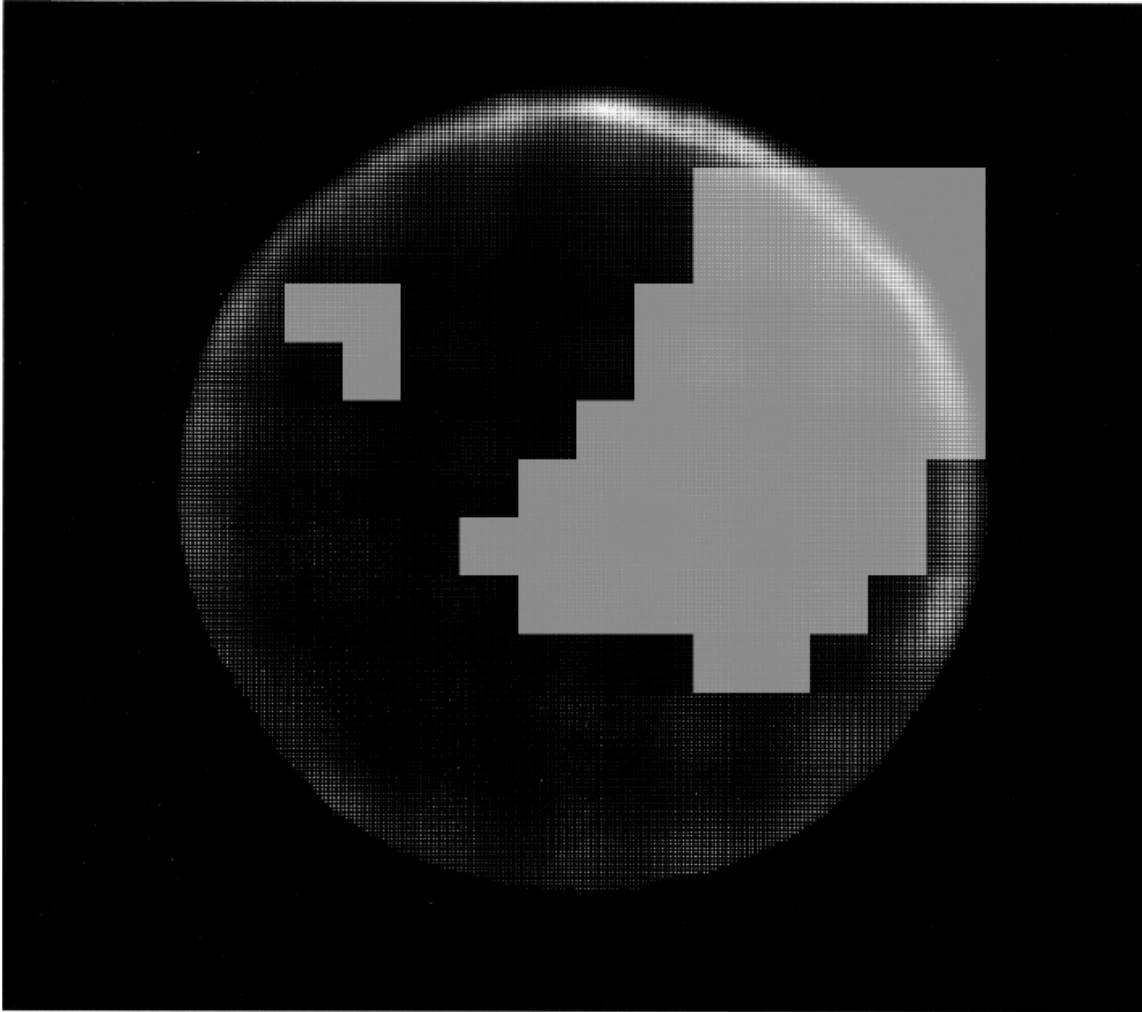


Figure 1 Auto-radiograph of 47-mm, soaked filter standard. (McFarland)

Standards may also be created using plastic simulants – a disk in the appropriate size of a filter made of a hard plastic. Plastic simulants are effective for several reasons. Materials can be deposited easily onto the flat, smooth surface of the plastic by pipetting, making it easy to determine, visually, if there is sufficient and equal coverage across the surface. Moreover, there are little to no burial losses using a plastic. However, if the purpose of the standard is to mimic the behavior of a true filter, then these losses must be accounted for.

Pipetting material onto an actual filter may be one of the best methods of producing a filter standard which most reasonably approximates the response expected from a filter collected in the field. Several studies have been performed to justify the most effective pattern and number of droplets to use. When considering which are most effective, some other factors must be taken into account. The volume of each droplet is important to ensure the total volume deposited does not lead to breakthrough and a loss of material through the backside of the filter. Droplet volume may also be a limiting factor in determining how far apart the droplets may be spaced and therefore, how many total droplets may physically fit across the filter surface. Literature prescribe droplet numbers from 9 to 385 per filter ((McFarland) and (Ceccatelli, De Felice and Fazio)).

Research Goals

At the conclusion of this work, a better understanding of how the method used in radioactive material deposition on a filter can potentially affect counting efficiency will be gained. During this process, the sources of error and uncertainty will be examined in an effort to anticipate and minimize them. A secondary research goal is to determine the effect of adding liquid to the filter media. It is not unreasonable that a filter may become wet during the sampling period due to dew, rain, snow, etc. These gains in knowledge may affect environmental air sampling procedures.

Chapter 2 Literature Review

IAEA Method

Much work has been done to characterize filters themselves, however little data have been found regarding creating or characterizing radiation air filter standards. Moreover, an extensive search for vendors has only returned three major radiation standard vendors - Eckert & Zeigler, Capintec, Incorporated, and Environmental Research Associates. This is not to say that useful work has not been done to move forward in solving some of the concerns surrounding the creation of air filter standards. In fact, a recently published paper describes a reasonable to method to create these standards (Ceccatelli, De Felice and Fazio).

In this procedure, a plastic air filter simulant with a 47 mm diameter was used as the basis for the work. The researchers created a pattern of interconnected hexagons fitted to the size of the “filter”. A mixed gamma source was created to highlight certain common gamma spectrum anomalies such as coincidence counts and overlapping peaks. Nuclides in this mix included ^{57}Co , ^{60}Co , ^{133}Ba , ^{134}Cs , ^{137}Cs , ^{152}Eu , and ^{241}Am . This mixture was pipetted onto the disk in 19 different locations on the pattern. The material was dried onto the filter using an infrared drying system at 40 °C. The dried filter was sandwiched between plastic materials to seal the radioactive material and its edges were reinforced with aluminum.

Figure 3 demonstrates the first pattern attempt in which small dots of the standard solution were deposited to the outer edge of the filter. Mathematical comparisons were made of the efficiency at discrete points on the filter relative to that of the center. Values expected from the pattern were compared against a filter with continuous deposition. An

underestimation of activity equal to 20.0% was introduced using this first pattern. After a number of trials and recalculations the final accepted pattern in Figure 2 confines all of the material to the active counting area with enlarged deposition diameters of 5 ± 1 mm. The activity of the final pattern was calculated to be within 2.6% of the accepted value of the continuous source.

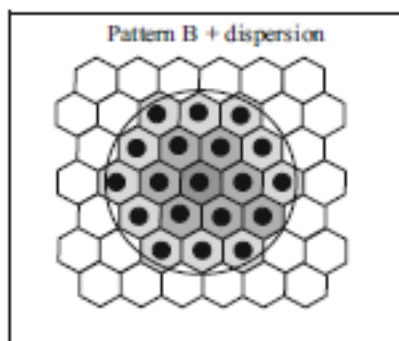


Figure 2 - Pattern B was the final pattern put forth by the research group. All material is confined within the active counting area and each deposition point had an average diameter of about 5 ± 1 mm (Ceccatelli, De Felice and Fazio).

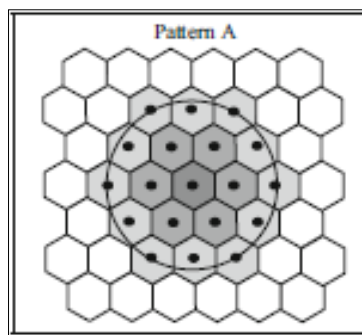


Figure 3 - Pattern A was the initial pattern attempted by researchers. Material was deposited in the center of 19 hexagons in concentric circles from center. The hexagon sides extended to the edge of the filter (Ceccatelli, De Felice and Fazio).

This study had however, some limitations. First, material spread was not well maintained, nor characterized. Second, the standards created in this work and those created by the International Atomic Energy Agency (IAEA), which were based on the same concept, analyzed only the gamma emissions of the radionuclides. Additional counting techniques must be investigated to account for losses of alpha and beta particles in the filter support and solvent. Lastly, the filter itself was not a true filter but, rather a plastic simulant.

Vendor Standards

As expected, vendors contacted for this work declined to comment on their exact procedure in creating filter standards citing trade secrets. However, some general information was provided by representatives over the phone and in sales materials. Customers may be quoted both the contained activity and the surface emission rate of the filter standard as in the Eckert & Ziegler Isotope Products catalog. Some form of deposition into the middle of the filter media occurs to create a somewhat uniform distribution of material throughout the filter. The standards are covered with thin sheets of mylar or acrylic to create a sealed source. Beyond these details not much more could be determined directly.

Chapter 3 Materials and Methods

Creating the JIG

The initial concern, consistency of droplet size, is potentially significant to this thesis. If droplets of radioactive material solution are expected to spread considerably, it is possible that uncontrollable and therefore unpredictable error would be introduced. As a result, a preliminary evaluation was conducted in effort to understand how stable liquid materials spread in filter media prior to collecting or assessing experimental data with radioactive liquid standards.

The first step in performing this assessment was to construct an apparatus which would offer a reproducible geometry for all droplet sizes and filter media. Using standard quarter inch sheets of Plexiglass, two sheets were machined into squares measuring approximately 4 inches x 4 inches. A circle with a diameter of 2 inches was cut into the center of the first sheet with a circular saw as seen in Figure 4.

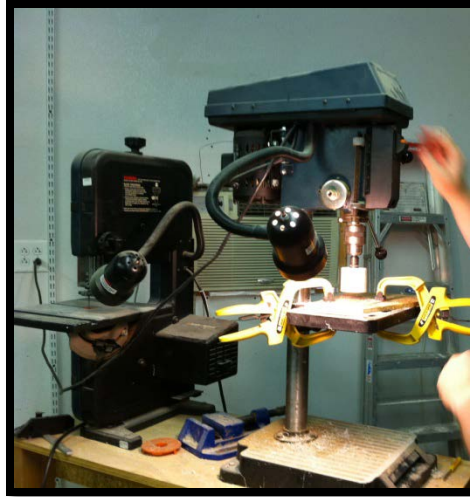


Figure 4 - Machining a circle into a Plexiglass sheet

The pattern from Figure 3 was affixed to the center of the second sheet of Plexiglass, Figure 5. Holes were machined into this sheet in locations indicated by the pattern to simulate the procedure put forth by the IAEA. The sheets were then bound together with set screws and plastic washers to add spacing, Figure 6. This apparatus was used to create a series of test filters to measure droplet spread.

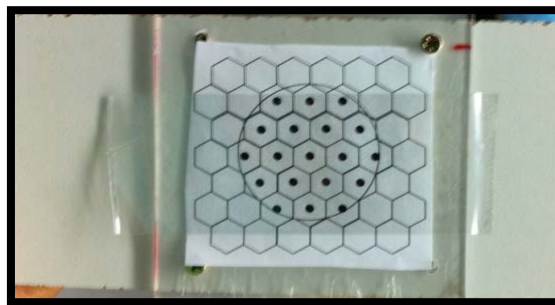


Figure 5 - Pattern affixed to the plastic sheet to machine holes for future pipetting

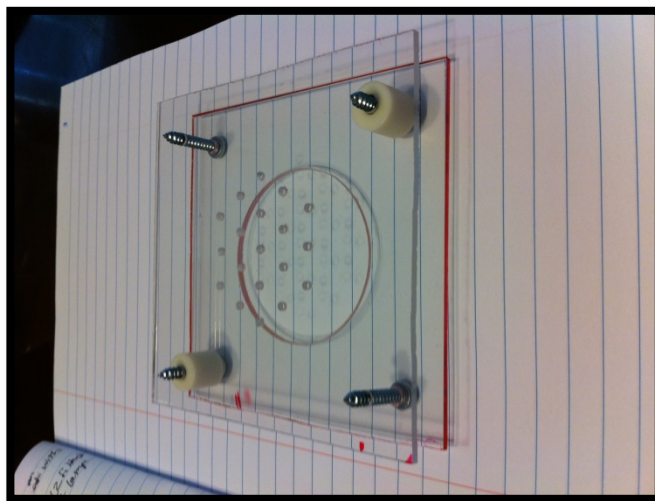


Figure 6 - The completed pipetting apparatus

Procedure for Depositing Materials

A solution of distilled water (250 ml) and McCormick brand red food coloring (5 large drops) were mixed to create an indicator dye. Filter materials were placed, one at a time, in the testing apparatus. Several filter media were used: Pall Corporation Supor®-200 membrane filters (pore size 0.2 μm , 47 mm), plastic discs cut from Plexiglass sheets (47 mm, to mimic those used by IAEA), and Hi-Q Environmental Products Company Part FP2063-20 glass fiber 47mm filters, also referred to as paper filters. Liquid was drawn into a VWR® Ergonomic High Performance pipette (volume range of 2 - 20 μL) at 5, 10, 15, and 20 μL and dispensed onto representative samples for each filter type, Figure 7.



Figure 7 - Pipetting dye onto filter matrix

The complete set was allowed to dry in Corning® Cell Culture Dishes (60mm x 15mm), Figure 8.

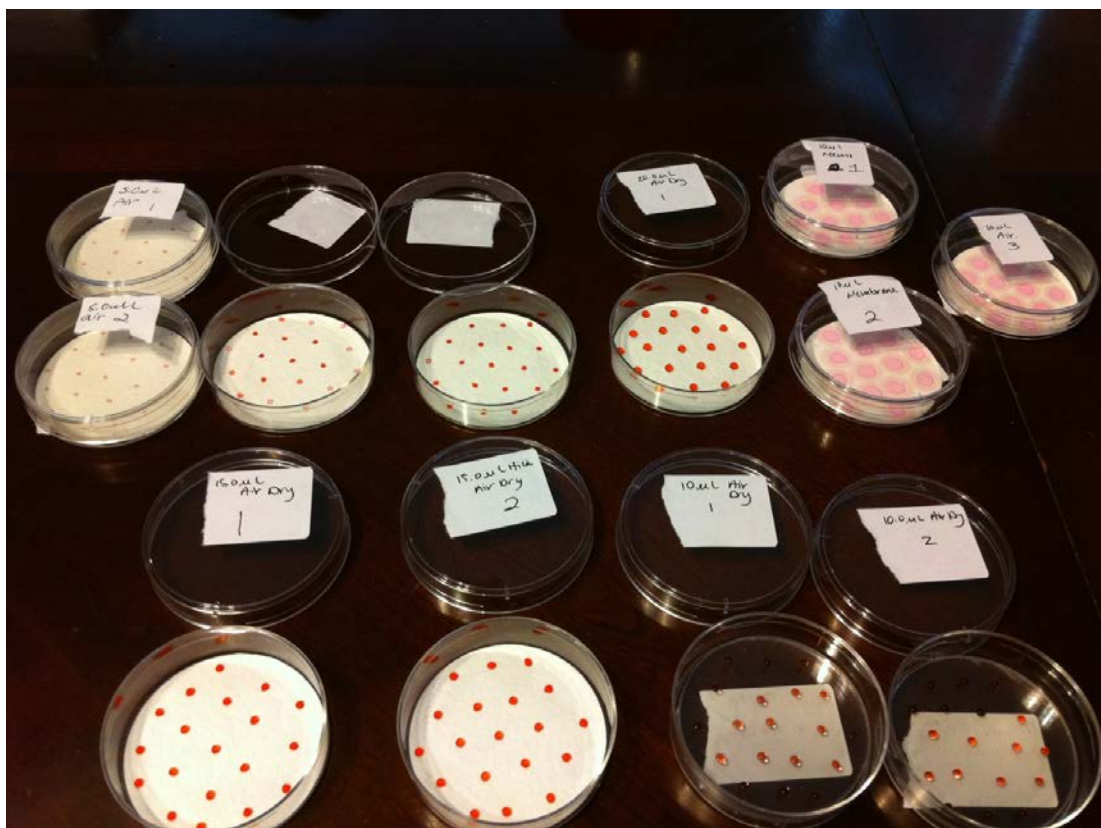


Figure 8 - Filter media completely dry in cell culture dishes. Note the unique spread of the dye across the membrane filter in the upper right corner of the image.

Upon review of the filter media after the above procedure was carried out some determinations were made. First, material deposited onto membrane filters tended to spread widely, however color patterns may be a function of the dye used rather than water diffusion. Second, the spread of liquids across the glass fiber filters appear to be reasonably controlled and do not bleed through the bottom of the filter paper. Overall, the media performed well under this test and therefore it is not necessary that the plastic simulant be used for the remainder of the analysis.

Creating Filter Standards

Choosing the Filter Media

At the conclusion of the droplet test it was determined that five sample media should be included in the experiments using radioactive materials. The details of these filter models are captured in Table 1.

Table 1 - Filter media used in experiments with radioactive materials

Model Name	Manufacturer	Size	Media Type	Comment
FP 2061-47	Hi-Q Environmental Products Company	47 mm	Glass fiber	Hydrophilic, acrylic resin binder
FP 2063-20	Hi-Q Environmental Products Company	2 inches	Glass fiber	Hydrophobic, acrylic resin binder
Fluoropore FSLW04700	EMD Millipore	47 mm	Membrane	Hydrophobic with laminated backing
Isopore TSTP04700	EMD Millipore	47 mm	Membrane; track-etched screen filter	Hydrophilic
PALL 60301	Supor®	47 mm	Membrane; polyethersulfone (PES)	Hydrophilic

The glass fiber filter models were chosen for two reasons. These particular models are in use today across the emergency response community as well as in routine environmental surveys. They are also the most commonly referenced in literature used in preparation for these experiments. The membrane filters are not as widely used however, some lapel air samplers may use them. These particular filters were chosen due to their diameter (field standard of about 47 mm for a standard low volume air sample pump head) and pore sizes (0.2 - 3.0 μm).

Deposition Procedure

When creating the standards the filters were treated using the same procedure as was performed with the dye. To fully explore sources of efficiency loss and error a number of variables were introduced. First, three radionuclides were chosen to represent the three radiation types of interest: alpha, beta, and gamma; Americium-241, Strontium-90, and Cesium-137, respectively. These are also significant as they are typically used as calibration sources therefore this work has operational significance. Second, a set of filters was made to represent

three different volumes of radioactive solutions. Third, for each radionuclide, two source strengths were used for each droplet volume. Differing source strengths provided an opportunity to observe errors in pipetting and stock solution uncertainties. Additionally, it provided options in the autoradiography phase of this work to enhance image quality.

As with the dye, the radioactive materials were deposited on the filters using the jig and pipette. Also, as observed with the dye, when the liquid was deposited on the glass fiber filters it formed beads on the filter surface. The membrane filters performed quite differently. When attempting to dispense 5 μ L size droplets onto the EMD Millipore Fluoropore FSLW04700 filters there was not enough frictional force to move the droplet from the pipette tip to the surface of the filter therefore, no 5 μ L droplet sized filters were created of any source strength. The Supor[®] Pall 60301 filters became fairly saturated at 10 μ L and therefore no attempts were made to create filters using a higher droplet volume. By far, the EMD Millipore TSP04700 filters were least suited for this procedure. When applying 5 μ L droplets to these filters there was immediate breakthrough and substantial loss of material. These filters were therefore not used at all in this experiment. Table 2 illustrates the sample inventory while Table 3 provides clarification of the phrases “high activity” and “low activity” in terms of the strength of the solution used.

Table 2 - Sample inventory

Low Activity Am-241						High Activity Am-241					
	FSL	TSTP	Hi-Q 20	Hi-Q 47	PALL 60301		FSL	TSTP	Hi-Q 20	Hi-Q 47	PALL 60301
5 µL	0	0	3	3	3	5 µL	0	0	3	3	3
10 µL	3	0	3	3	3	10 µL	3	0	3	3	3
15 µL	3	0	3	3	0	15 µL	3	0	3	3	0

Low Activity Sr-90						High Activity Sr-90					
	FSL	TSTP	Hi-Q 20	Hi-Q 47	PALL 60301		FSL	TSTP	Hi-Q 20	Hi-Q 47	PALL 60301
5 µL	0	0	3	3	3	5 µL	0	0	3	3	3
10 µL	3	0	3	3	3	10 µL	3	0	3	3	3
15 µL	3	0	3	3	0	15 µL	3	0	3	3	0

Low Activity Cs-137						High Activity Cs-137					
	FSL	TSTP	Hi-Q 20	Hi-Q 47	PALL 60301		FSL	TSTP	Hi-Q 20	Hi-Q 47	PALL 60301
5 µL	0	0	3	3	3	5 µL	0	0	3	3	3
10 µL	3	0	3	3	3	10 µL	3	0	3	3	3
15 µL	3	0	3	3	0	15 µL	3	0	3	3	3

Table 3 - Activity concentrations of low and high activity standard solutions

Radionuclide	Low Activity	High Activity
Am-241	1.7 Bq/ml	100 Bq/ml
Cs-137	1.7 Bq/ml	170 Bq/ml
Sr-90	1.7 Bq/ml	170 Bq/ml

Counting Methods

The alpha spectroscopy performed in this study was accomplished using an Oasis Tenelec System. This system features a Passivated Implanted Planar Silicon (PIPS) detector. Alpha particles interact with the “passified” silicon wafer creating a set of charged particles. The

energy of these particles is linearly related to the energy of the incident particle therefore making the instrument capable of producing spectral data. The thin windows etched into the wafer preserve well the peak energy resolution (Knoll).

The samples were all counted using the same detector in the 8-detector system. The area of the detector window was larger than all of the filters used at 1200 mm^2 . The filters were loaded onto a plastic sample holder about 2 mm from the face of the detector. This distance is approximate as the detector was slightly tilted to one side with upper end being about 5 mm away from the source and the lower end about 2 mm away. This is shown in Figure 9 below.



Figure 9 - The PIPS detector position was not parallel to the filter.

The samples were counted based on the number of counts accumulated in a previously identified region of interest (ROI) defined for the Am-241 5.486 MeV and 5.443 MeV peaks. This count time was adjusted throughout the study of these filters therefore, not all filters were

analyzed according to this protocol. In general, high activity filters were counted until 2,000 counts were observed in the ROI while, low activity filters were counted until 1,000 counts were observed in the same region.

The filters treated with Sr-90 were analyzed using a Canberra Series 5 XLB – Automatic Low Background Alpha/Beta Counting System; a gas flow proportional counter. The detector in this system contains a chamber filled with inert gas with an anode wire running along its length. When a voltage is applied to this anode, the charged particles created from incident radiation move along to their respective regions (Knoll). Gas proportional counters make use of the phenomenon described by the Townsend Equation (Knoll):

$$\frac{dn}{n} = \alpha dx \quad \text{Equation 1}$$

The equation indicates that there is a fractional increase in the number of electrons per unit length of an anode under high voltage. As the voltage increase the number of charge carriers freed and subsequently multiplied increases until a charge avalanche arises. This occurs until the proportional region of voltage response is reached and there is a linear relationship between the incident radiation and the output pulse. This system also features a guard detector which is used to remove from the resulting count rate any contribution from external activity such as cosmic radiation.

This counter has a stacking system which automatically changes sample carriers as they are processed according to the protocol established for the set. Samples were mounted into the carrier trays of the system using a combination of different types of tape (masking and

double sided) to secure them during the analysis period. The samples were counted for 10 minutes each with background samples being counted for an hour.

Gamma spectroscopy in this study was performed using a NaI(Tl) detector in a well with 4π geometry. In a NaI(Tl) detector, the incident gamma rays interact within the crystal exciting electrons in its valence band to the conduction band. As the electron de-excites it may do so to an activator excited state available due to the presence of the doping agent, thallium. The photons created in the de-excitation from this state produce photons in the visible region of light. These photons interact with a photomultiplier tube which increases their signal strength. The result is a series of counts recorded in energy bins representing the energy spectrum of the incident radiation source.

The NaI(Tl) detector used in this work was a Canberra NaI(Tl) system utilizing a 3 inch x 3 inch crystal in lead shielding. Each filter sample (encased in its petri dish) was placed into the detector for each count. The samples were counted until at least approximately 1000 channels were detected in the region of interest. The detection system was operated using the ProSpect Gamma Spectroscopy Software.

Autoradiography

To verify source locations in the filter media and relative concentration, autoradiography was performed on a representative set of filters. The Perkin Elmer Cyclone[®] Plus Storage Phosphor System was used for this analysis. The Cyclone[®] Plus takes advantage of the autoradiographic properties of the material being processed by using charged particle interactions in the film to produce light. The light intensity and relative flux are used to

produce an image of the filter media representing the concentration of the radioactive materials contained therein.

Beginning in a darkened imaging room, the unprocessed film was placed onto a light box used clear it from previous images or lingering artefacts from any contact with light. Next, the standards were placed into an imaging cassette along with the film screen and allowed to stand for enough time for incident radiation to produce a useful image. It was noted in a previous work that filters with low-level activity such as air sampling standards may need at much as three hours to produce an image (Kelly 2009). However, high activity standards used in this work took only one hour to produce an image of sufficient quality to determine material location and relative abundance of activity.

Chapter 4 Results and Discussion

Fluid Spread Analysis

Assessing the liquid spread visually, it could be observed that filters made of glass fiber tended to cause it to form a bead on most of the filter media. This is also true when considering simulant filters made of Plexiglass, see Figure 10. Liquid deposited on the membrane filters, however did not behave this way. When applied to membrane filters, the dye immediately spread throughout the membrane filter, soaking through to the backside. Yet, no bleed through was observed.

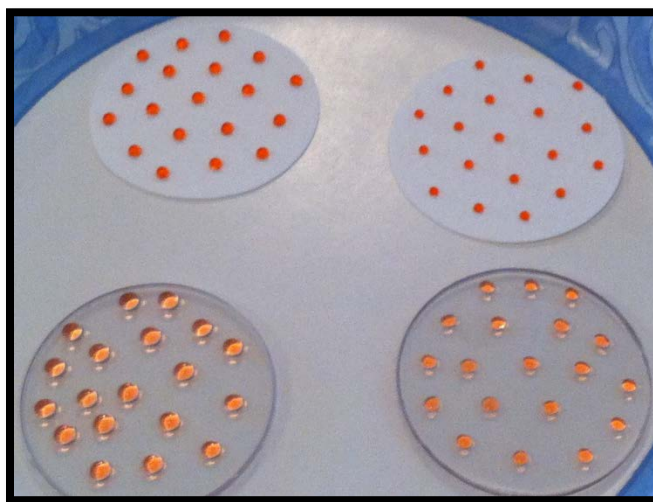


Figure 10 - The same beading effect was observed in the plastic simulant as in glass fiber filter paper.

The droplets were measured using an optical microscope and accompanying analysis software. The software allows the user to draw polygons representing the shape of the image presented on the stage and provides several data for analysis. Of importance in this case: the

diameter of the droplets and their estimated area. Most droplets dried as approximate circles, Figure 11 and for the purpose of simplifying analysis will be treated as such.

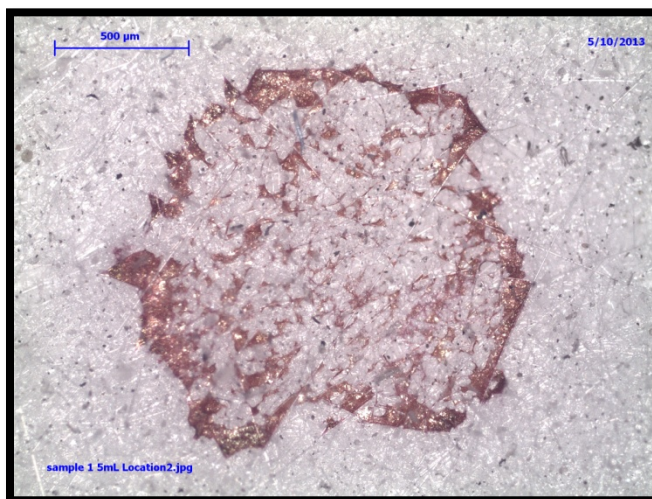


Figure 11 - An image capture using the optical microscope camera from a glass fiber filter with a 5 µl droplet.

The data captured can be seen in Table 4 below. The data for each droplet are averaged per droplet volume per medium. Therefore, for example, all 38 droplets analyzed for 10 µl on glass fiber filters will be summarized on line two of the chart. The datum L_{ave} represents the average diameter of the droplets. For each droplet (where possible) the diameter was measured in three different locations and recorded. The average per droplet was then averaged over all droplets of the same volume and filter media. The area, A_{ave} , was measured using an analysis tool where the user defines the boundaries of the shape of the droplet, and an area of the shape is calculated automatically. To gain an understanding of how much the droplets varied, the standard deviation of the diameter and area were also calculated, σ_L and σ_A , respectively.

Table 4 - Data collected for various droplet volumes and filter media.

Volume (μL)	Medium	L_{ave} (μm)	σ_L	A_{ave} (μm^2)	σ_A
5	Paper	1.53E+03	1.15E+02	1.68E+06	2.42E+05
10	Paper	1.99E+03	1.01E+02	2.82E+06	2.69E+05
15	Paper	2.37E+03	7.21E+01	3.65E+06	1.15E+05
10	Plastic	1.78E+03	2.39E+02	2.34E+06	5.71E+05

Figure 12 and Figure 13 illustrate how droplet sized varied with respect to volume. It should be noted that the error bars in these figures represent 5% error. However, despite the error, a linear trend can be observed where the spread of the droplet can be well approximated by the volume of the droplet itself when using a glass fiber filter paper.

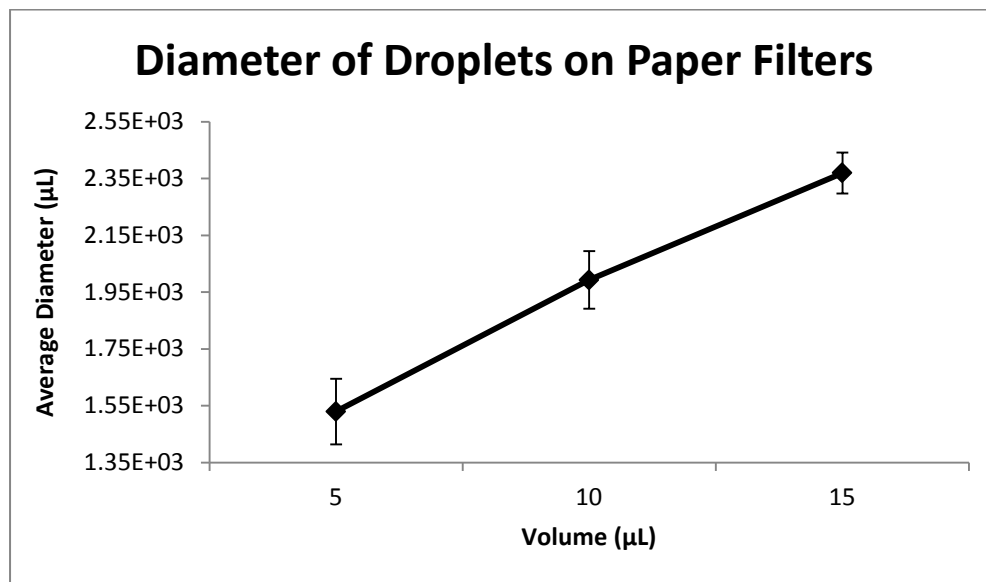


Figure 12 - Average diameter [μm] and droplet volume area compared using paper filters

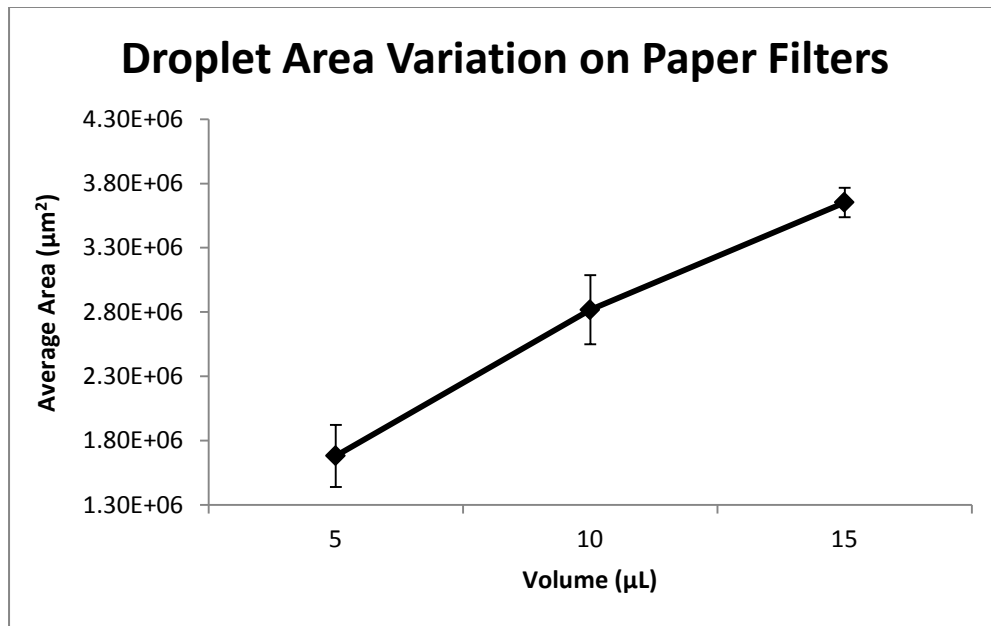


Figure 13 - Average area [μm2] and droplet volume are compared using paper filters

When comparing the filter paper results with a sampling of plastic filter simulants (10 μl droplet size) it can be said that in regard to droplet spread they are equivalent, see Figure 13 and Figure 14 for analysis.

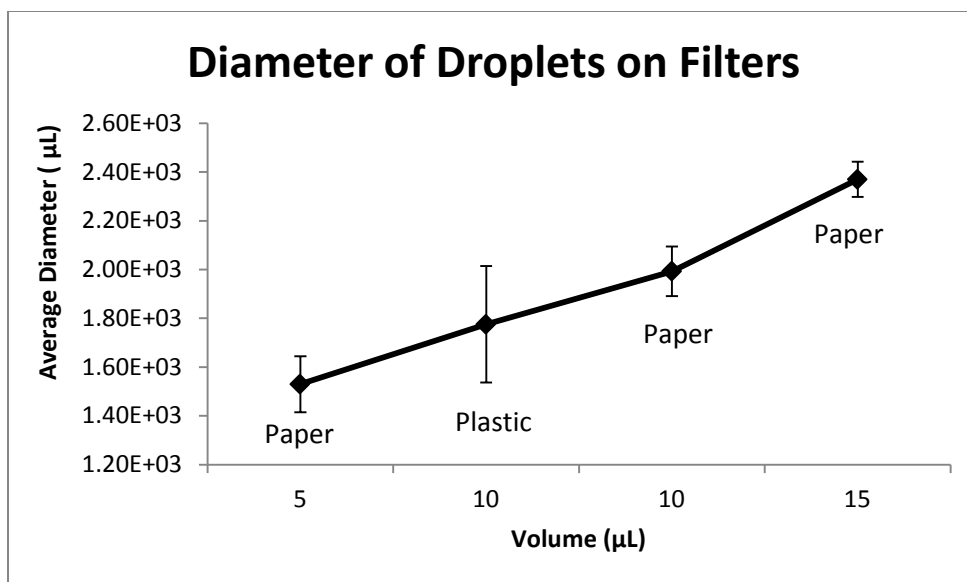


Figure 14 - Comparison of droplet diameter size between plastic simulants and glass fiber filter paper. The 10 μL droplets were within the margin of error for both filter matrices.

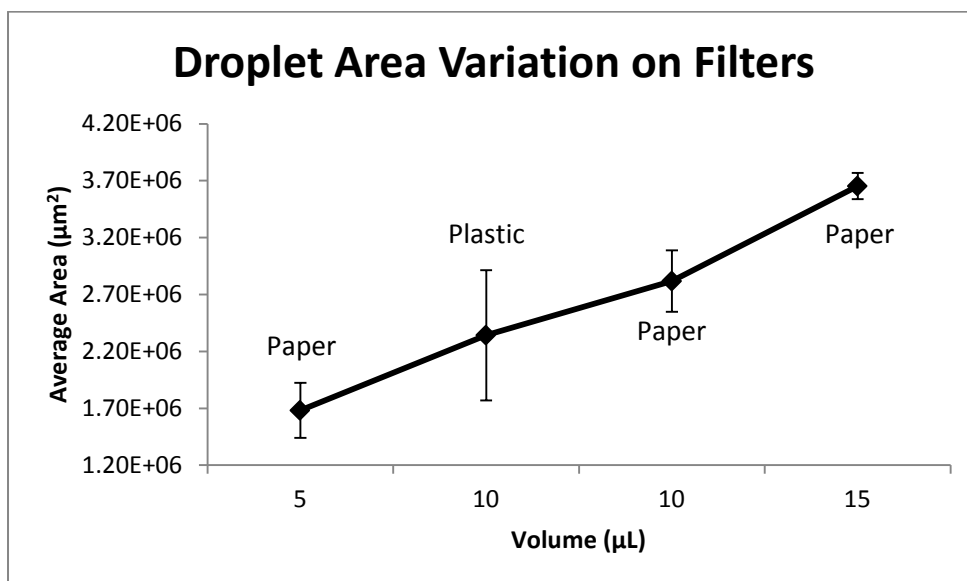


Figure 15 - Comparison of the relative average droplet area between plastic simulants and glass fiber filter paper. As seen in the diameter comparisons, the areas measured for each were within the margin of error for all matrices for a given droplet volume.

Autoradiography Analysis

The imaging screen was exposed for one hour to two sets of representative filters treated with the high activity Am-241 solution to verify the placement of the droplets on each filter. The results of this assessment are in line with the activity calculations and visual observations. The Fluoropore filters show distinct locations of activity with a spread consistent with the earlier dye test. The image of the other membrane filter, the Pall 60301 filter, indicates the radioactive material spread evenly throughout the filter and accumulated somewhat at the edge. The glass fiber filters have a fainter image when imaged from the front. However, as seen in Figure 17, when imaged on the reverse side, it is clear that the material has migrated largely to the back of these filters.

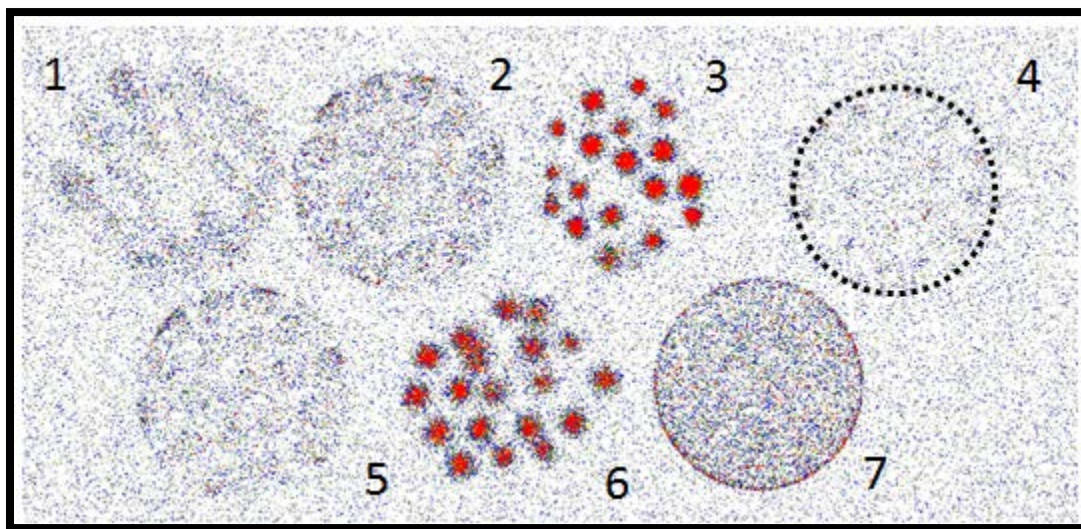


Figure 16 - 1 hour exposure of a series of filter paper media. (1) Hi-Q FP2063-20 high activity Am-241 using 15 uL droplets (2) Hi-Q FP2061-47 high activity Am-241 using 15 uL droplets (3) Millipore Fluoropore high activity Am-241 using 15 uL droplets (4) Hi-Q FP2063-20 high activity Am-241 using 10 uL droplets (5) Hi-Q FP2061-47 high activity Am-241 using 10 uL droplets (6) Millipore Fluoropore high activity Am-241 using 10 uL droplets (7) Pall 60301 high activity Am-241 using 10 uL droplets

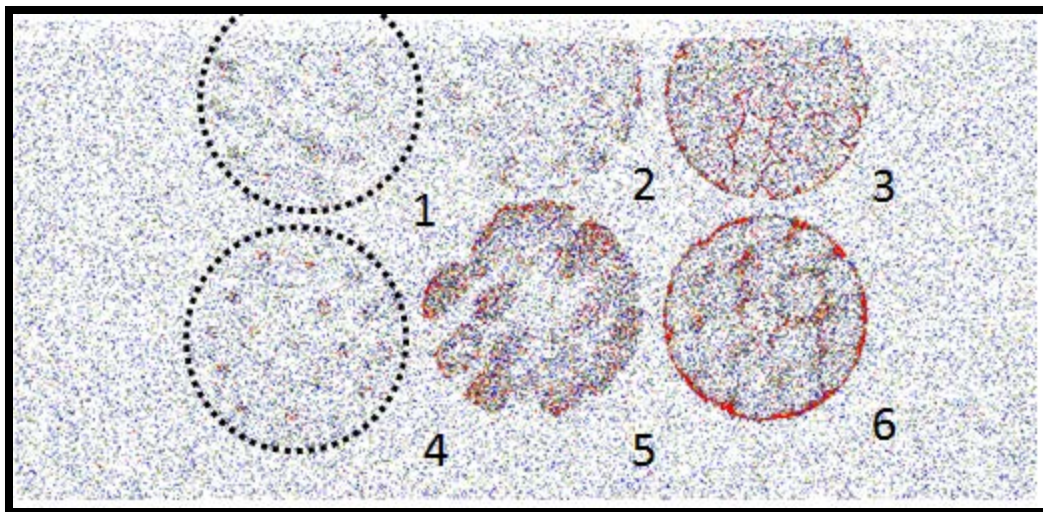


Figure 17 - 1 hour exposure of a series of filter paper media. (1) Hi-Q FP2063-20 high activity Am-241 using 5 uL droplets (2) Hi-Q FP2061-47 high activity Am-241 using 5 uL droplets (3) Pall 60301 high activity Am-241 using 5 uL droplets (4) Hi-Q FP2063-20 high activity Am-241 using 10 uL droplets (5) Reverse side of Hi-Q FP2063-20 high activity Am-241 using 15 uL droplets (6) Reverse side of Hi-Q 2061-47 high activity Am-241 using 15 uL droplets

Analysis of Americium-241 Samples

Genie 2K software was used in the acquisition of the Am-241 alpha spectra. The resulting .cnf files were converted to .csv files using Canberra ProSpect software. Subsequent analyses were performed using Microsoft Excel 2010. The key metrics recorded for each spectrum included the full width at half maximum (FWHM) and measured activity. Also, the spectra generated for the filters were statistically noisy, and determining the FWHM directly was impossible. Therefore a smoothing 7-point triangular algorithm (O'Haver) was applied to even out highly variable peaks in the spectra.

Smoothing the spectra also assisted in resolving the different peaks areas present. In figure 18, an interesting spectral feature is shown. Below the maximum energy peak, there is an area with increased activity that is not present in background spectra with an almost Gaussian shape suggesting that it is a function of the Am-241 activity. This is especially apparent in glass fiber filters.

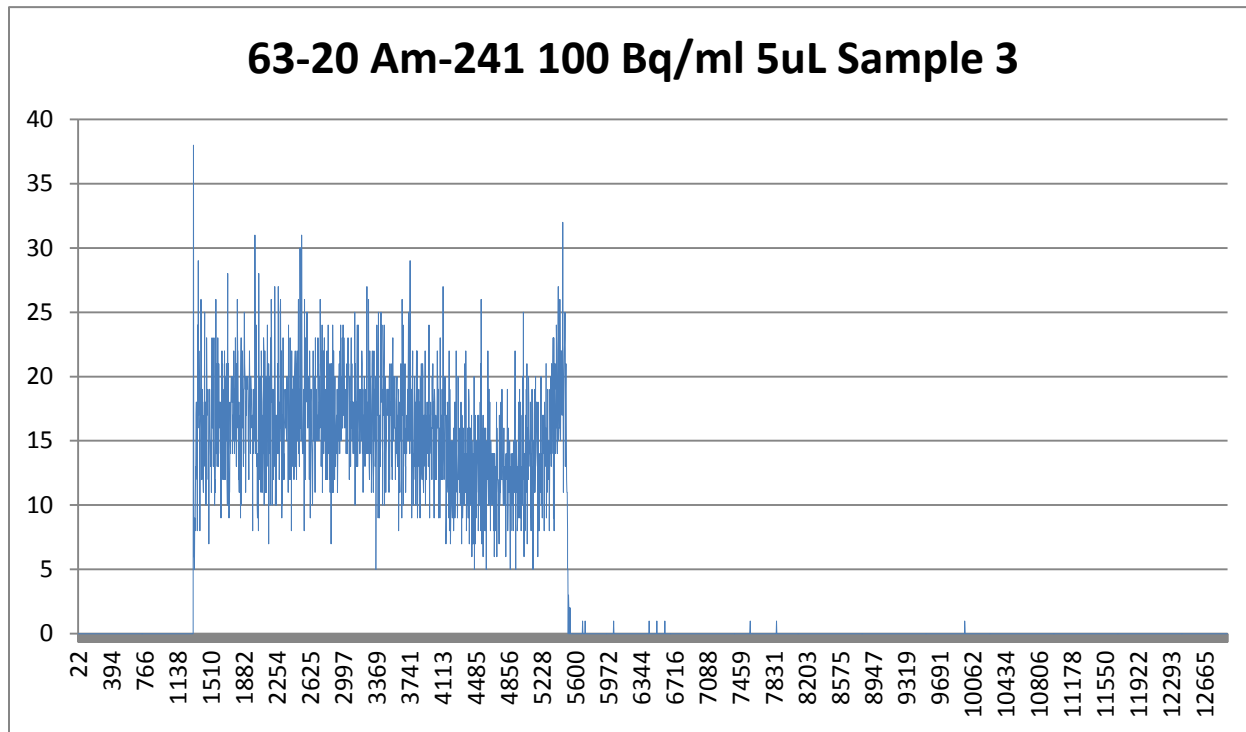


Figure 18 - An example of a spectrum resulting from a glass fiber filter (Hi-Q 2063-20) treated with the high activity Am-241 solution.

Using the smoothing algorithm (see Figure 19), this difference becomes more obvious, and more importantly, quantifiable. The FWHM and ratio of peak area to total active area became a means by which filter attenuation effects could be determined if the total area is assumed to be related to the Am-241 in the sample.

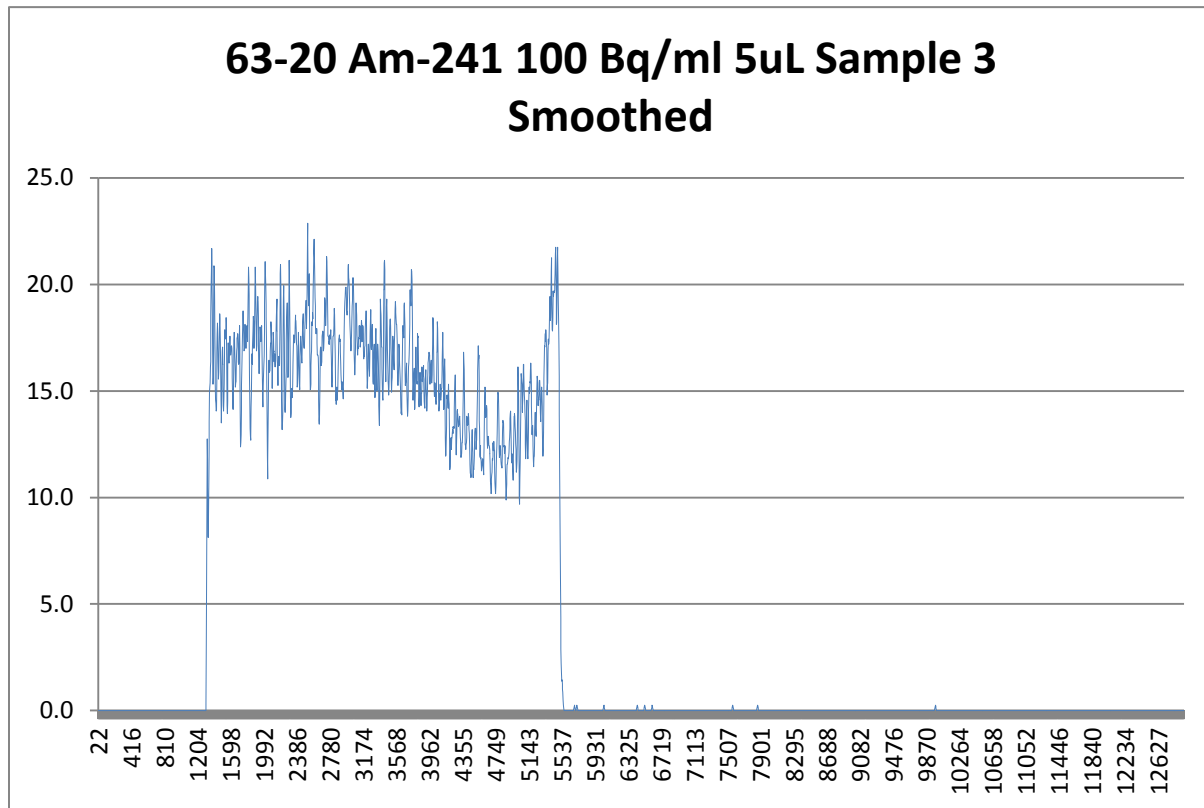


Figure 19 - The same spectrum with the smoothing algorithm applied.

In Table 5, the ratio of the area under the peak to the total area of the spectrum has been averaged over all filters treated with high and low activity solutions. This is further summarized to compare the effects on membrane filters with the effects on glass fiber filters. It may be noted that in glass fiber filters the fraction of the activity captured in the peak is 0.15 ± 0.15 of the total activity for high activity samples but, much better in the low activity samples averaging between 0.67 ± 0.02 and 0.89 ± 0.02 . In membrane filters, this relationship is reversed. The high activity filters have less low energy tailing with fractions of activity under

the peak averaging between 0.73 ± 0.08 to 0.82 ± 0.10 . This collection efficiency drops slightly for low activity membrane samples with 0.52 ± 0.11 to 0.70 ± 0.20 of the activity being captured under the peak. The range describes the discrepancies in peak identification between smoothed and raw spectra. It should be noted that there is an average of 91% agreement between these values in high activity samples and 76% agreement in low activity samples.

Table 5 - Summary of the peak to total area ratios between all filters.

Filter (Treatment)	Peak Area/Total Area (raw)	Standard Deviation	Peak Area/Total Area (smoothed)	Standard Deviation
63-20 (high activity)	0.15	0.13	0.16	0.12
63-20 (low activity)	0.70	0.03	0.92	0.03
61-47 (high activity)	0.15	0.17	0.16	0.19
61-47 (low activity)	0.63	0.01	0.86	0.02
60301 (high activity)	0.68	0.07	0.75	0.09
60301 (low activity)	0.36	0.12	0.53	0.29
FSL (high activity)	0.78	0.09	0.88	0.10
FSL (low activity)	0.67	0.09	0.87	0.11
Summary				
Glass fiber high activity	0.15	0.15	0.16	0.16
Glass fiber low activity	0.67	0.02	0.89	0.02
Membrane high activity	0.73	0.08	0.82	0.10
Membrane low activity	0.52	0.11	0.70	0.20

This assessment may be explained by filter attenuation effects. As the material settles into the filter fibers, some settles near the surface while some migrates toward the back of the filter. The material buried deep in the filter will either be attenuated completely or experience significant energy degradation, which is expressed in activity in lower energy regions of the spectrum appearing as tailing or a secondary peak. Figure 20 is an example of a smoothed

spectrum from a high activity sample using a Hi-Q 2063-20 glass fiber filter. In this spectrum, two distinct areas can be seen, the first starts at 1314 keV to 4755 keV, and the second (the Am-241 peak) picks up at 4756 keV ending at 5537 keV.

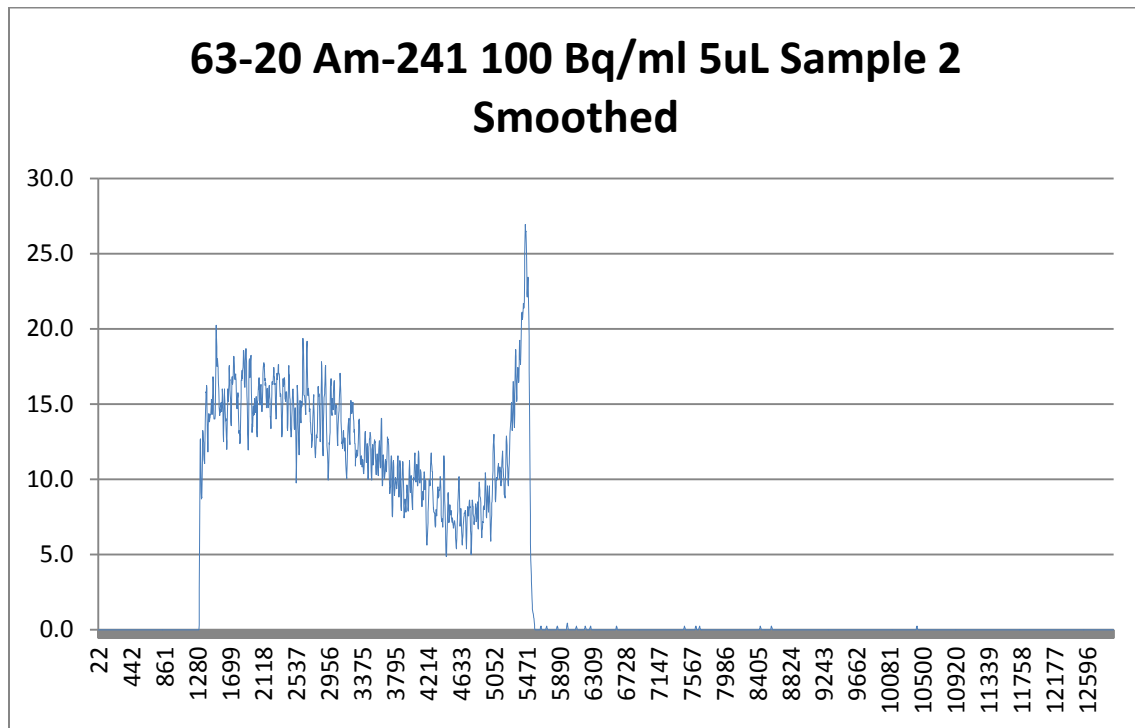


Figure 20- This high activity Am-241 spectrum has been smoothed to show two distinct areas of activity.

This can be contrasted with Figure 21, the spectrum resulting from the same filter type treated with the low activity Am-241 solution. This spectrum contains only one continuous peak with some low energy tailing.

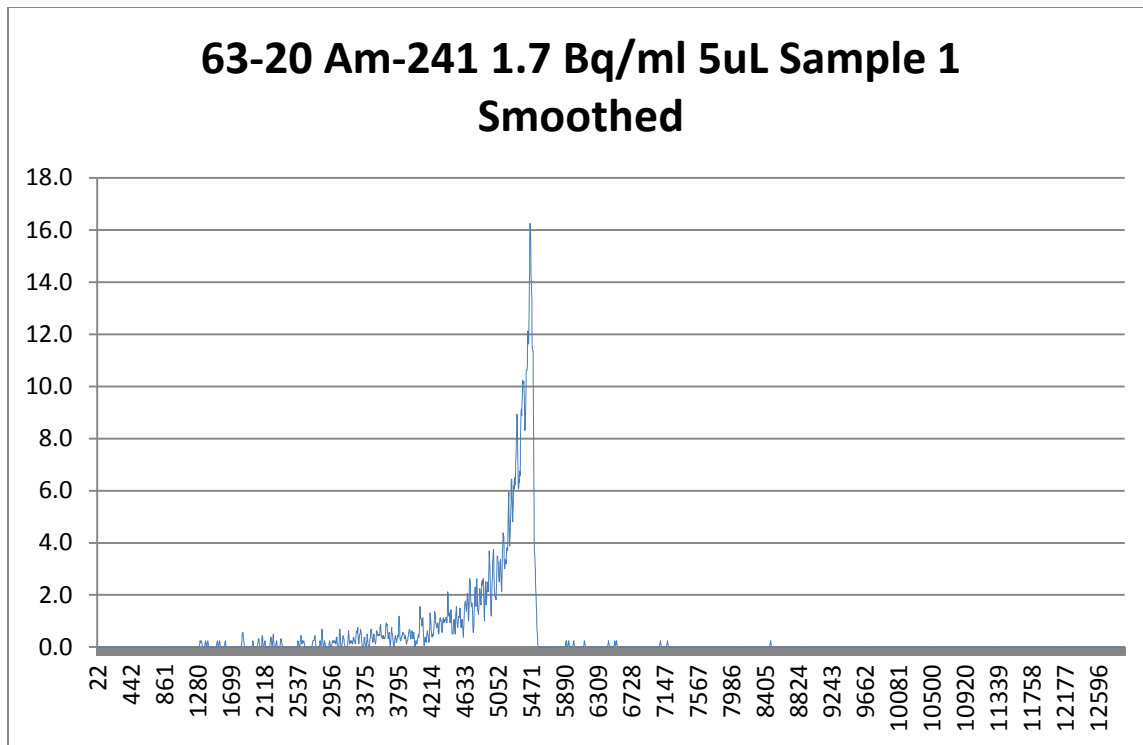


Figure 21 - Smoothed low activity glass fiber filter Am-241 spectrum.

This is also reflected in the measured activity values for the filters. The glass fiber filters showed significant inconsistencies in measured activities with 1σ standard deviation greater than half of the mean value. Figure 22 through Figure 25 represent the measured activities of the glass fiber filters.

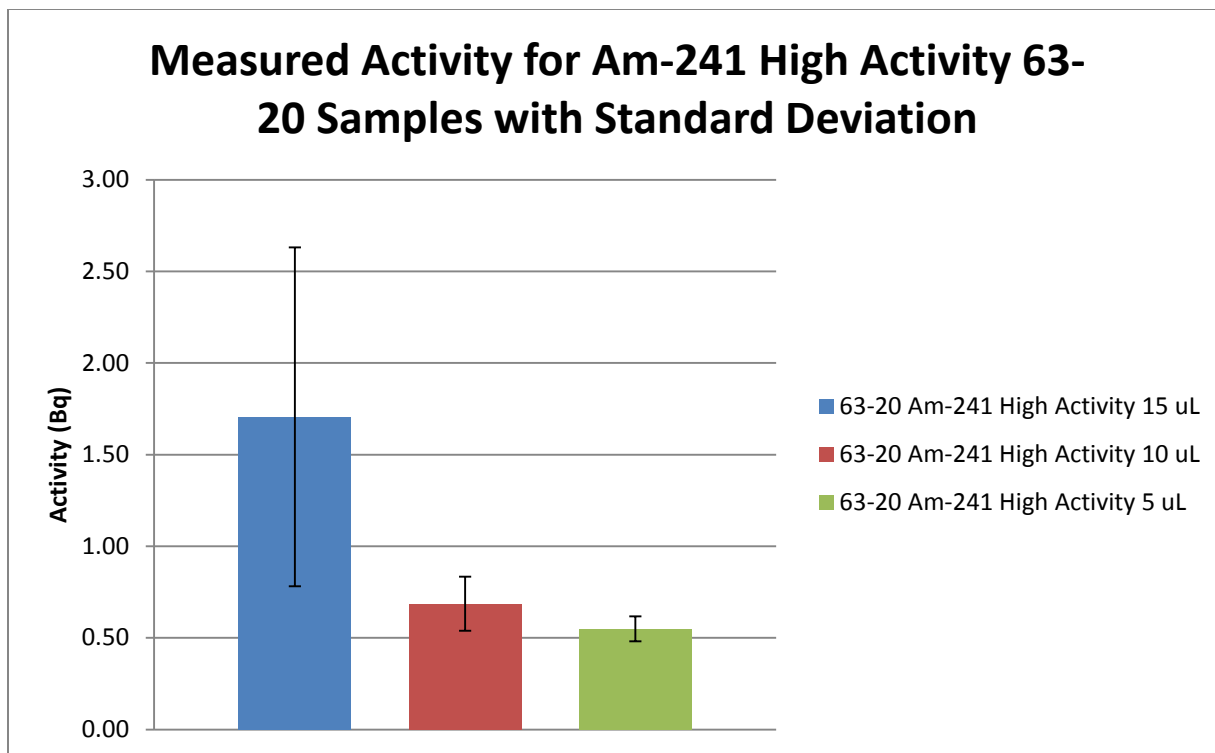


Figure 22 - Measured activity in Hi-Q 2063-20 filters treated with high activity solution of Am-241.

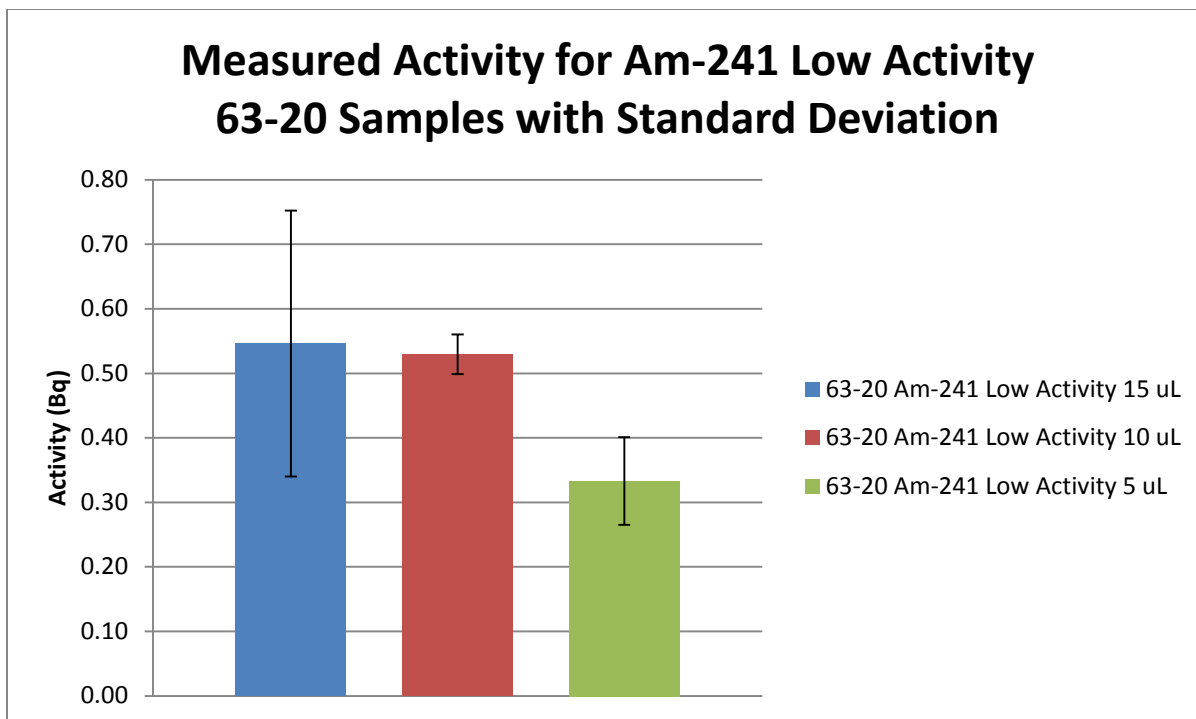


Figure 23 -Measured activity in Hi-Q 2063-20 filters treated with low activity solution of Am-241.

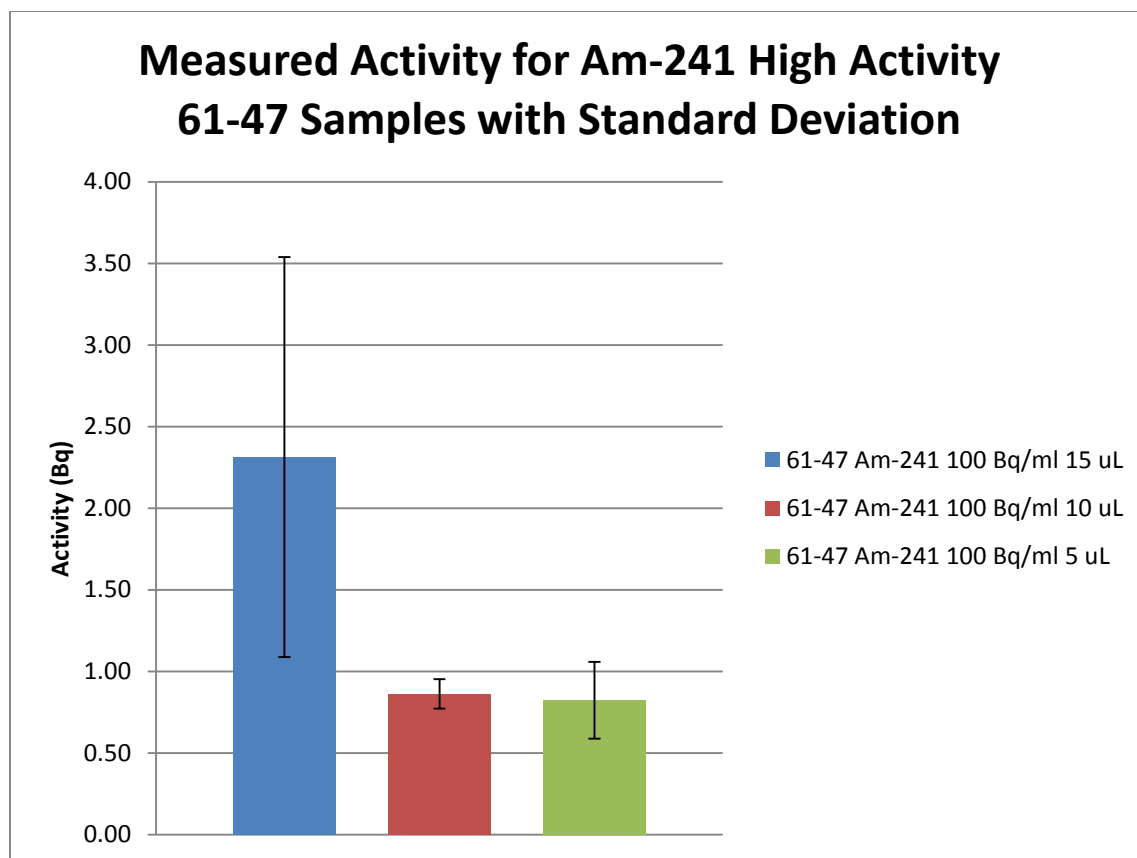


Figure 24 -Measured activity in Hi-Q 2061-47 filters treated with high activity solution of Am-241.

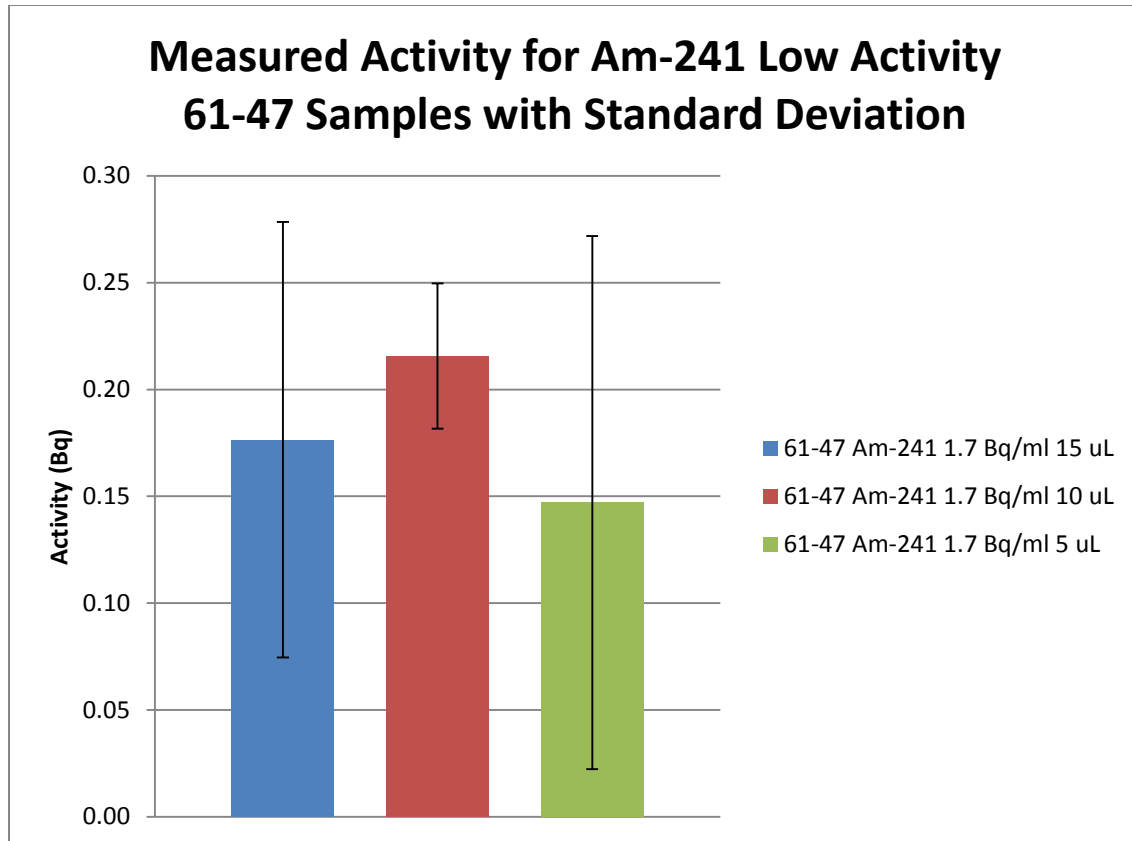


Figure 25 -Measured activity in Hi-Q 2061-47 filters treated with low activity solution of Am-241.

However, though incredibly imprecise, the FWHM was relatively consistent for all glass fiber filters. In almost all cases, excluding the low activity FSL filters, the FWHM was maintained across all droplet volumes. Figure 26 through Figure 29 demonstrate how FWHM varied across all of these parameters.

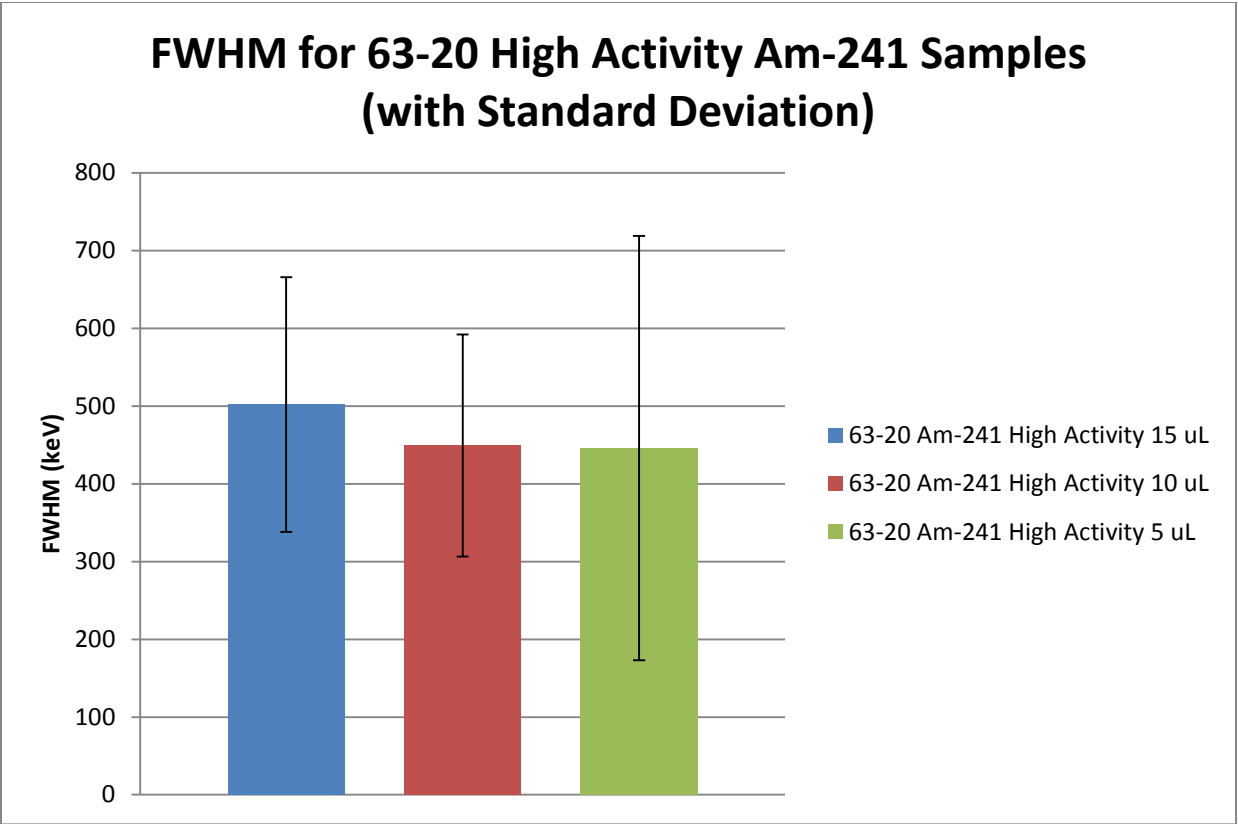


Figure 26 -FWHM measured in Hi-Q 2063-20 filters treated with high activity solution of Am-241.

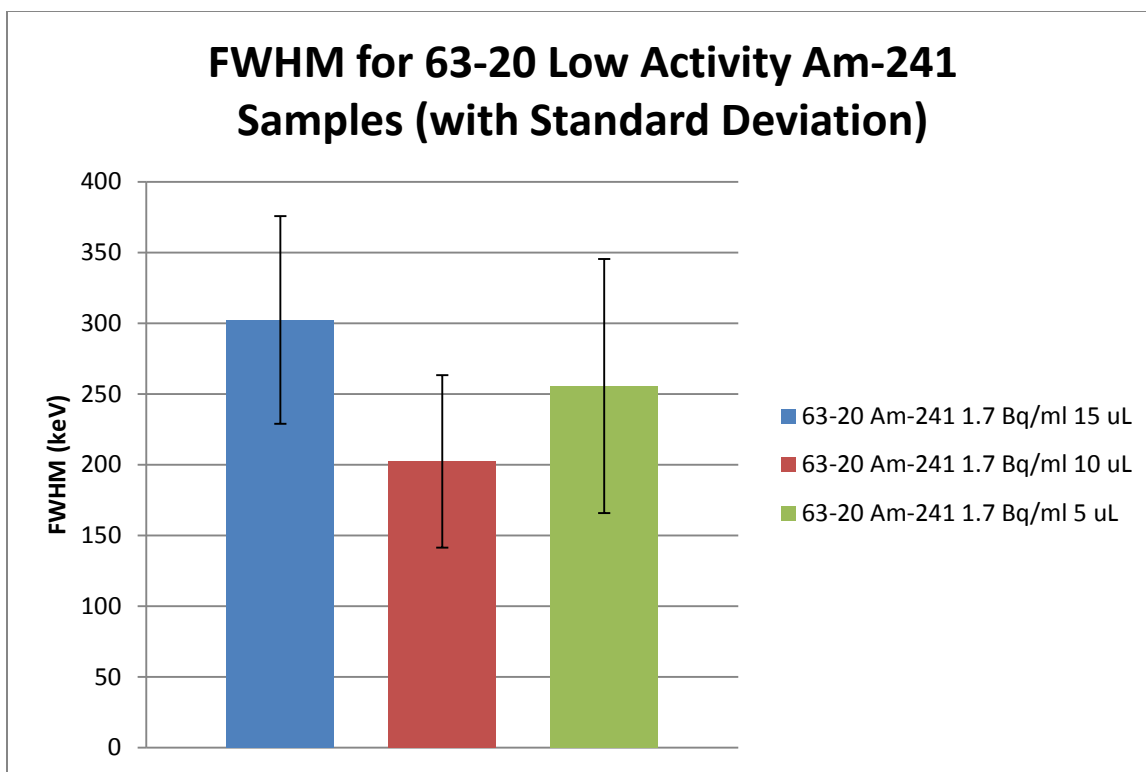


Figure 27-FWHM measured in Hi-Q 2063-20 filters treated with low activity solution of Am-241.

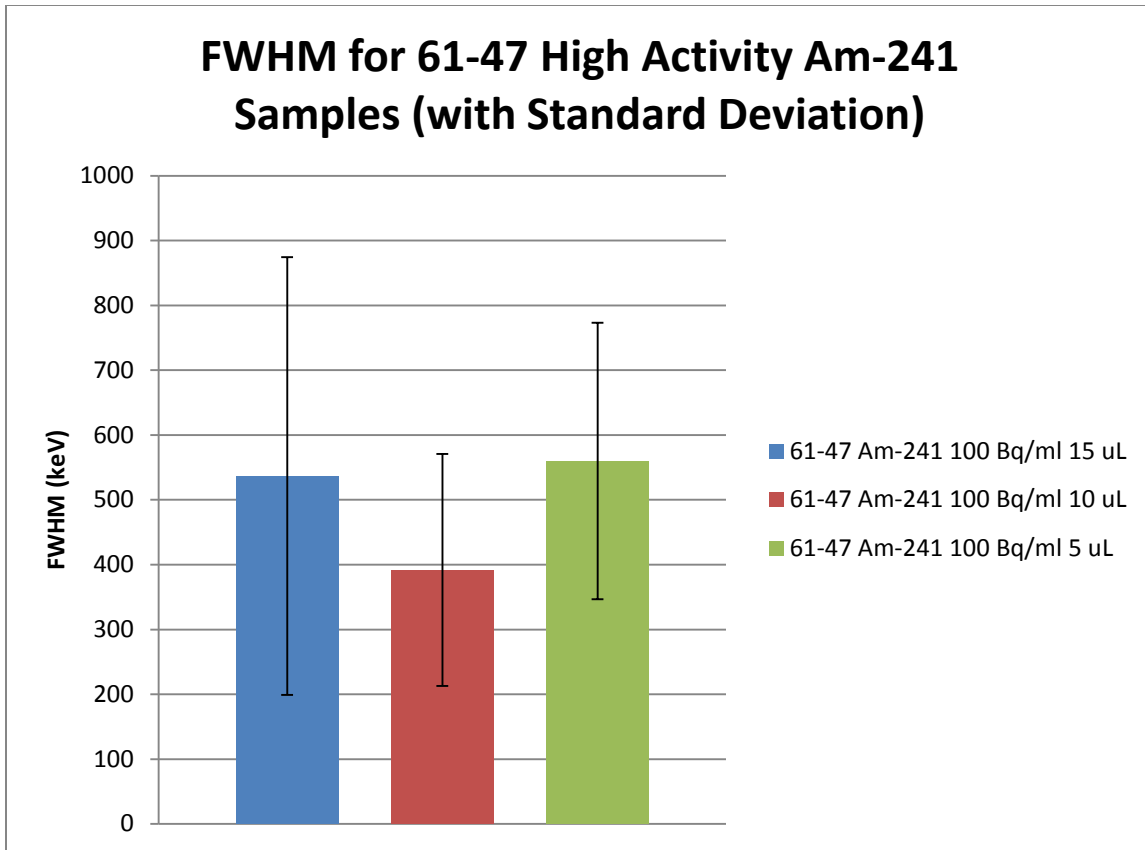


Figure 28-FWHM measured in Hi-Q 2061-47 filters treated with high activity solution of Am-241.

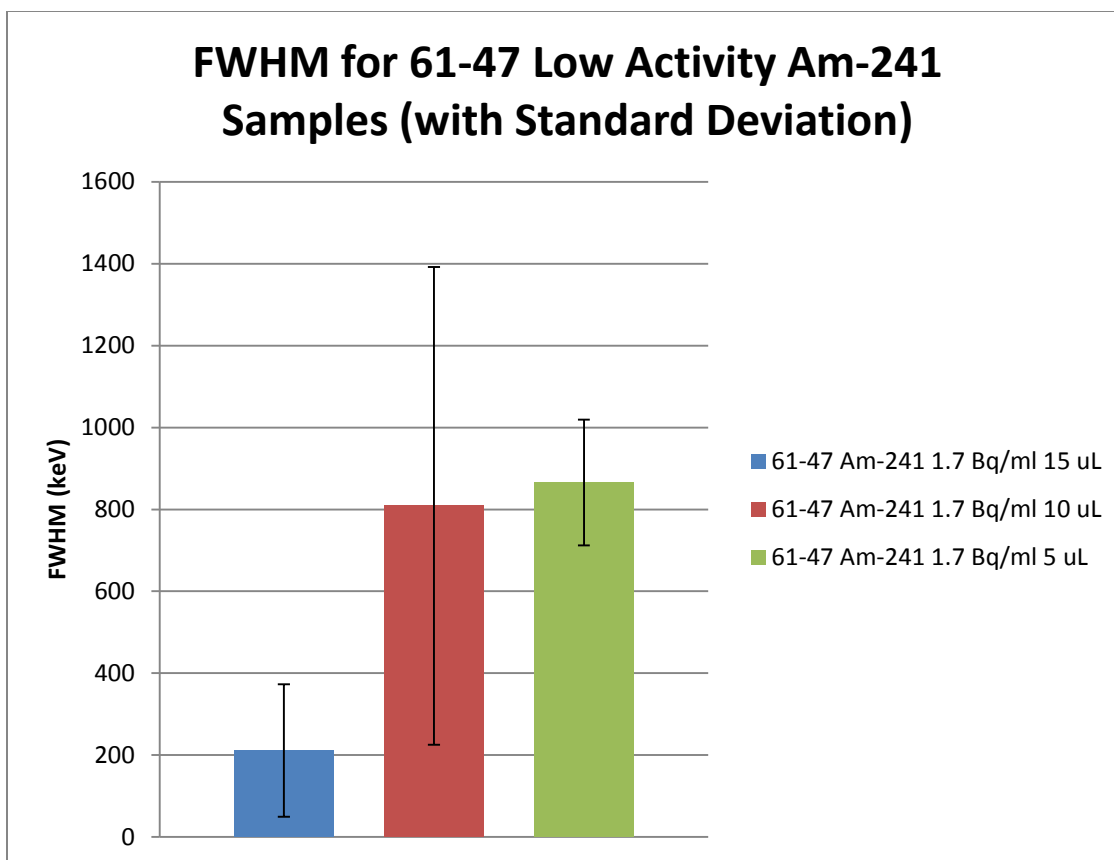


Figure 29 - FWHM measured in Hi-Q 2061-47 filters treated with low activity solution of Am-241.

Membrane filters, on the other hand, performed much more consistently with respect to precision of measurement of the activity on each filter. However, the activity contained in filters with 15 μ L of solution was calculated as equal to those with 10 μ L. This was true for 10 μ L samples compared with 5 μ L samples as well. These differences are a function of burial losses and other sources of error as described later in the Error section of this document. Figure 30 to Figure 33 demonstrate the activity in the membrane filters and associated 1σ error.

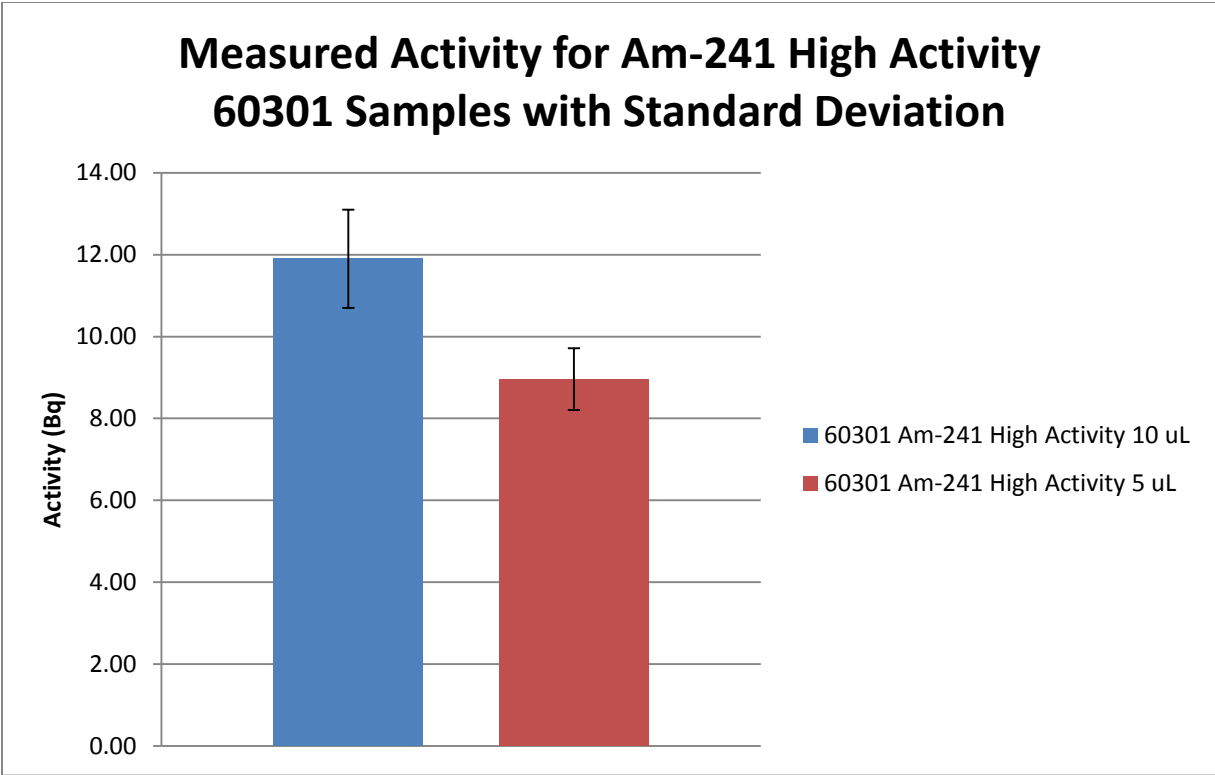


Figure 30 - Measured activity in Pall 60301 filters treated with high activity solution of Am-241

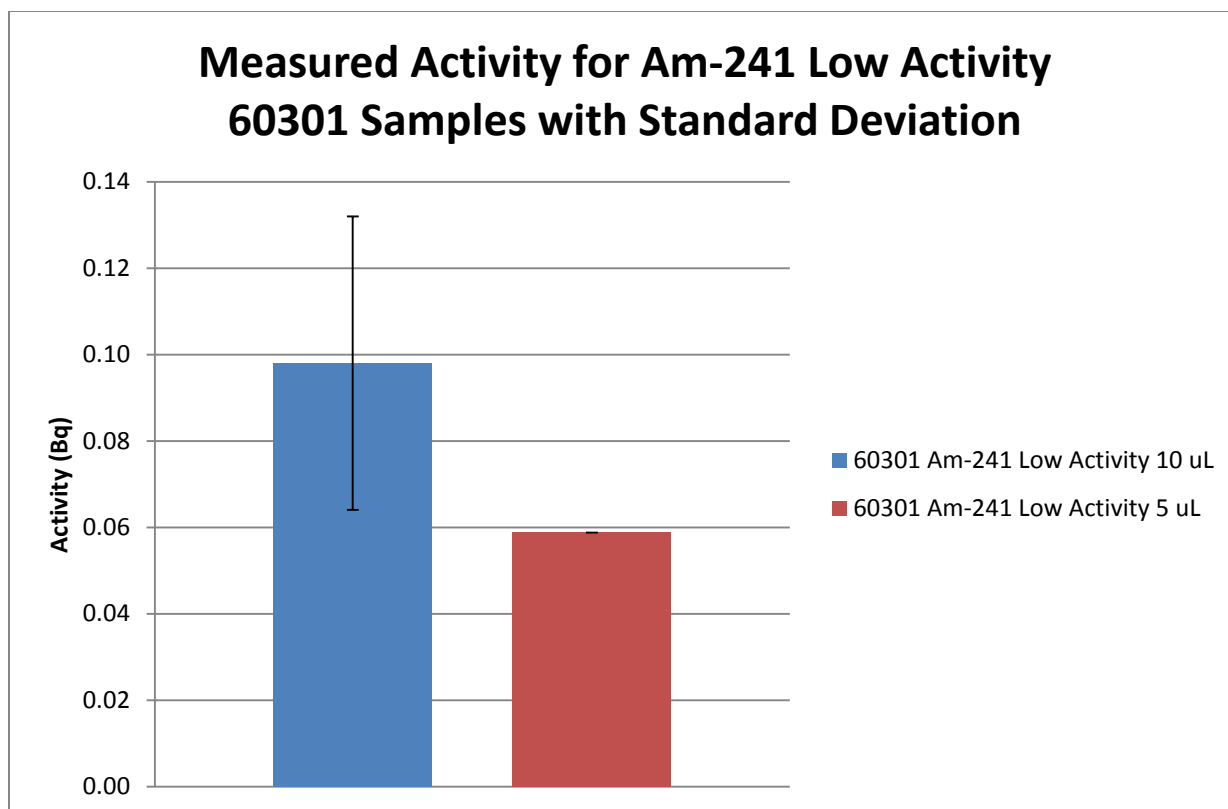


Figure 31 - Measured activity in Pall 60301 filters treated with low activity solution of Am-241.

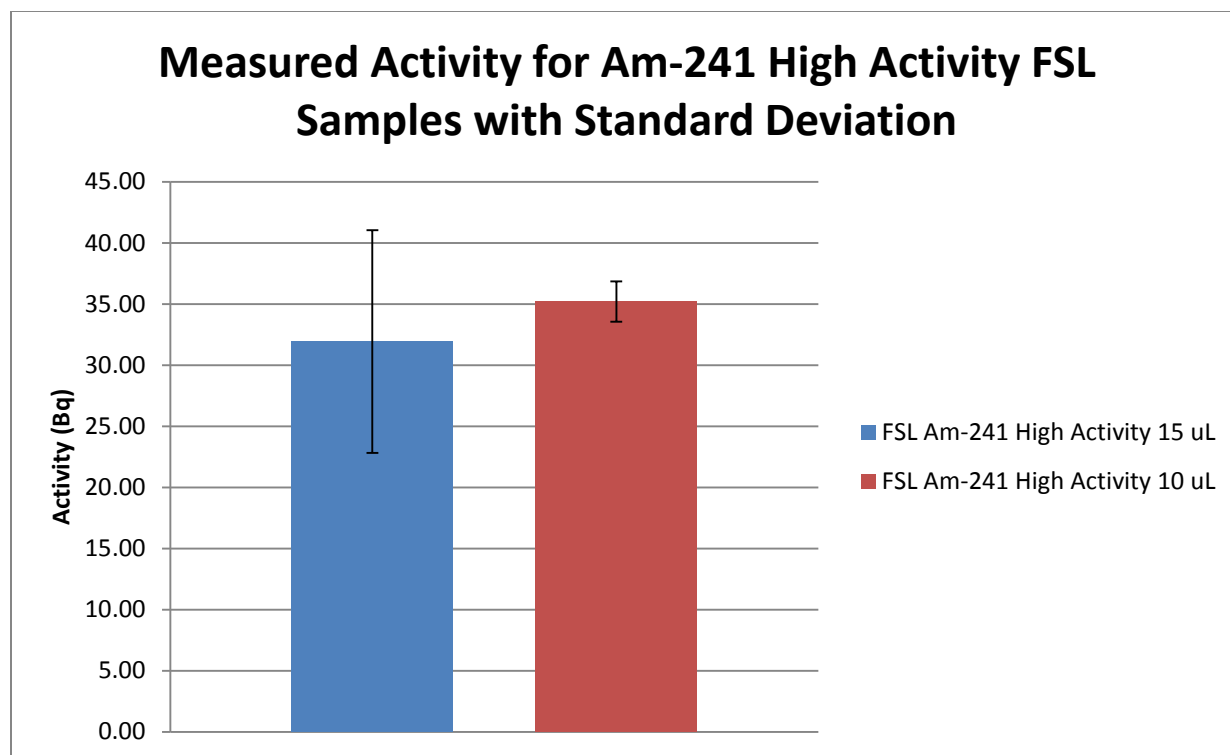


Figure 32 - Measured activity in Millipore Fluopore (FSL) filters treated with high activity solution of Am-241

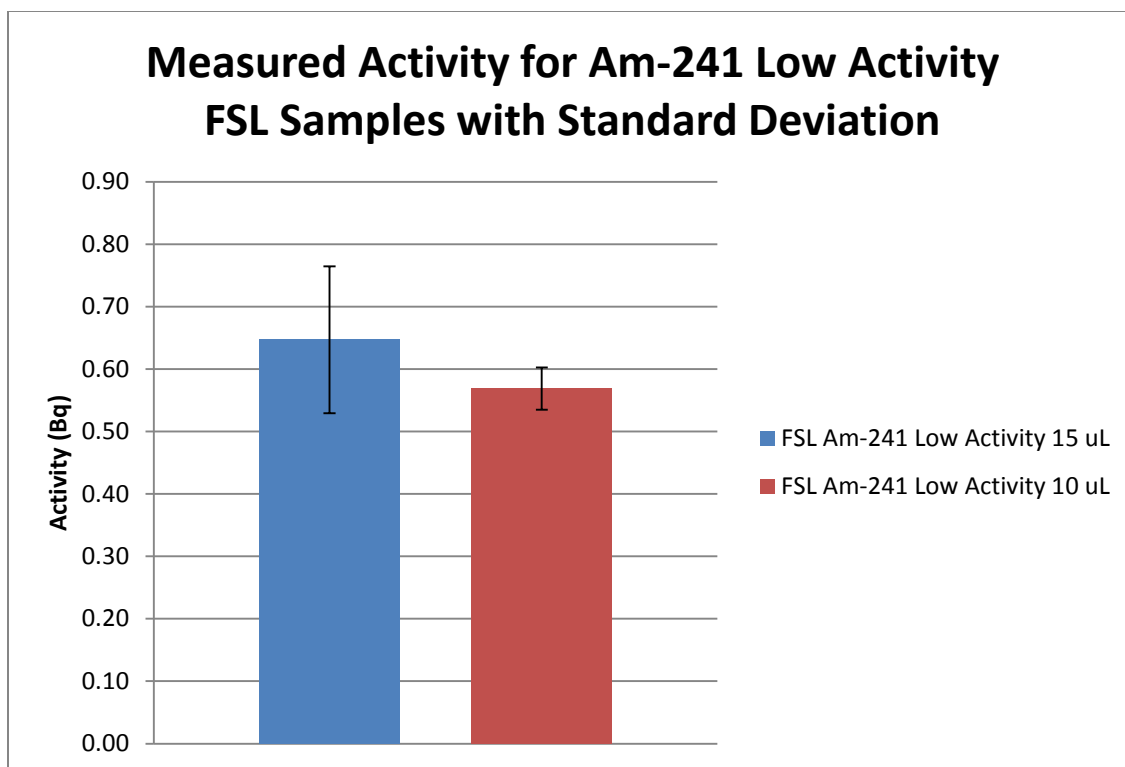


Figure 33 - Measured activity in Millipore Fluoropore (FSL) filters treated with low activity solution of Am-241

As seen with the glass fiber filters, the FWHM of the Am-241 peak in the membrane filters remained fairly consistent across all filters in this cohort. Figure 34 to Figure 37 represent the FWHM calculated for these filters.

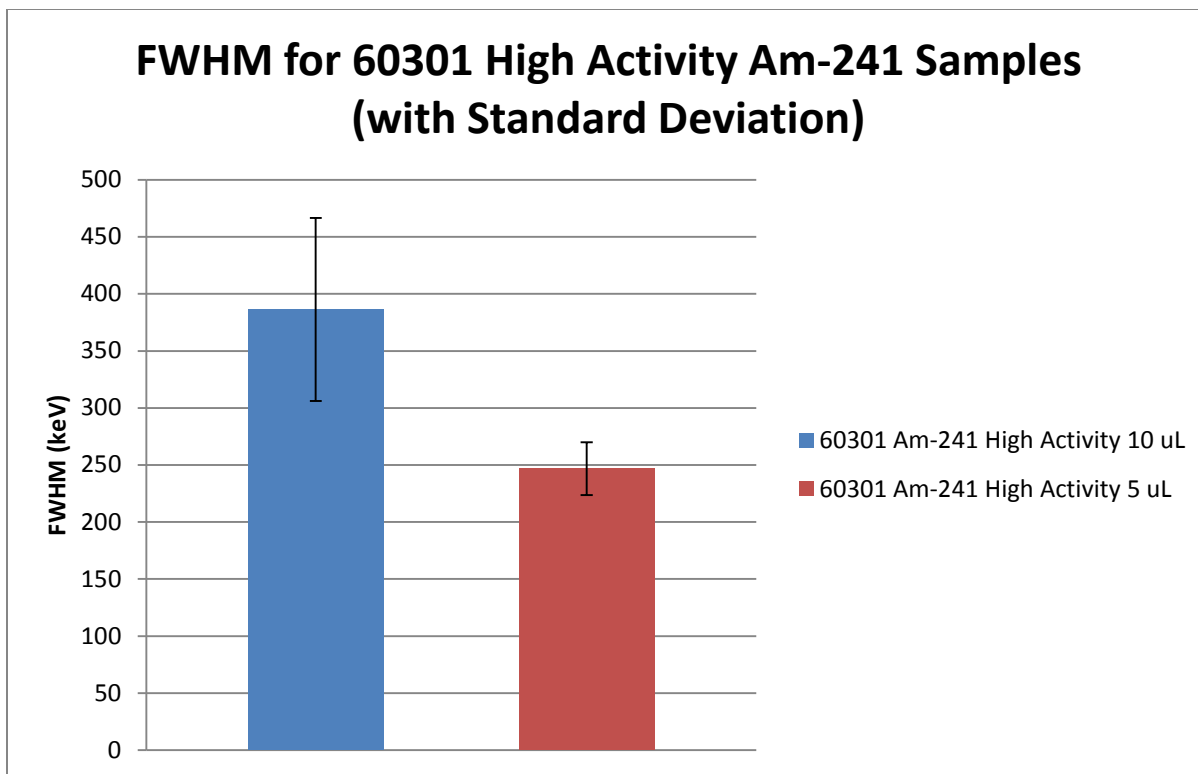


Figure 34 - FWHM measured in Pall 60301 filters treated with high activity solution of Am-241.

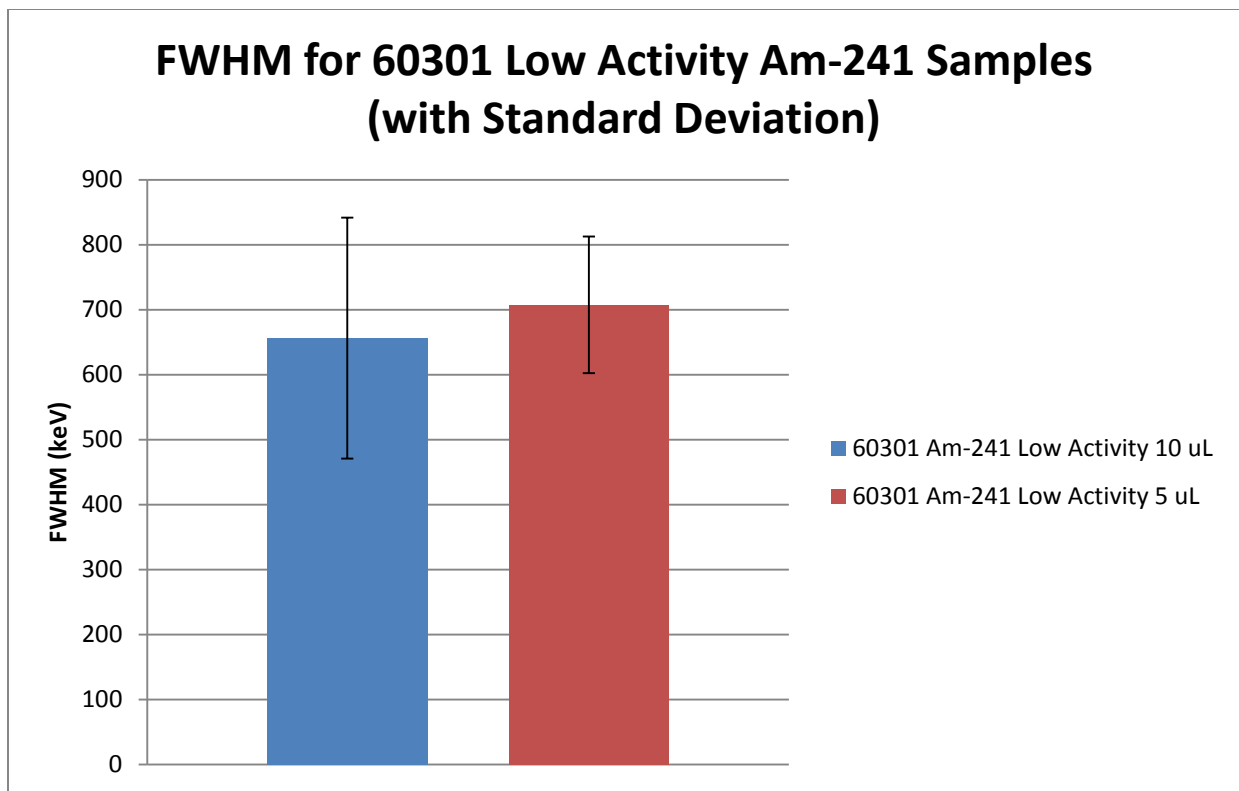


Figure 35 - FWHM measured in Pall 60301 filters treated with low activity solution of Am-241.

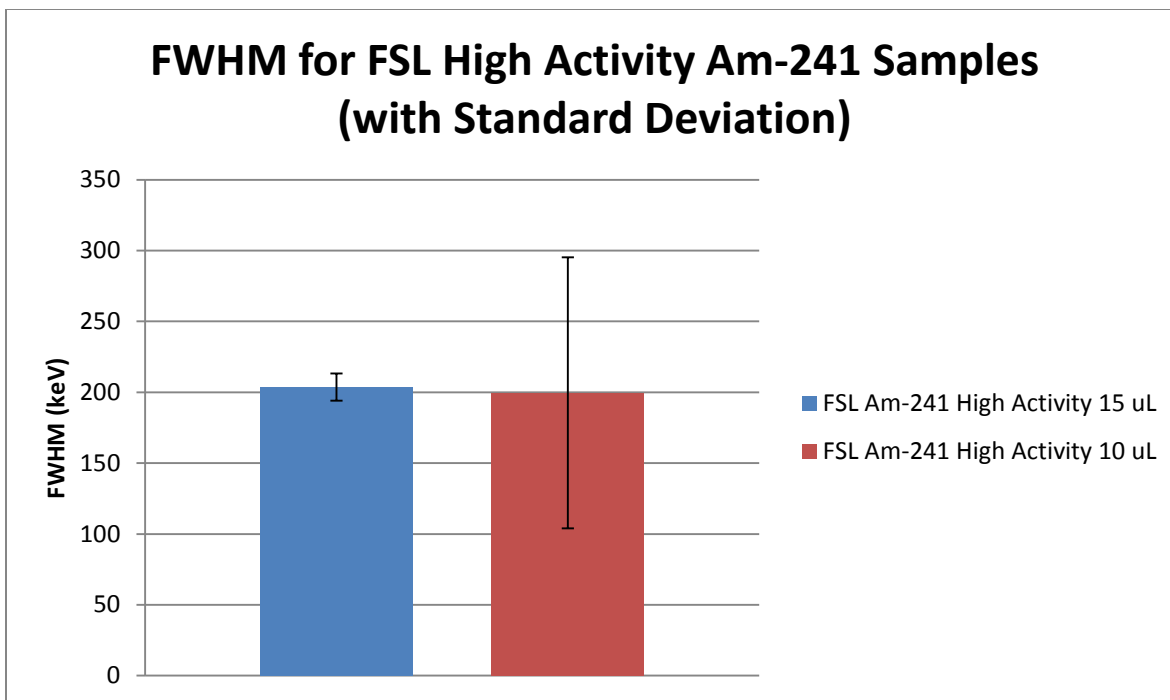


Figure 36 - FWHM measured in Millipore Fluopore (FSL) filters treated with high activity solution of Am-241.

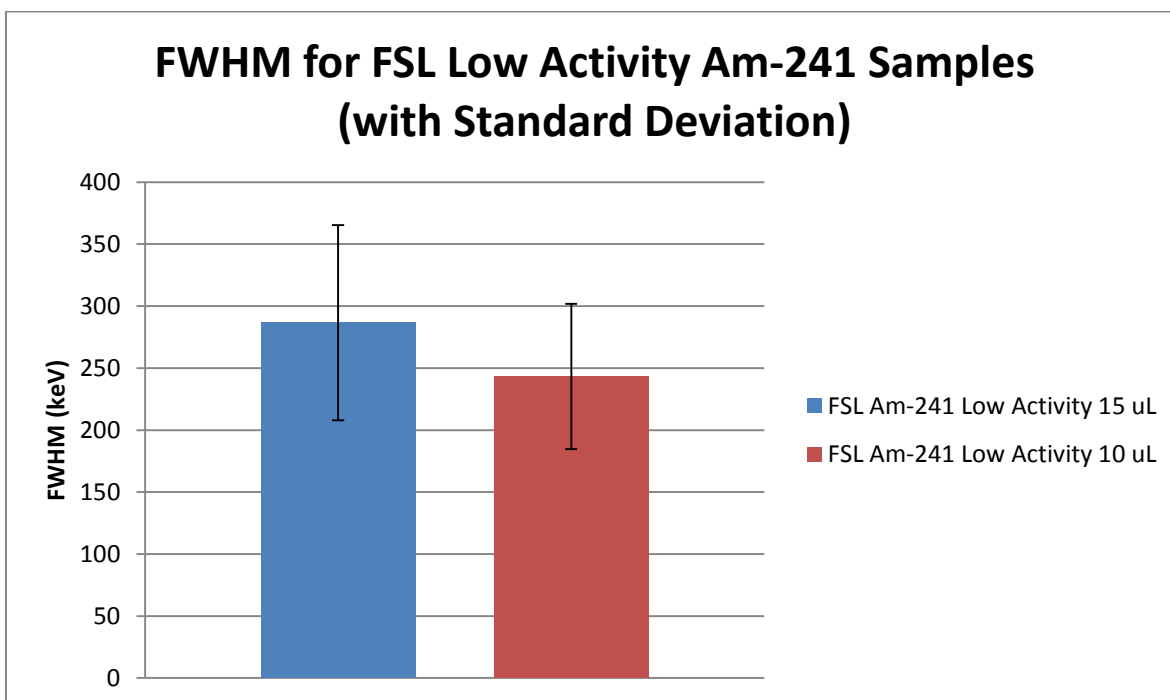


Figure 37 - FWHM measured in Millipore Fluopore (FSL) filters treated with low activity solution of Am-241.

The activity measured in all samples was compared with the theoretical values based on droplet volume, activity concentration of the standard solution, and number of droplets used corrected for pipetting error (Figure 38). For high activity glass fiber filter samples, percent difference between these values varied between 63% and 85%. Membrane filter activity measured was significantly different from expectation values. Activity measured was up to a factor of three greater than theoretical values. In low activity samples the response was very different. In almost every case, the activity on the filter was over reported by 50% up to nearly three times the expected value; the exception being the Milipore FSL filters which were within 20%. Figure 39 provides details on the percent difference in the measured and theoretical values for filter activity for low activity samples.

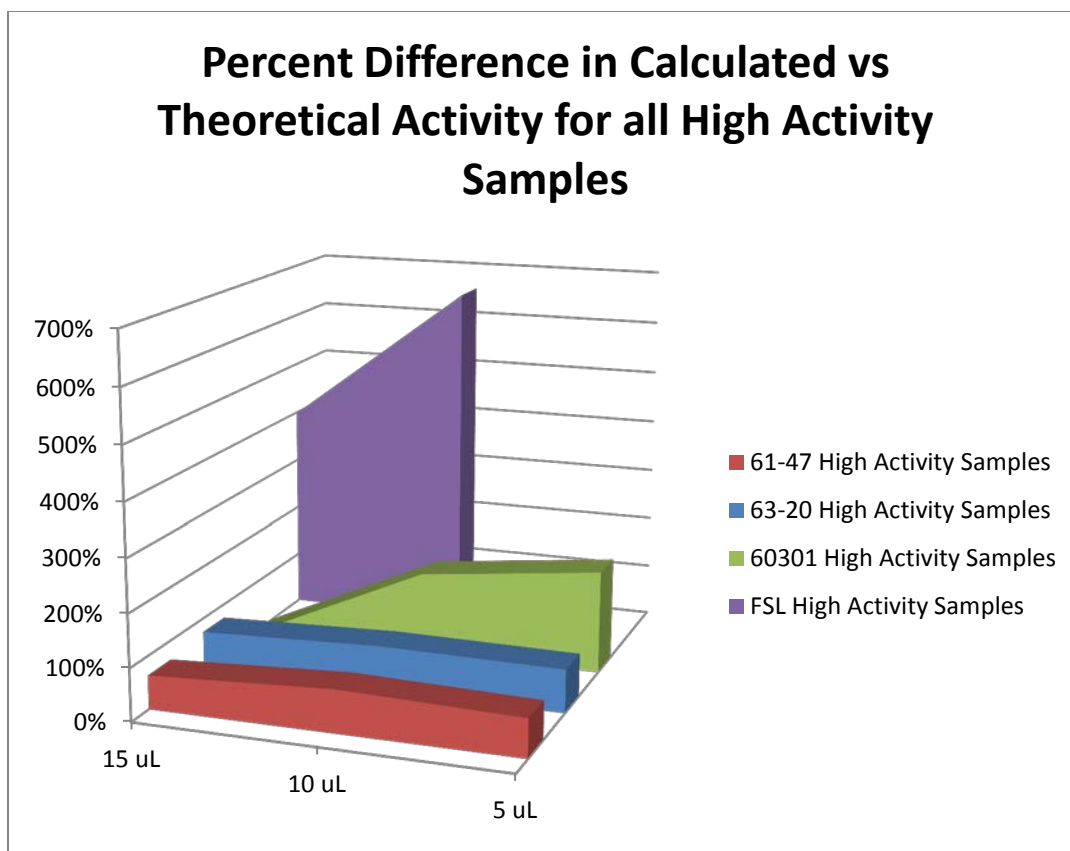


Figure 38 - Percent difference in calculated activity versus theoretical activity for all samples treated with high activity solution of Am-241.

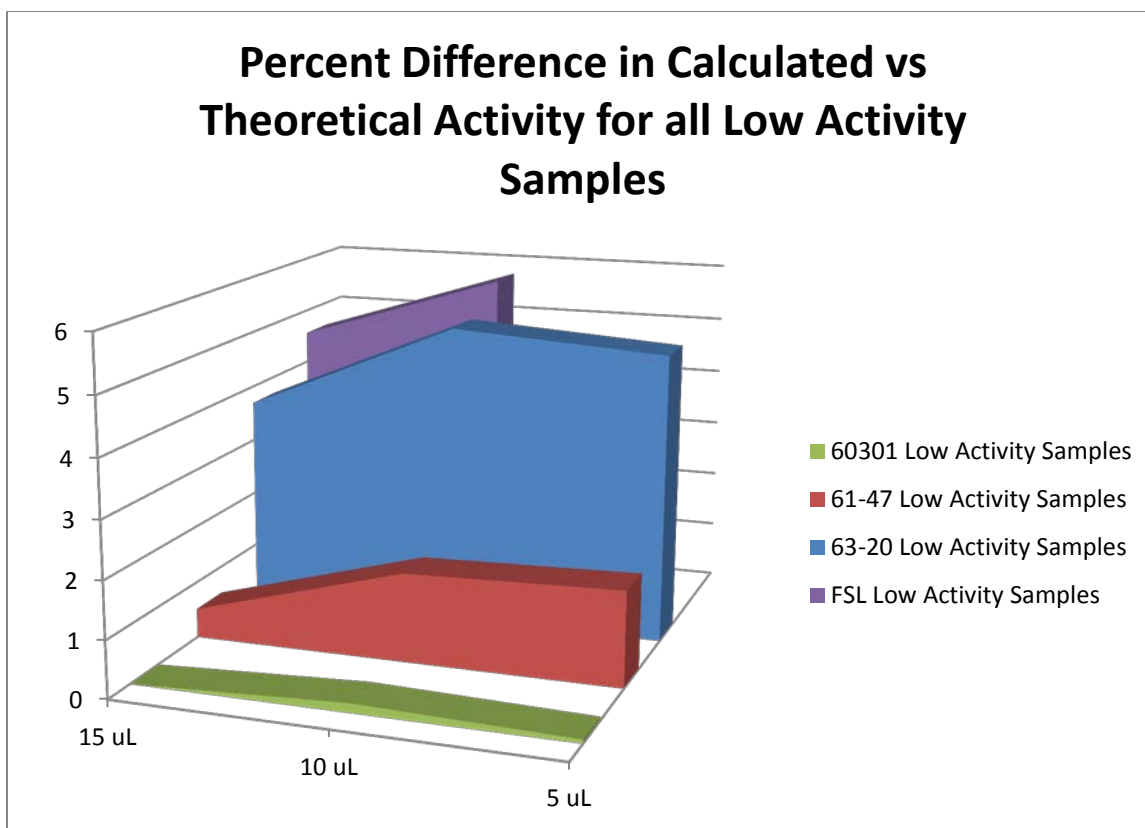


Figure 39 - Percent difference in calculated activity versus theoretical activity for all samples treated with low activity solution of Am-241.

Analysis of Cesium-137 Samples

The ProSpect software used for gamma ray analysis has an Excel export function creating a .csv file with sample analysis details and counts per channel. These files were used to generate spectra for each sample created. The spectra were evaluated based on peak resolution, FWHM of the Cs-137 662 keV peak, and measured activity.

To evaluate the full width at half maximum, first the peak height was determined within the region of interest. Dividing this value by two, the corresponding channels (below and above the peak) with this value were determined. The energy values associated with those channels were then subtracted from one another to yield the FWHM value expressed in keV. The

resolution was calculated by dividing the FWHM by the peak energy and multiplying by 100 to return a percent. The activity of the samples was calculated by dividing the area under each peak by the sampling time. The activity is reported in terms of counts per second.

As expected, the resolution of the Cs-137 characteristic 662 keV peak was relatively unaffected by the filter media differences. This is especially true for samples created with the higher activity standard for which the resolution was recorded between 5.0% and 8.1% with an average around 7.5%. There was a higher variability associated with the lower activity samples with resolution being reported in the range of 6.4% - 11.9%. Figure 40 illustrates the spread of the data for high activity samples while Figure 41 demonstrates the resolution calculated for samples created using the low activity solution.

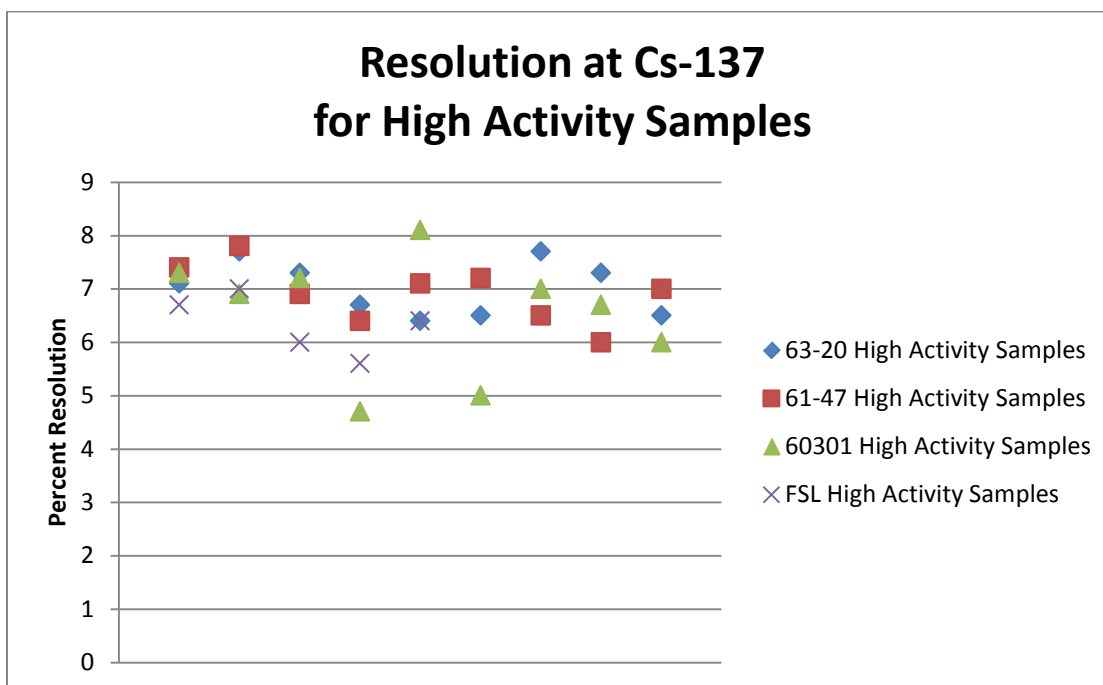


Figure 40 - Resolution of the Cs-137 662 keV peak for all samples treated with the high activity standard solution.

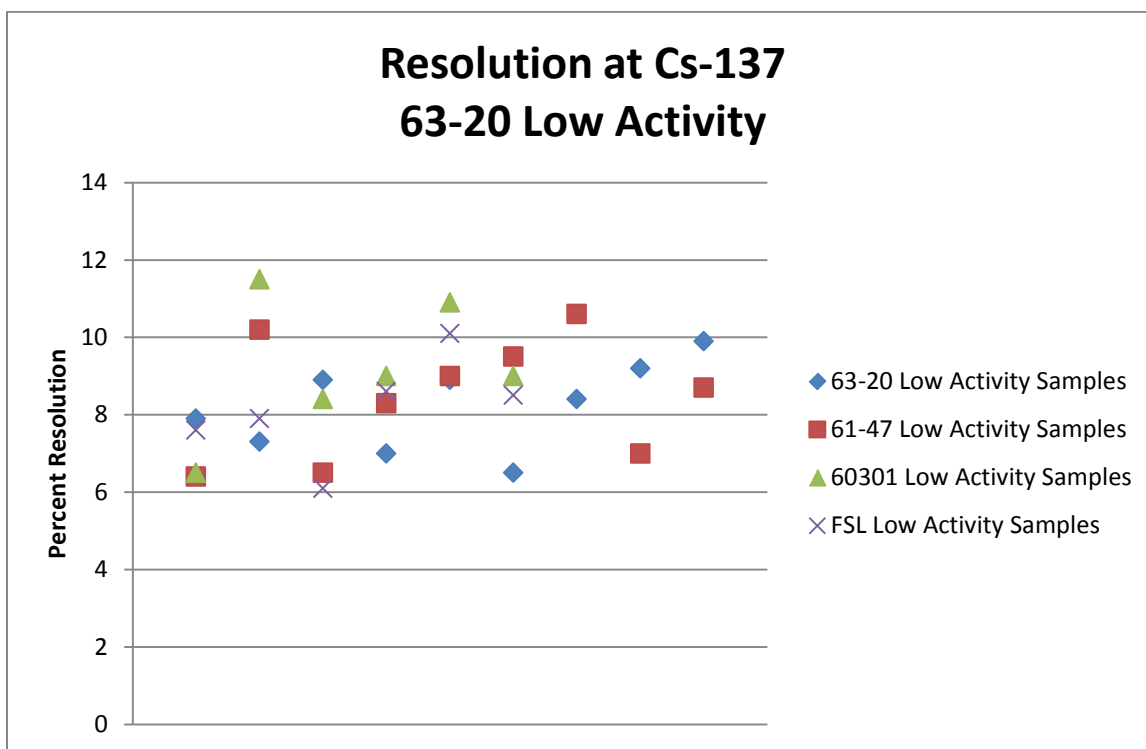


Figure 41 - Resolution of the Cs-137 662 keV peak for all samples treated with the low activity standard solution.

The second characteristic of the Cs-137 peak was its full width at half of the maximum peak height (FWHM). This metric evaluates the broadness of the peak which can be attributed to several factors. The most important factor is statistical fluctuations present in the detector (Knoll). Similarly, as FWHM is dependent upon the number of charge carriers, lower activity samples will tend to have wider peaks. The charge carriers are recoded in the spectrum according to their relative energies. Therefore, any attenuating media reduce the signal of the peak of interest and have the effect of peak broadening. In general, the samples in this study behaved accordingly. Figure 42 through Figure 45 show the FWHM for high activity samples while Figure 46 through Figure 49 demonstrates the FWHM spread for the low activity samples.

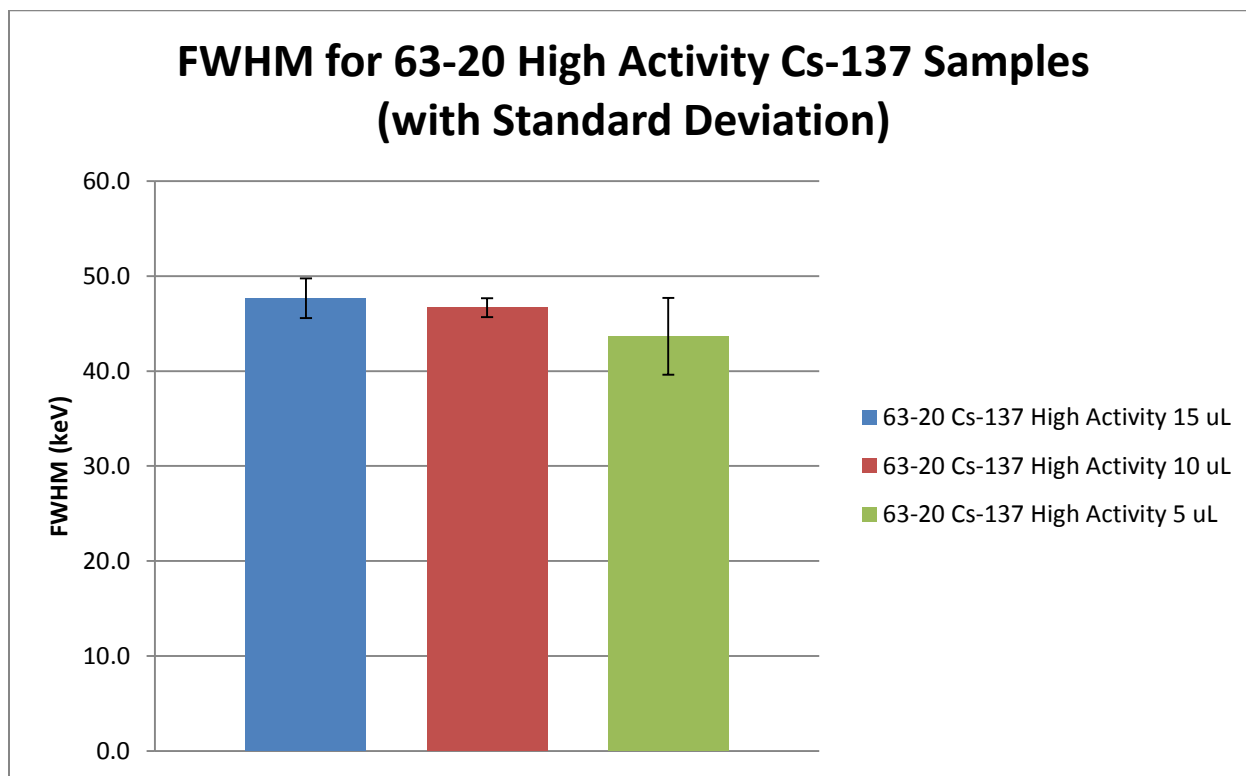


Figure 42 - FWHM for Hi-Q 2063-20 filters treated with high activity Cs-137 solution. Error bars are indicative of the standard deviation for all three samples created for each filter set.

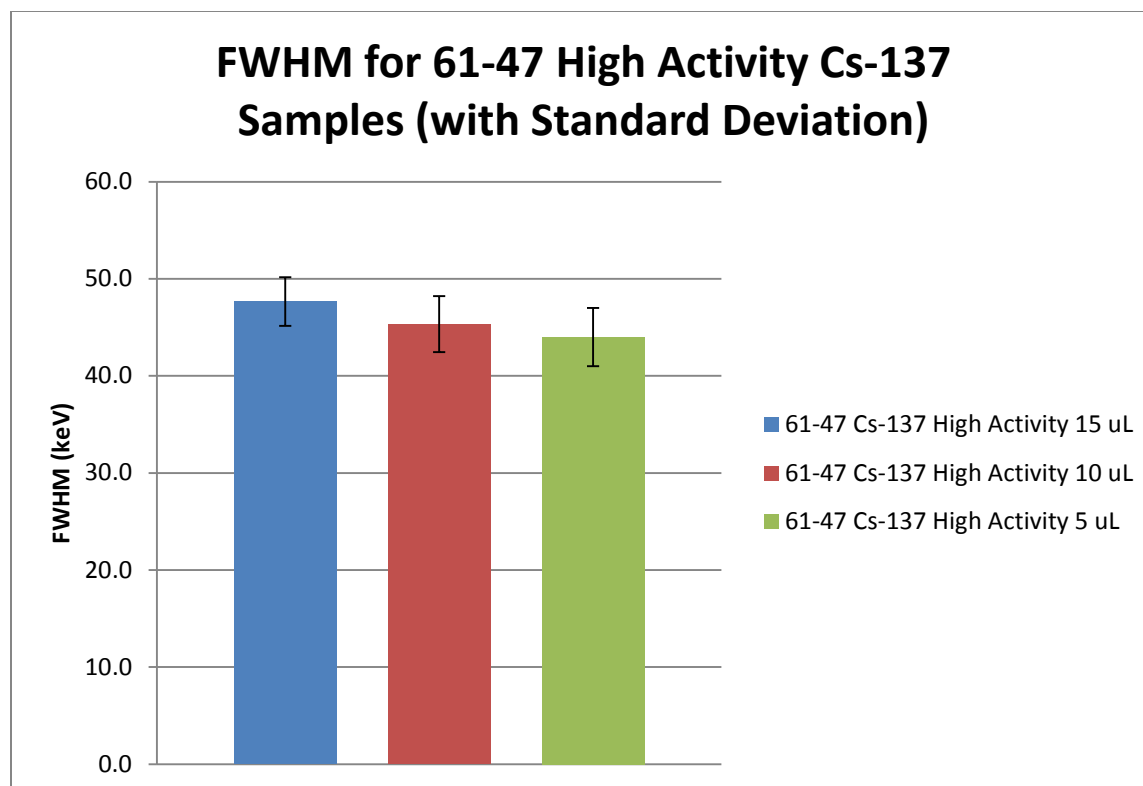


Figure 43 - FWHM for Hi-Q 2061-47 filters treated with high activity Cs-137 solution. Error bars are indicative of the standard deviation for all three samples created for each filter set.

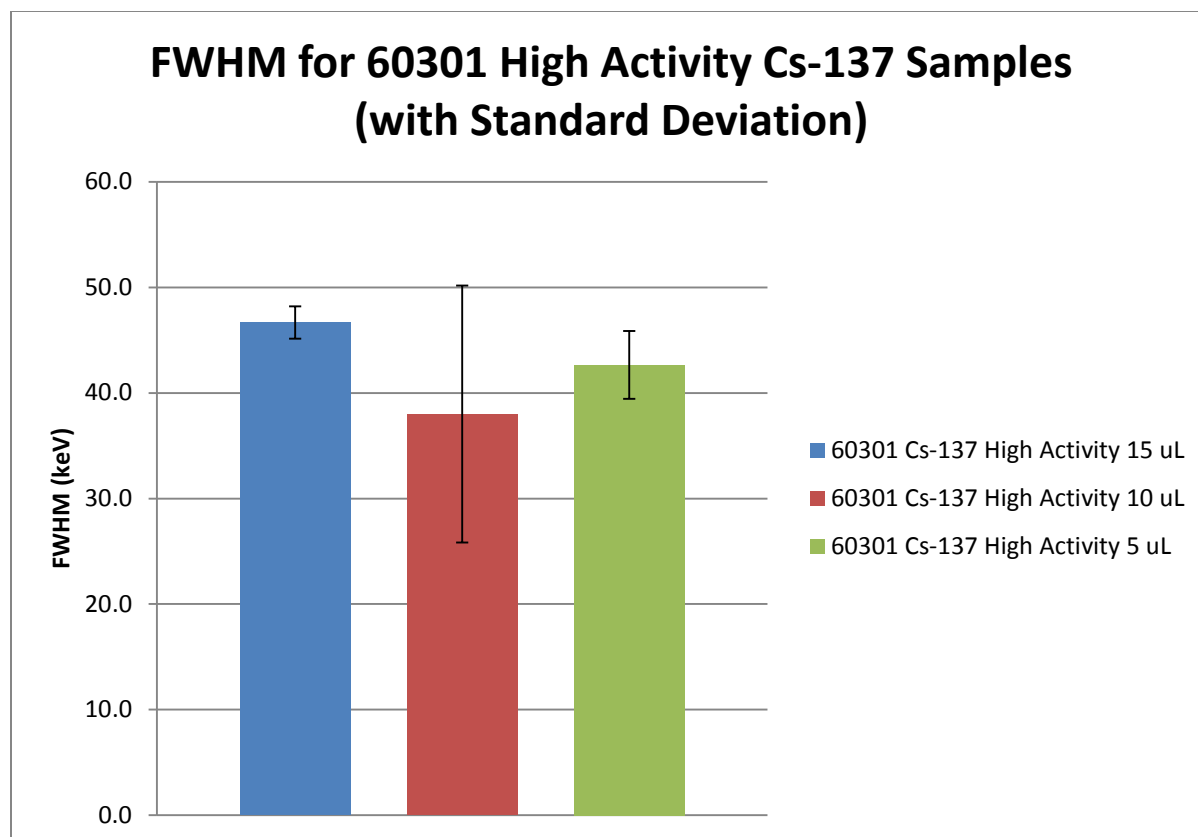


Figure 44 - FWHM for Pall 60301 filters treated with high activity Cs-137 solution. Error bars are indicative of the standard deviation for all three samples created for each filter set.

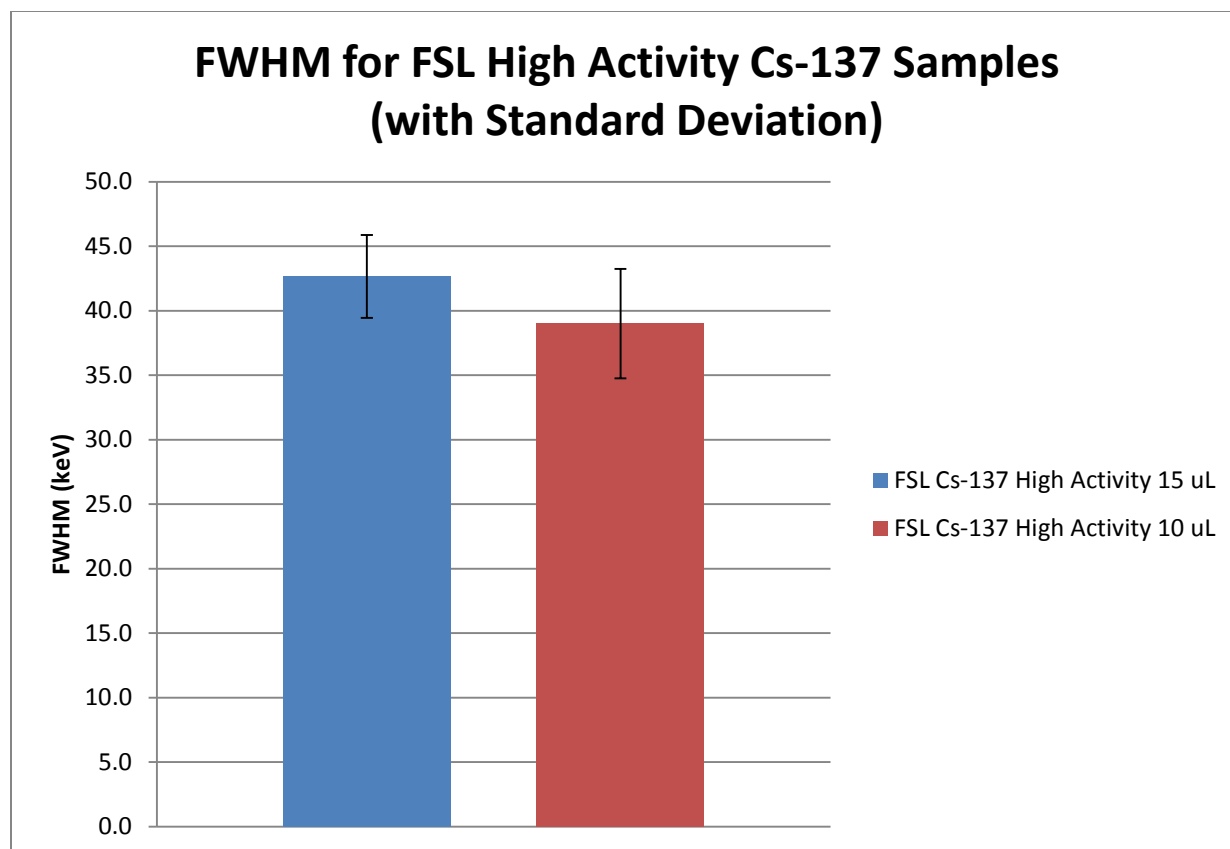


Figure 45 - FWHM for Millipore Fluoropore (FSL) filters treated with high activity Cs-137 solution. Error bars are indicative of the standard deviation for all three samples created for each filter set.

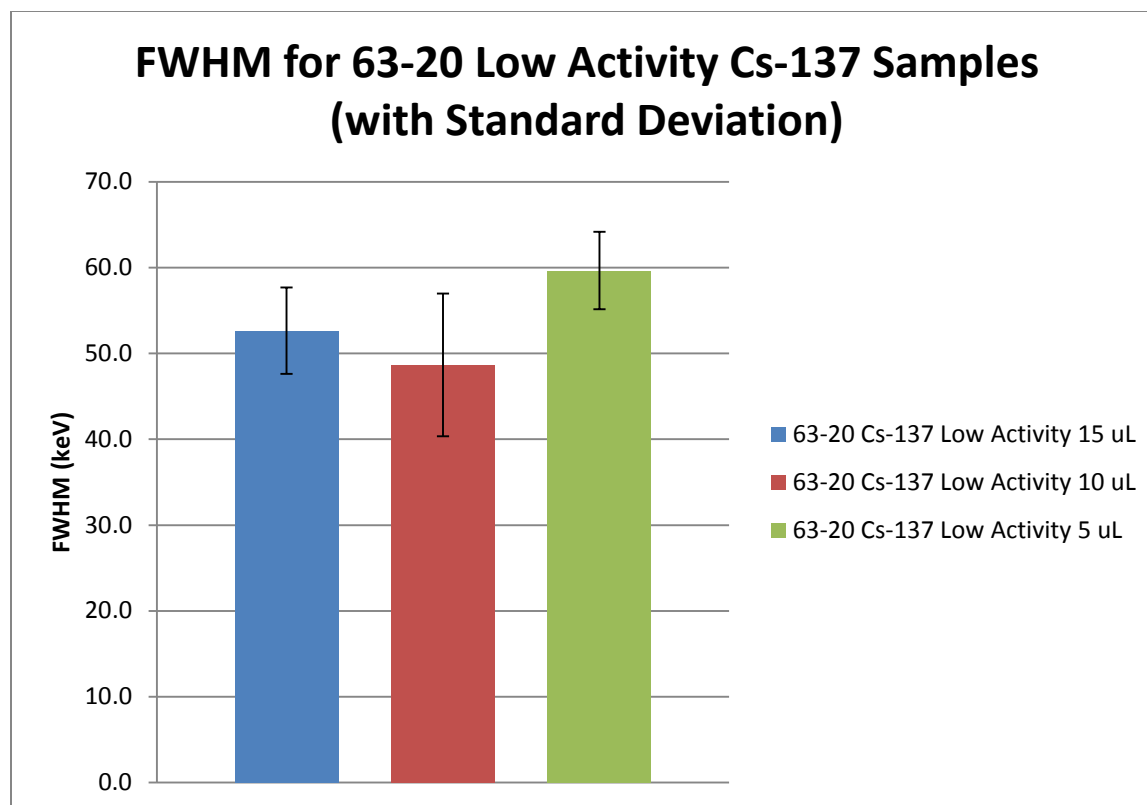


Figure 46 - FWHM for Hi-Q 2063-20 filters treated with low activity Cs-137 solution. Error bars are indicative of the standard deviation for all three samples created for each filter set.

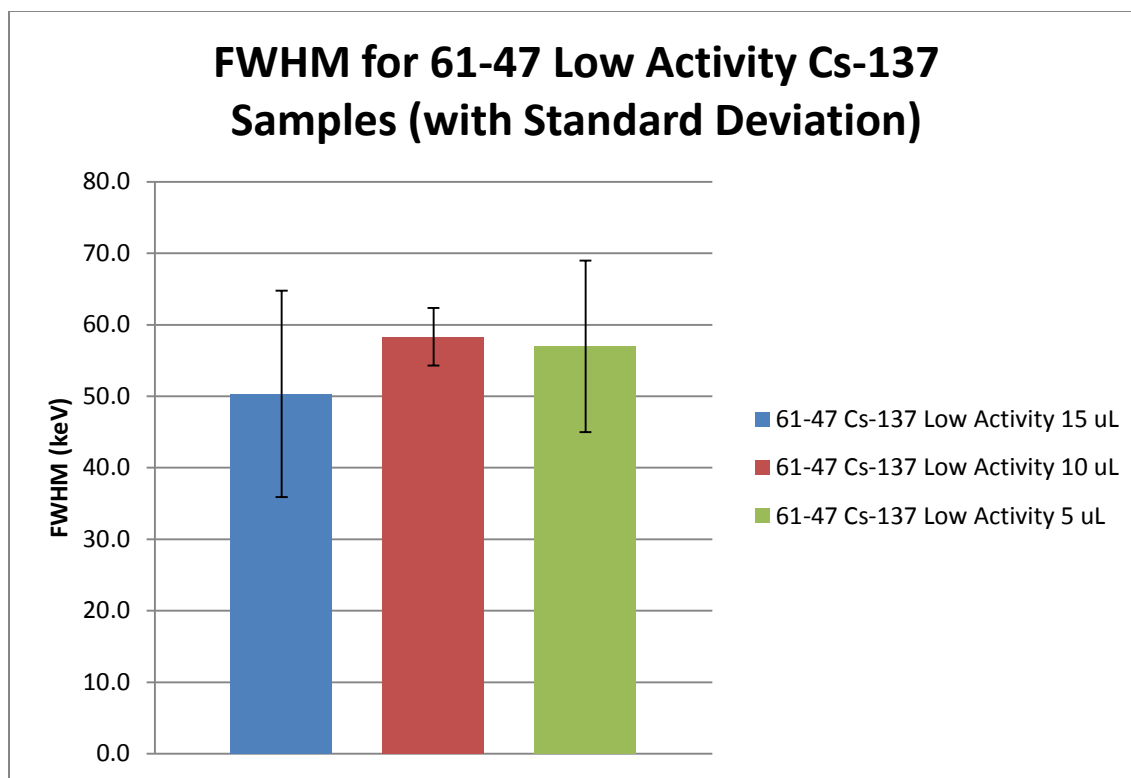


Figure 47 - FWHM for Hi-Q 2061-47 filters treated with low activity Cs-137 solution. Error bars are indicative of the standard deviation for all three samples created for each filter set.

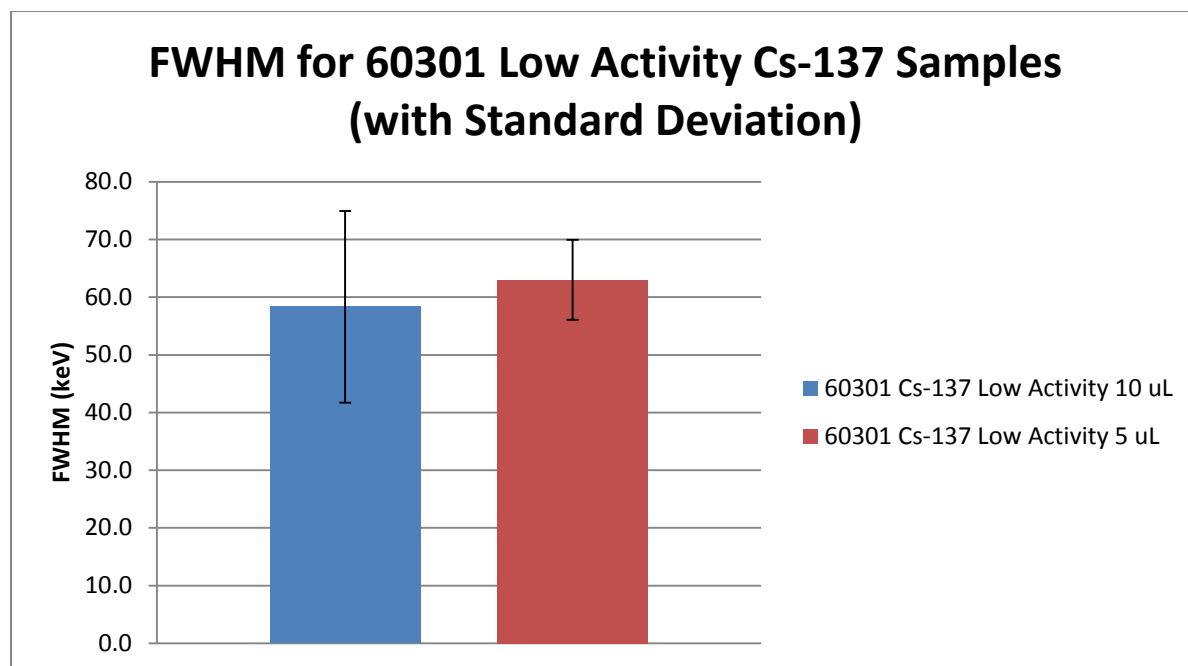


Figure 48 - FWHM for Pall 60301 filters treated with low activity Cs-137 solution. Error bars are indicative of the standard deviation for all three samples created for each filter set.

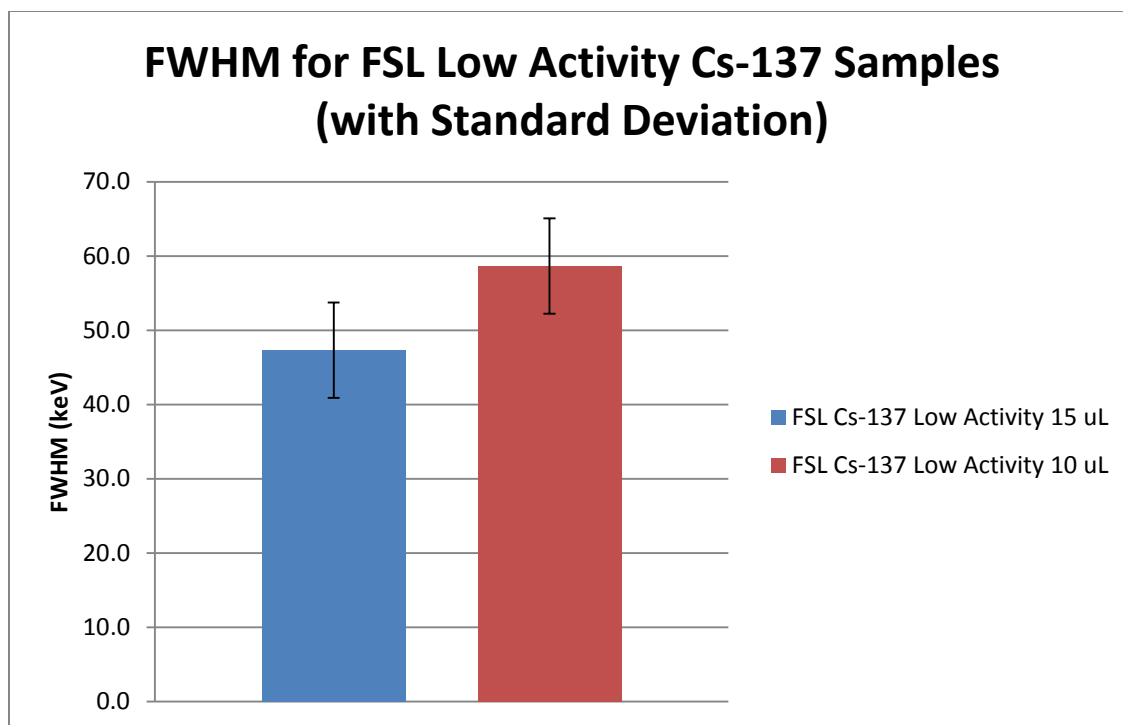


Figure 49 - FWHM for Millipore Fluoropore (FSL) filters treated with low activity Cs-137 solution. Error bars are indicative of the standard deviation for all three samples created for each filter set.

The final metric captured during the assessment of the Cs-137 treated samples was the measured activity for each sample. Each triplicate sample activity value was averaged, and the standard deviation for these values was calculated. These values were compared against the theoretical sample activity calculated based on stock solution concentration, number of droplets, and volume of solution contained in each droplet.

The glass fiber filters tended to perform well in terms of precision of measurement. The standard deviation around the mean of each triplicate sample tended to be smaller than the standard deviation calculated for the activities of the membrane filters. This could be indicative of higher evaporative loss or losses through the filter backing material during the pipetting procedure. The results of the glass fiber filter analysis can be found in Figure 50 through Figure 53. The results of the membrane filter analysis can be found in Figure 54 through Figure 57.

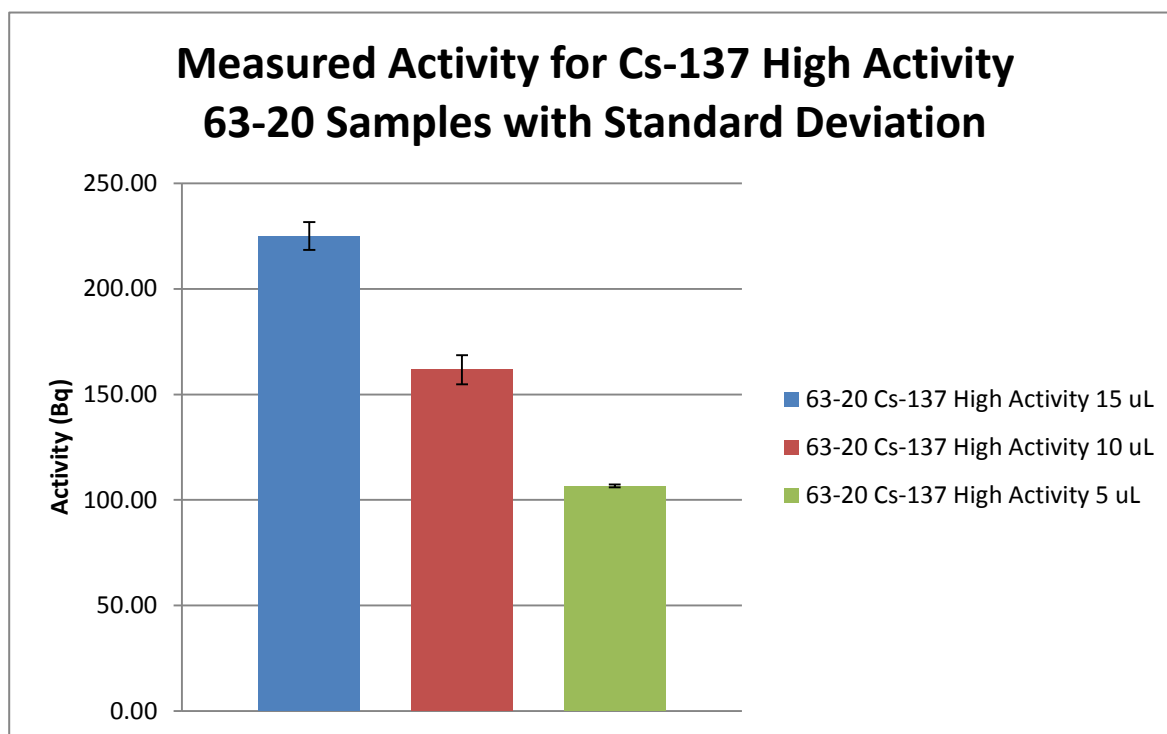


Figure 50 - Measured activity for Cs-137 high activity for Hi-Q 2063-20 samples with standard deviation

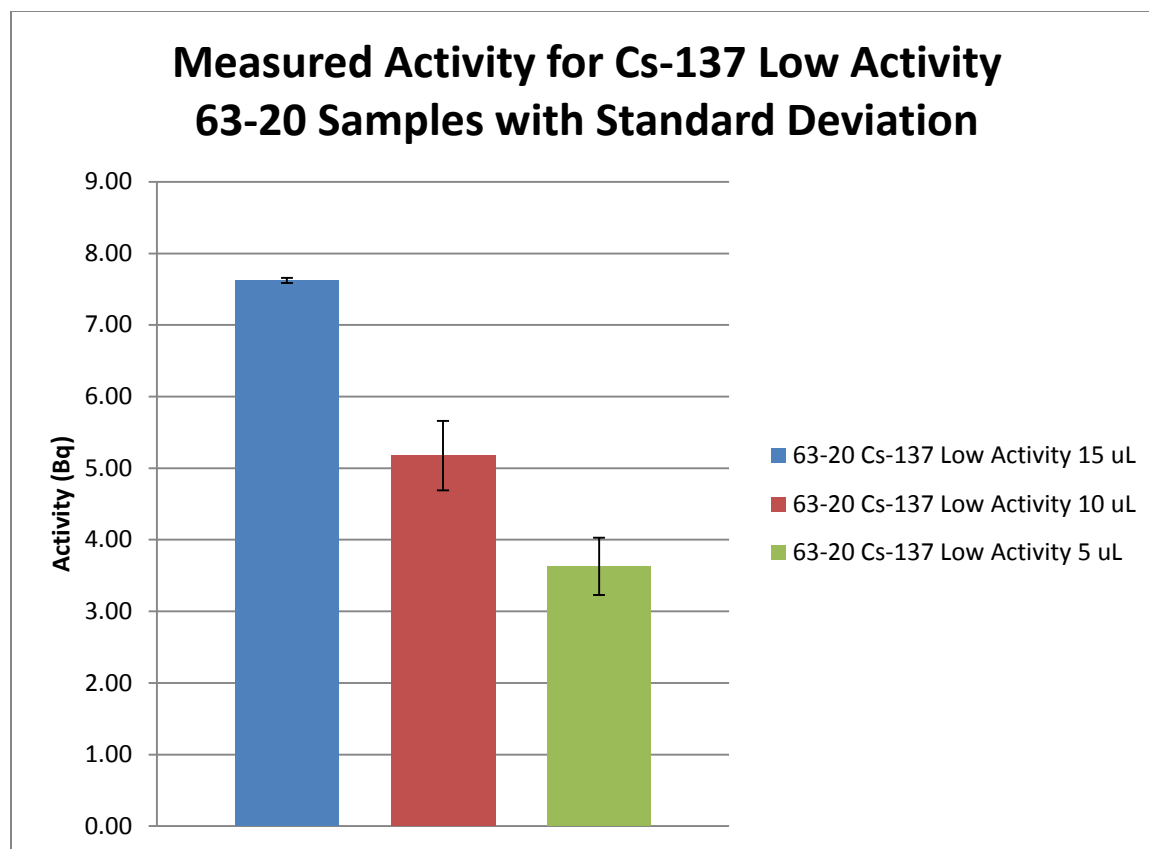


Figure 51 - Measured activity for Cs-137 low activity for Hi-Q 2063-20 samples with standard deviation

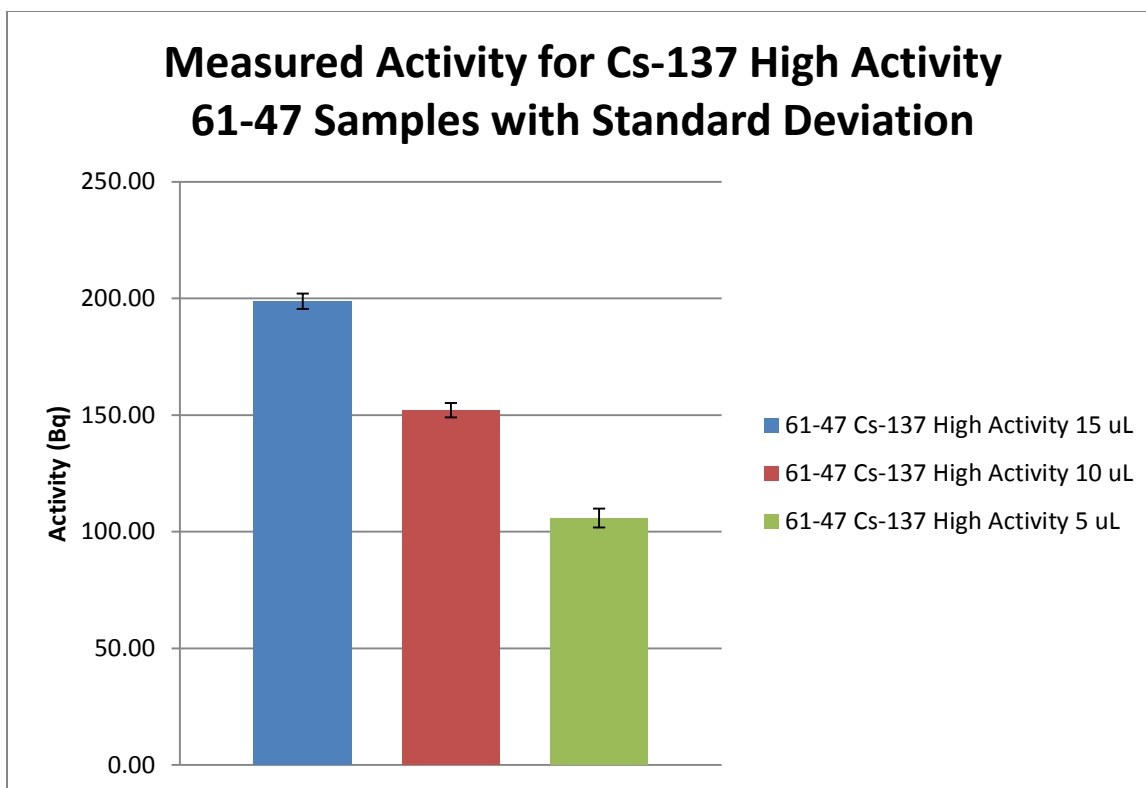


Figure 52 - Measured activity for Cs-137 high activity for Hi-Q 2061-47 samples with standard deviation

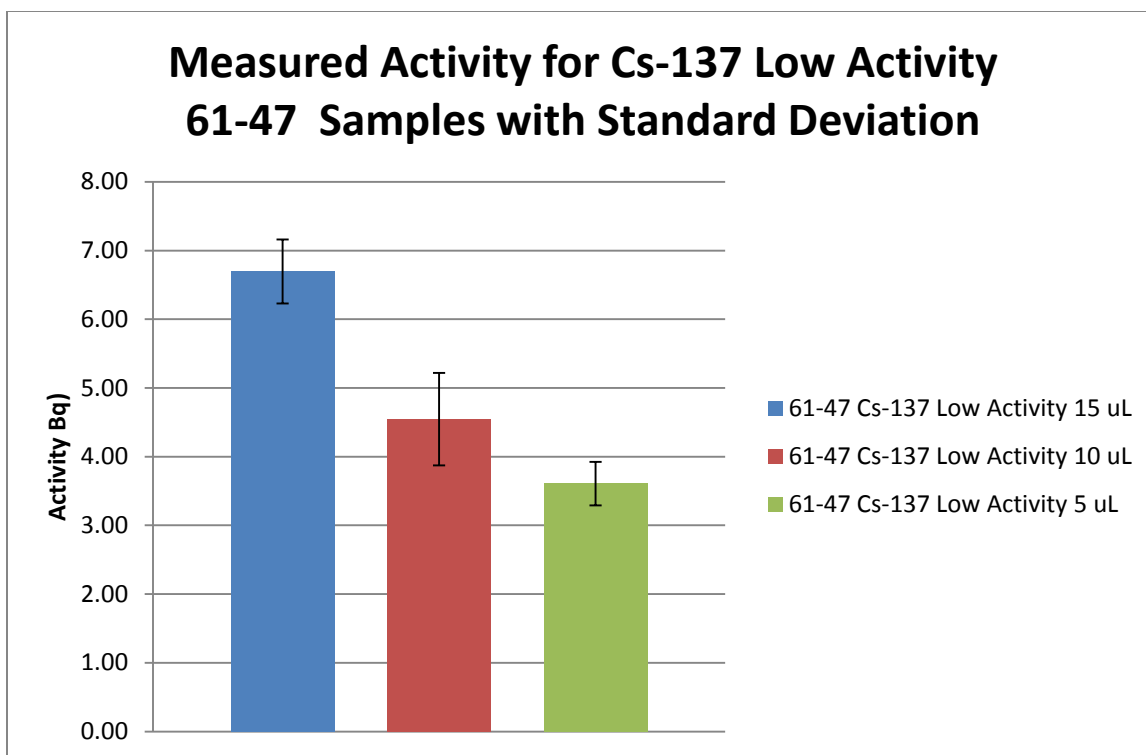


Figure 53 - Measured activity for Cs-137 low activity for Hi-Q 2061-47 samples with standard deviation

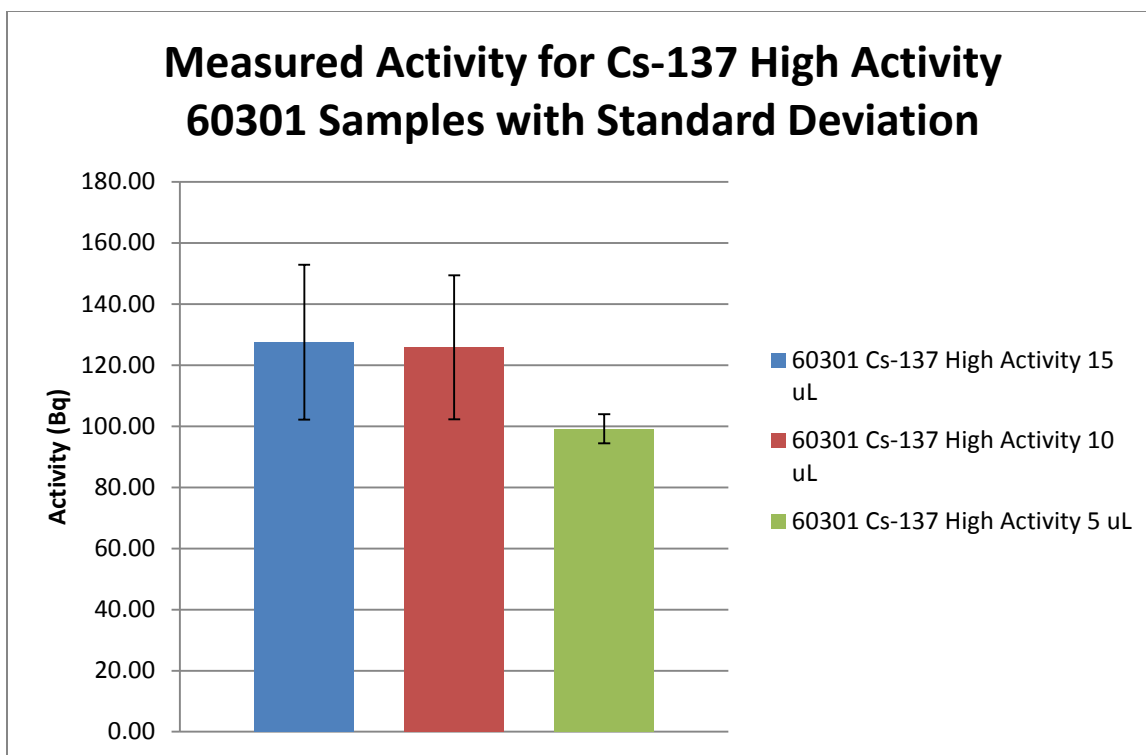


Figure 54- Measured activity for Cs-137 high activity for Pall 60301 samples with standard deviation

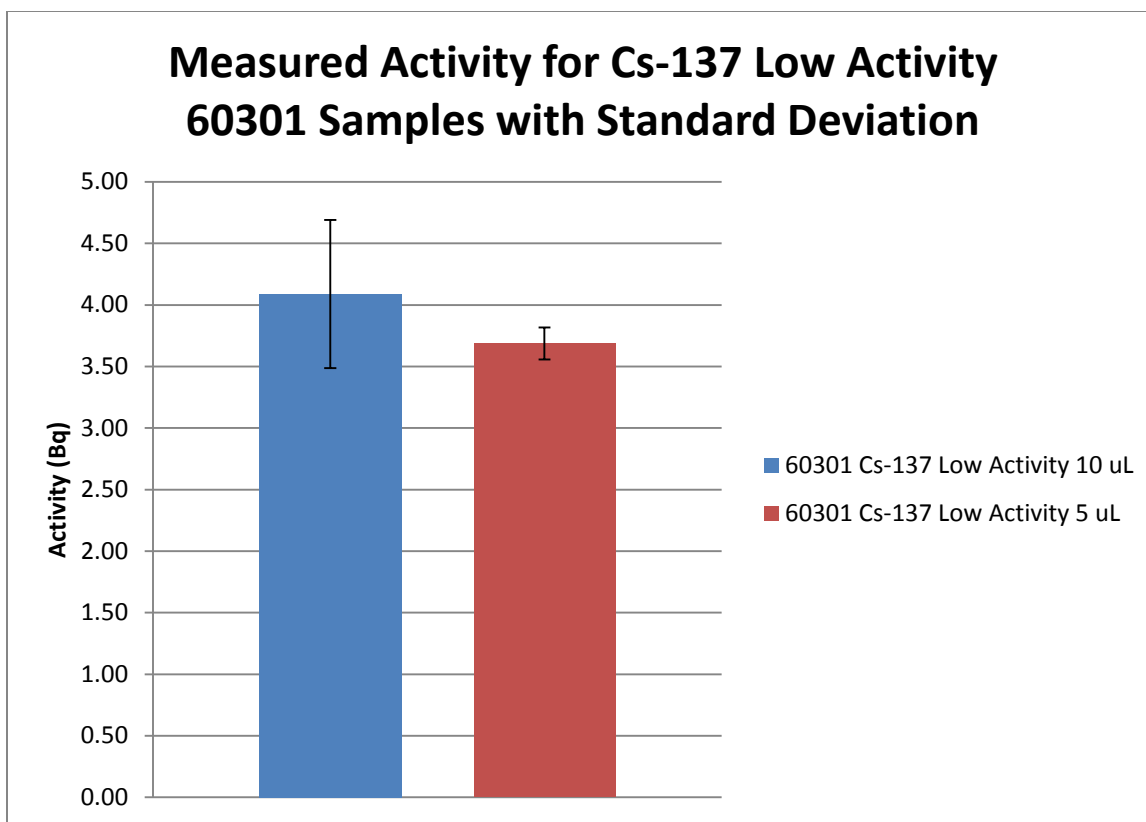


Figure 55- Measured activity for Cs-137 low activity for Pall 60301 samples with standard deviation

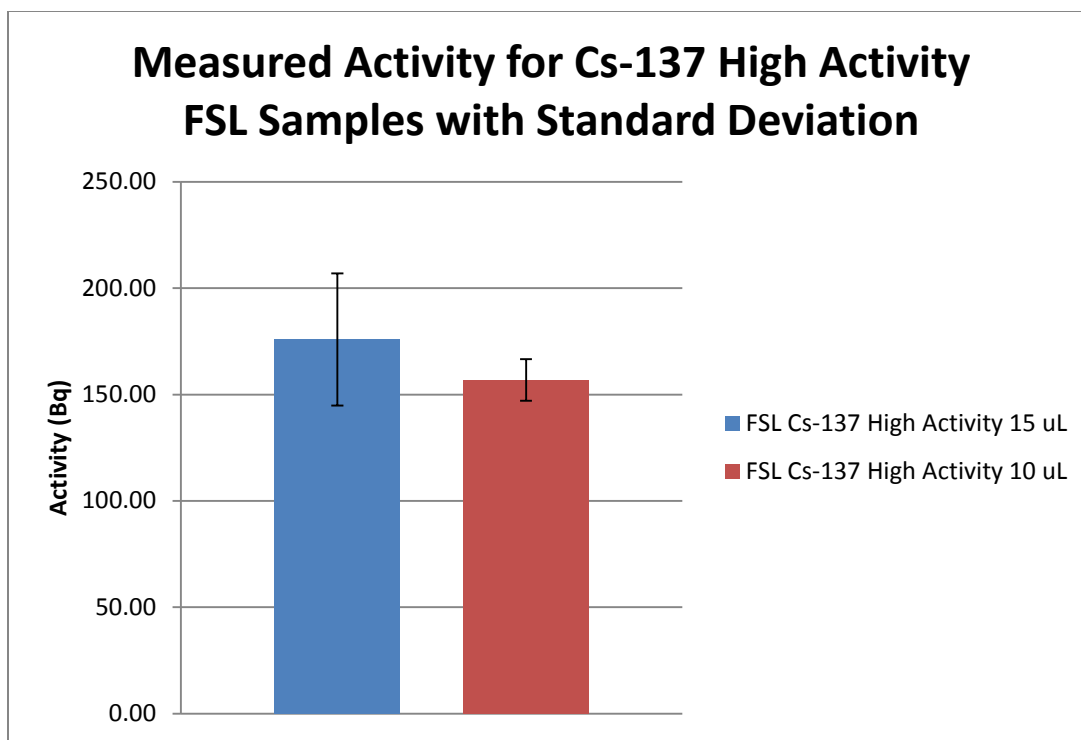


Figure 56- Measured activity for Cs-137 high activity for Millipore Fluoropore (FSL) samples with standard deviation

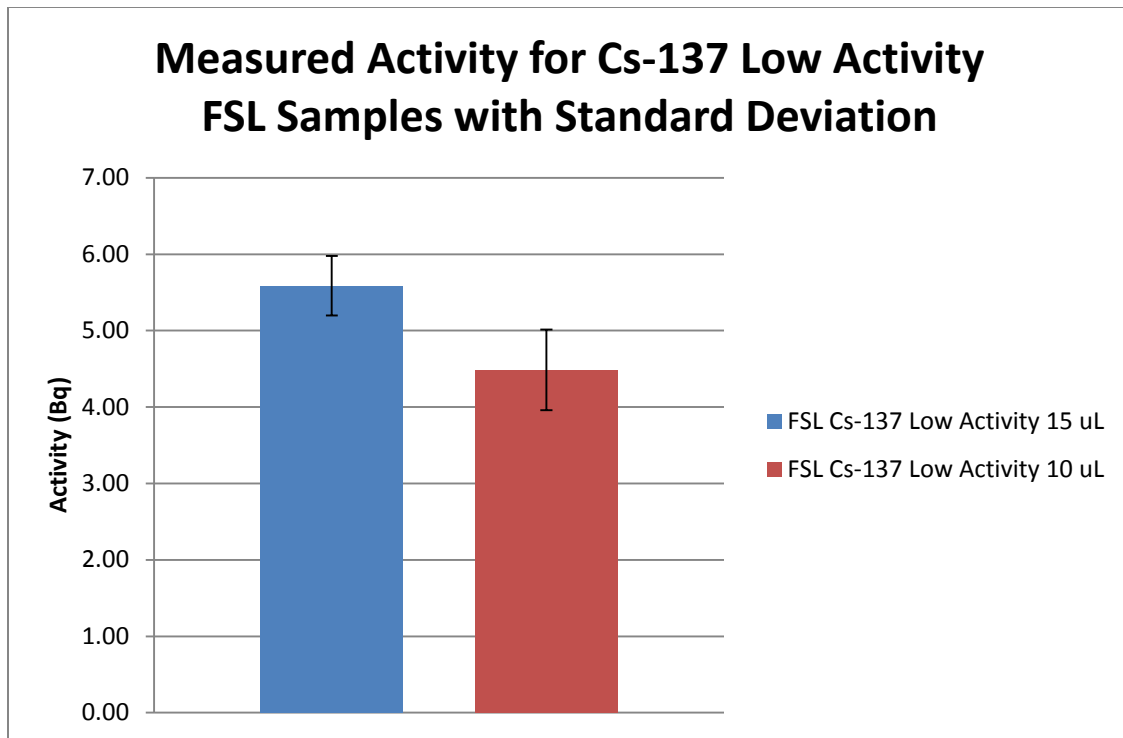


Figure 57 - Measured activity for Cs-137 low activity for Millipore Fluoropore (FSL) samples with standard deviation

When comparing the measured activity in samples created using high and low activity solutions, an interesting trend emerges. Figure 58 demonstrates percent difference between the mean for all of the samples sets created using the high activity solution and the expected or calculated activity. For these samples, the activity was under-recovered by between 24% and 63% from the expected activity based on the protocol used to generate the sample. For low activity samples, the opposite situation is found, see Figure 59. All samples report having more activity than what was expected with recovery gains ranging from 10% to 25%.

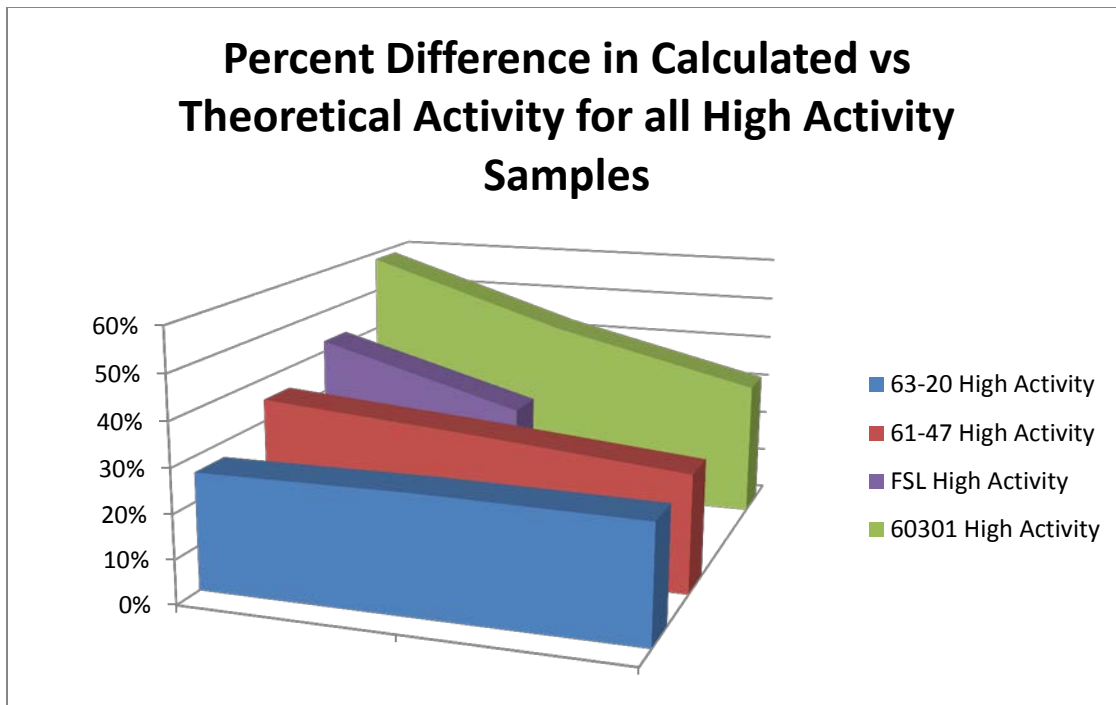


Figure 58 - The percent difference in the measured activity of all high activity samples versus their expected value.

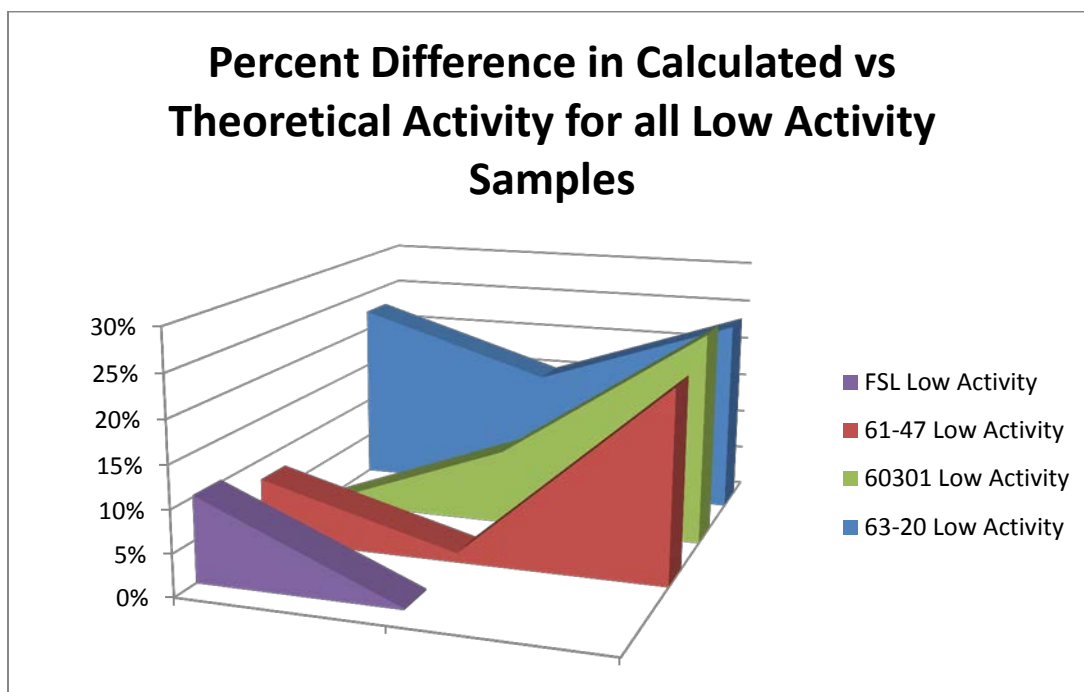


Figure 59 - The percent difference in the measured activity of all low activity samples versus their expected value.

Analysis of Strontium-90 Samples

The gas proportional counter software returned a series of results including counts per minute (cpm) for alpha and beta activity as well as the uncertainty associated with those counts. The net activity per second was calculated for each sample. The average of the replicates was taken as the mean, accepted value for each filter variable set (i.e. all Hi-Q 2063-20 filters treated with the high activity Sr-90 solution at 15 uL). The standard deviation for these values was also calculated. The theoretical value for the sample includes the count rate expected from Y-90 which would be in equilibrium with Sr-90 in solution. The figures below illustrate the results of this assessment.

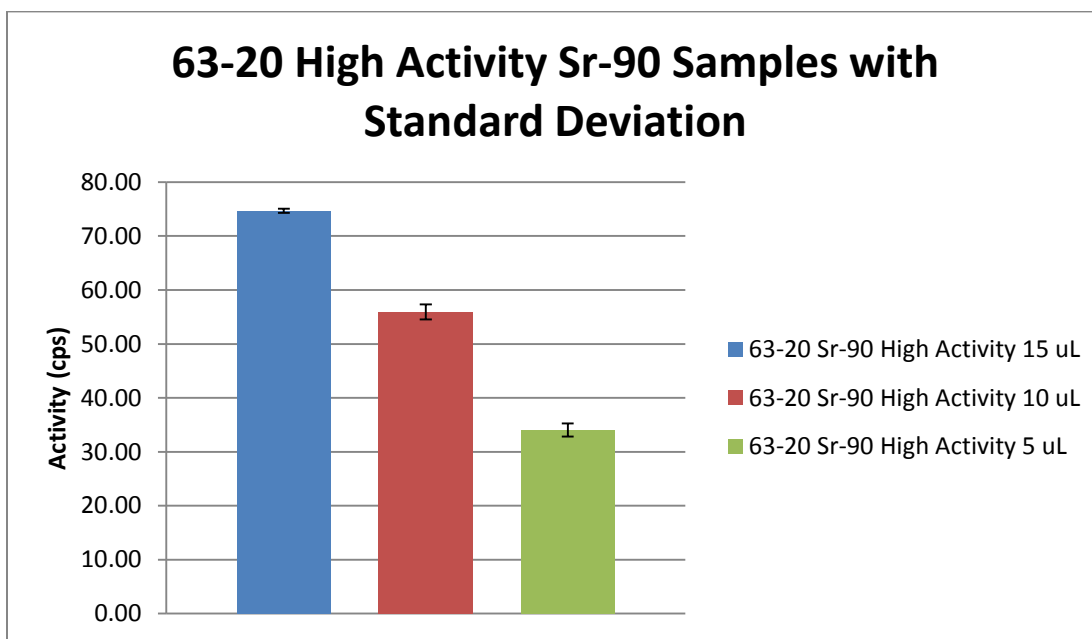


Figure 60 – Hi-Q 2063-20 High Activity Sr-90 Samples with Standard Deviation Calculated

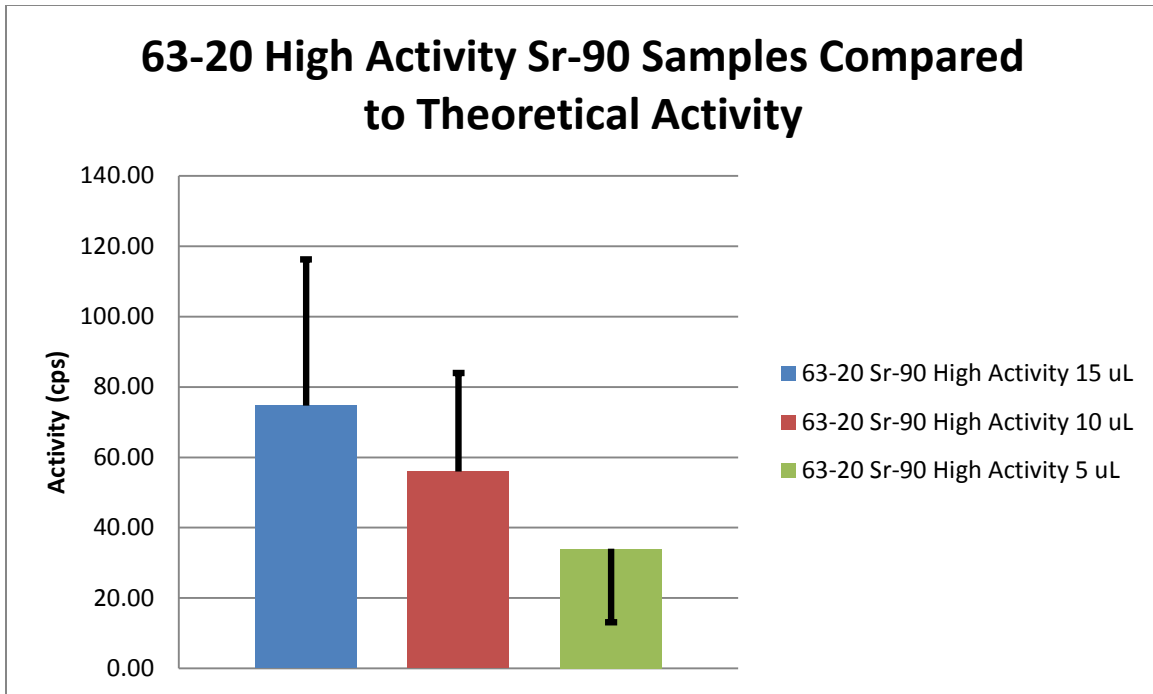


Figure 61 - Hi-Q 2063-20 High Activity Sr-90 Samples with Theoretical Activity

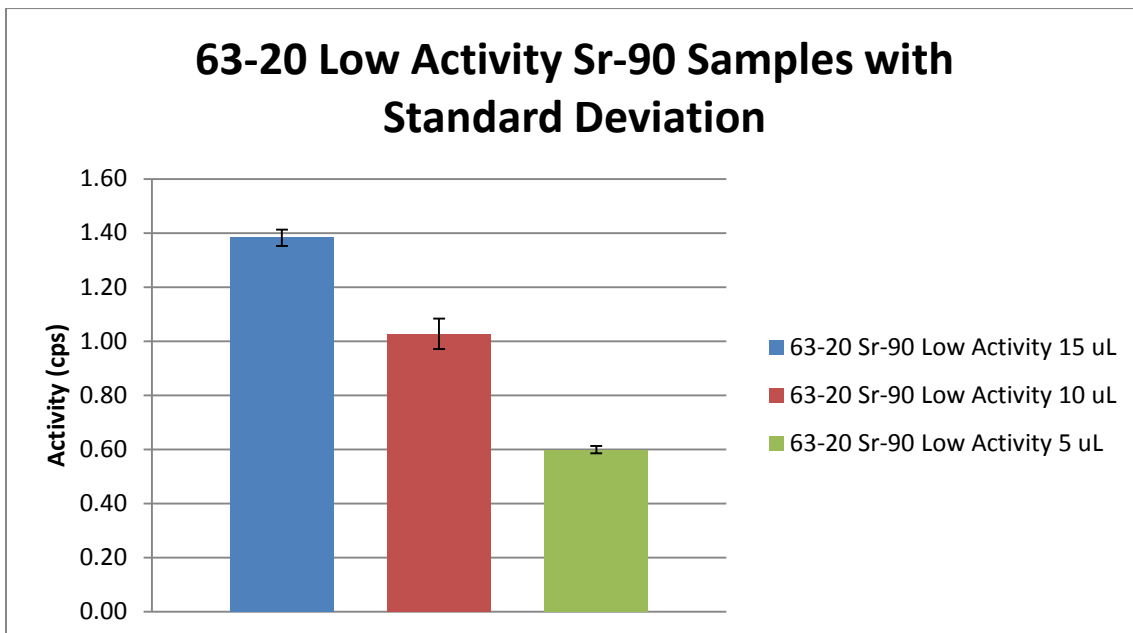


Figure 62 - Hi-Q 2063-20 Low Activity Sr-90 Samples with Standard Deviation Calculated

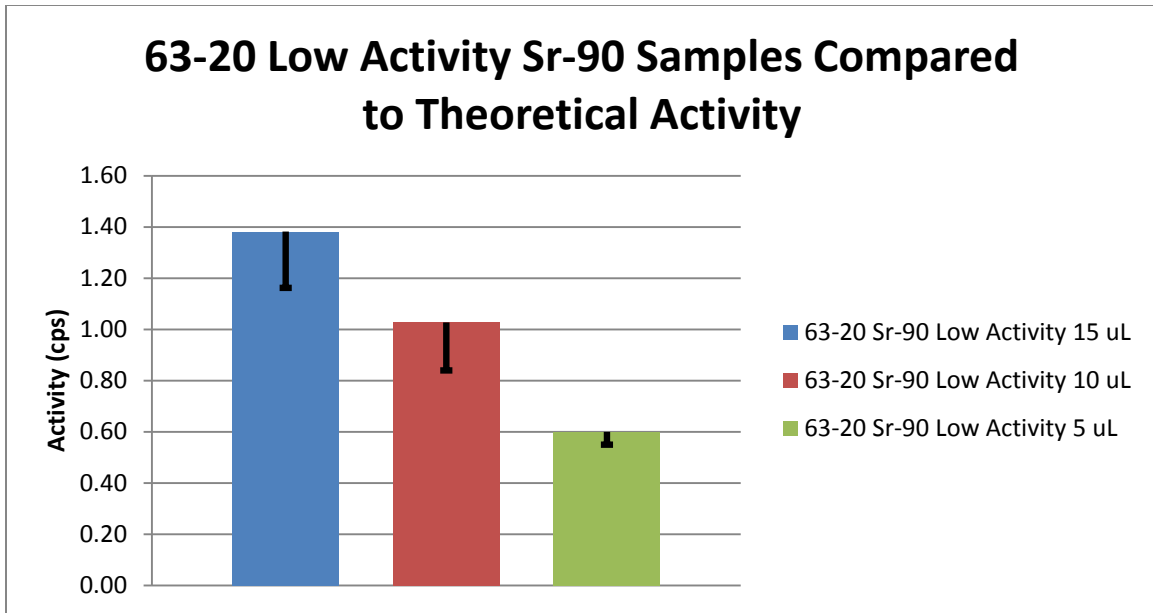


Figure 63 - Hi-Q 2063-20 Low Activity Sr-90 Samples with Theoretical Activity

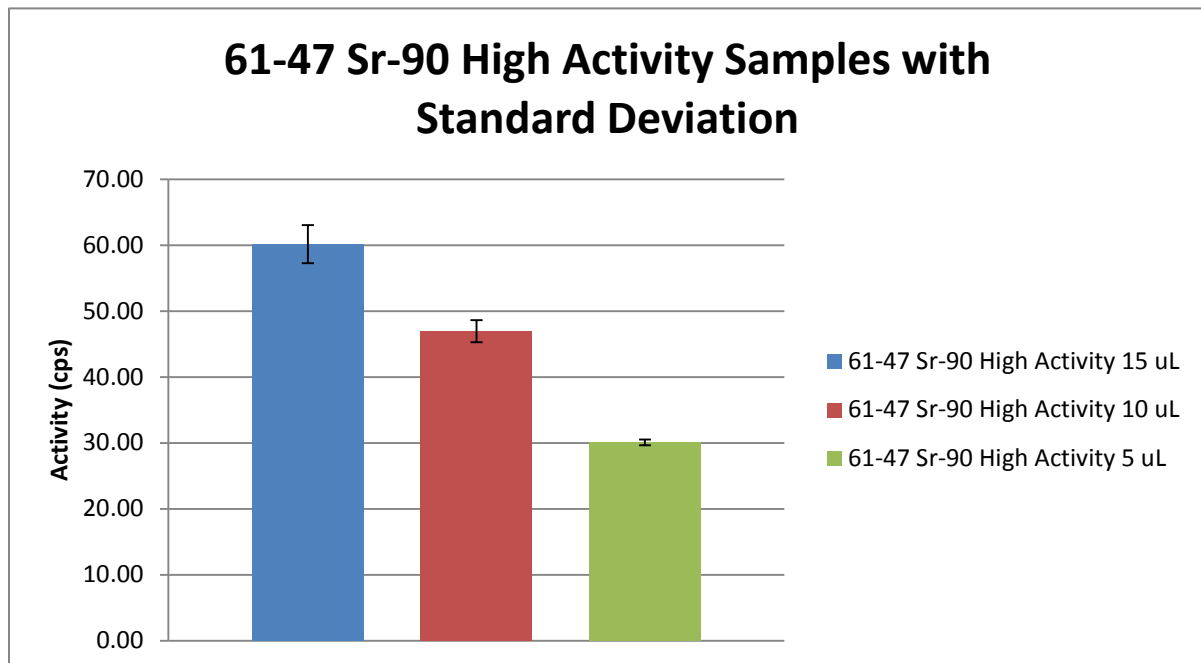


Figure 64 - Hi-Q 2061-47 Sr-90 High Activity Samples with Standard Deviation Calculated

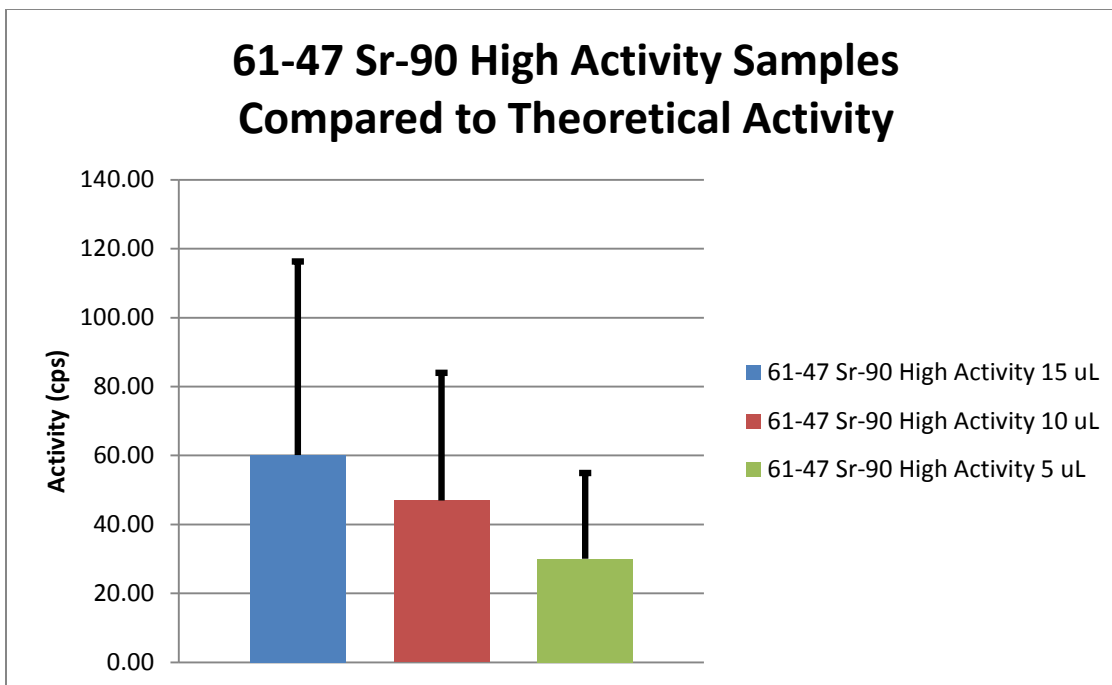


Figure 65 - Hi-Q 2061-47 Sr-90 High Activity Samples with Theoretical Activity

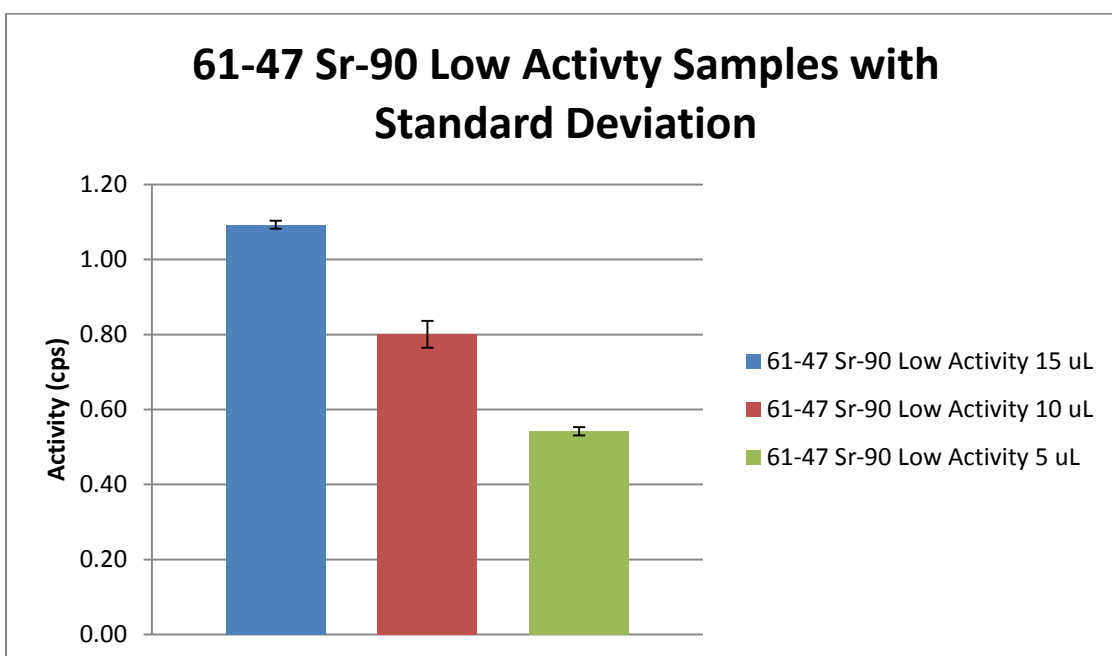


Figure 66 - Hi-Q 2061-47 Sr-90 Low Activity Samples with Standard Deviation Calculated

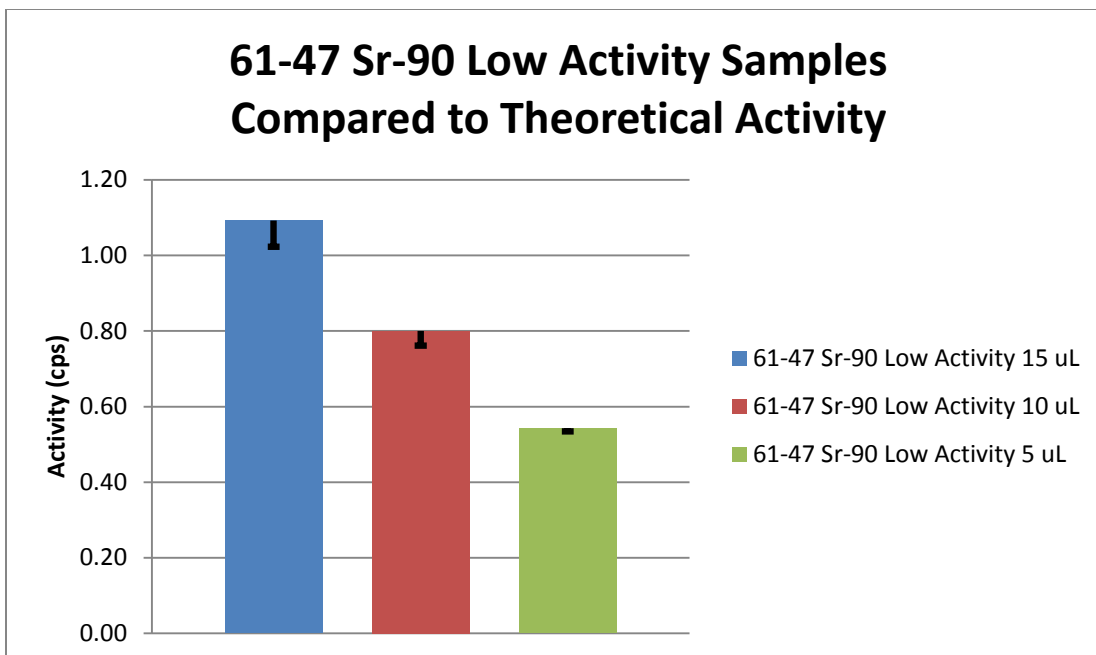


Figure 67 - Hi-Q 2061-47 Sr-90 Low Activity Samples with Theoretical Activity

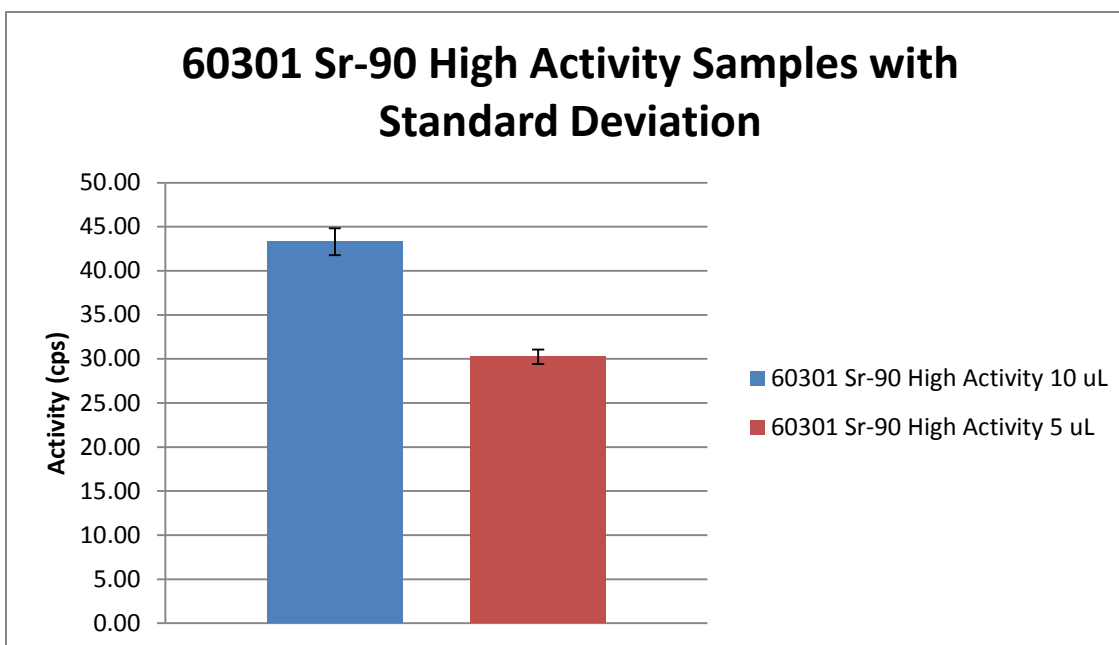


Figure 68 - Pall 60301 Sr-90 High Activity Samples with Standard Deviation Calculated

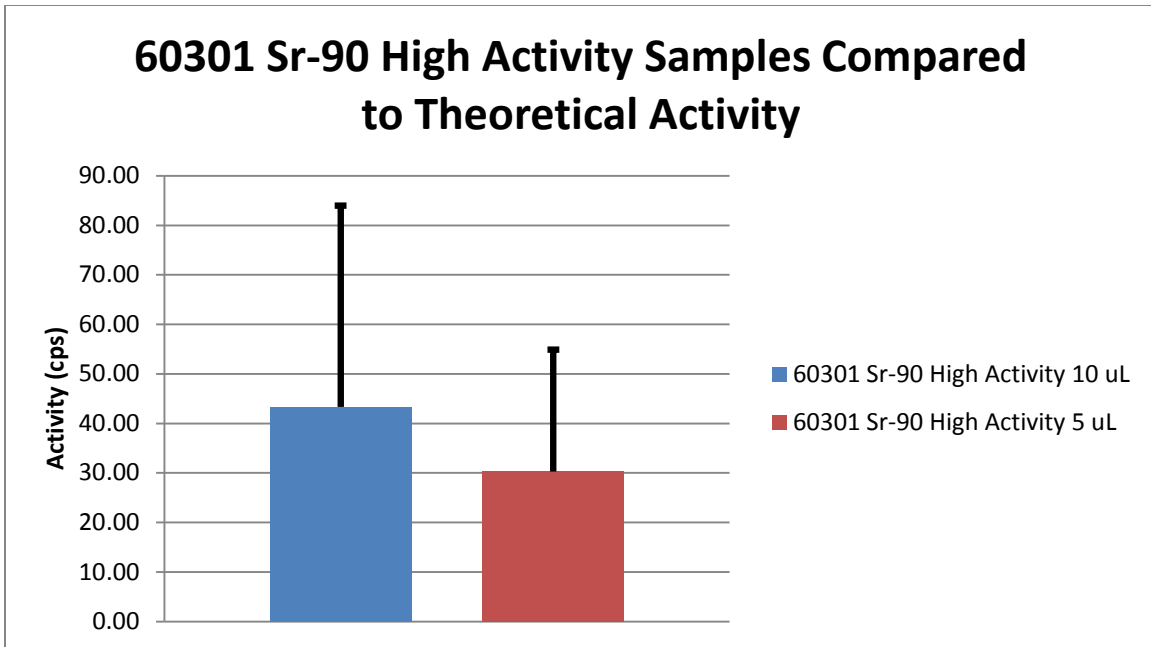


Figure 69 - Pall 60301 Sr-90 High Activity Samples with Theoretical Activity

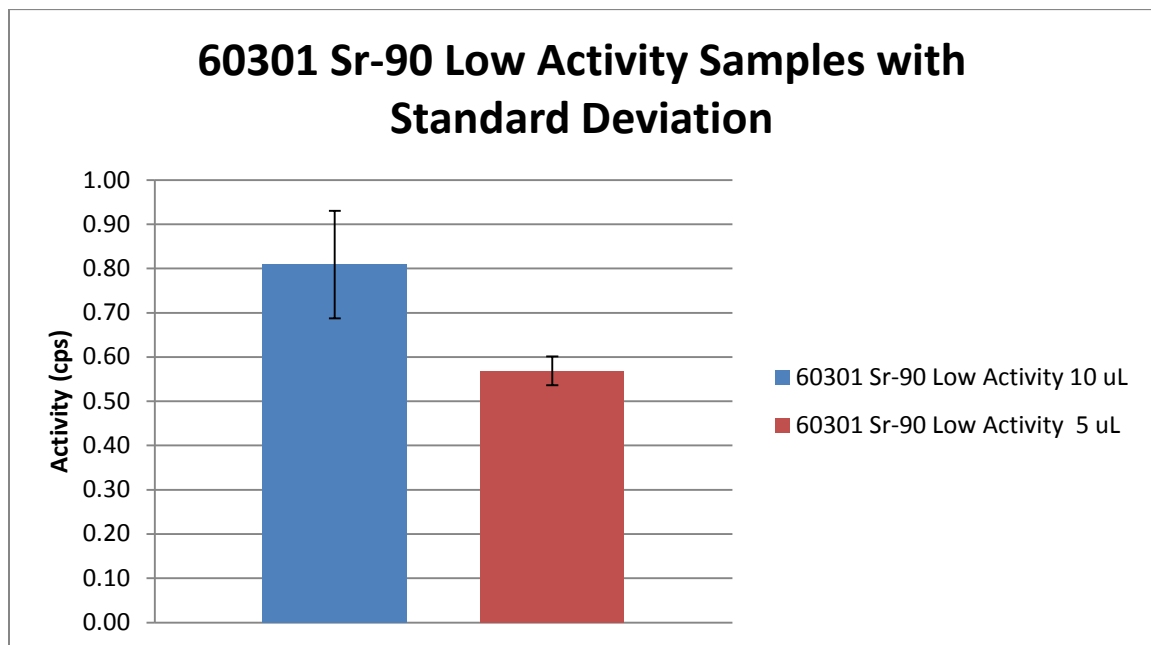


Figure 70 - Pall 60301 Sr-90 Low Activity Samples with Standard Deviation Calculated

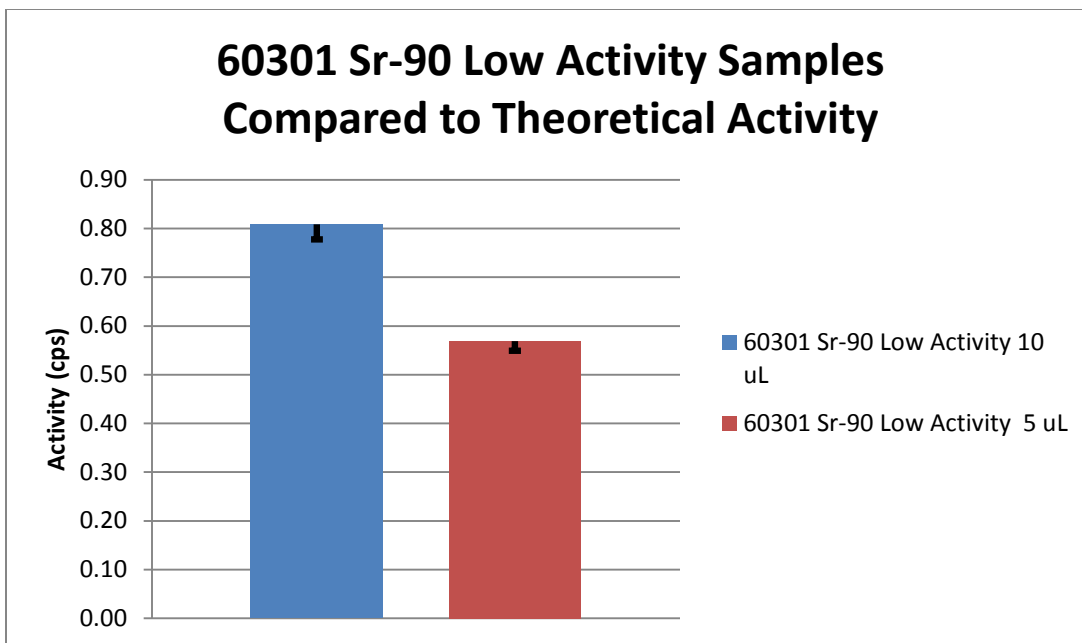


Figure 71 - Pall 60301 Sr-90 Low Activity Samples with Theoretical Activity

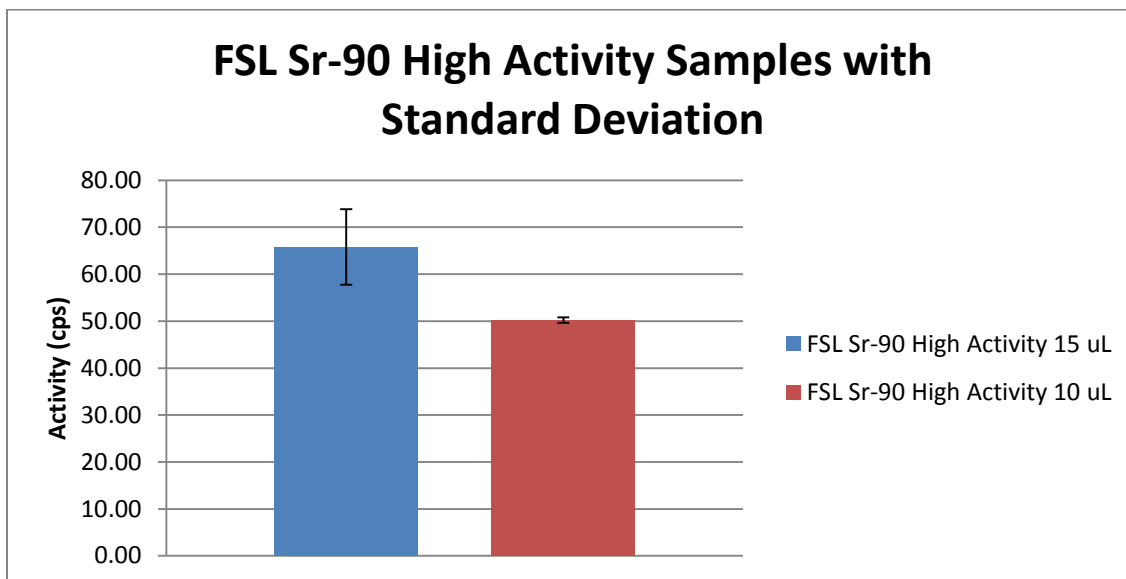


Figure 72 – Millipore Fluoropore Sr-90 High Activity Samples with Standard Deviation Calculated

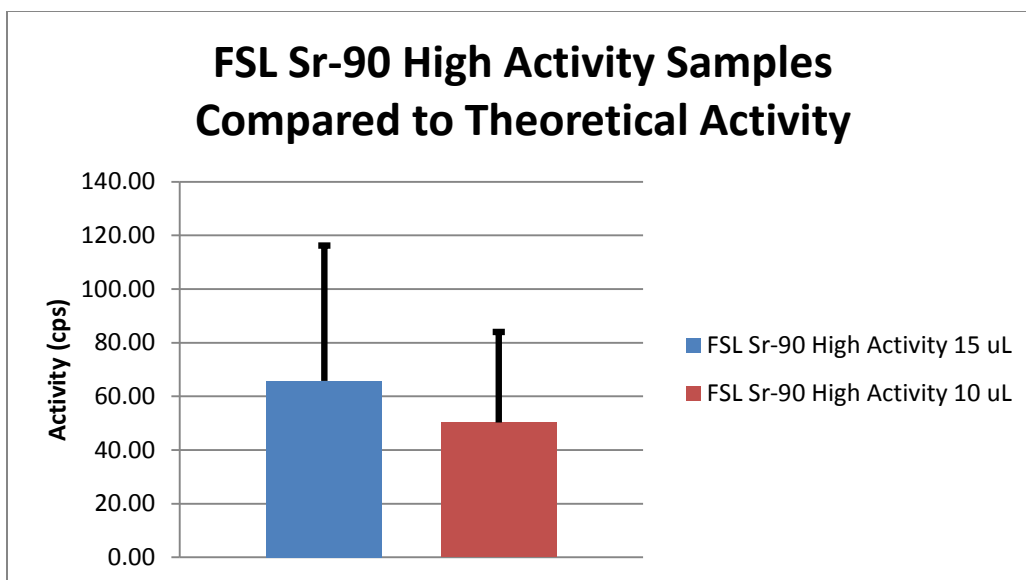


Figure 73 – Millipore Fluopore Sr-90 High Activity Samples with Theoretical Activity

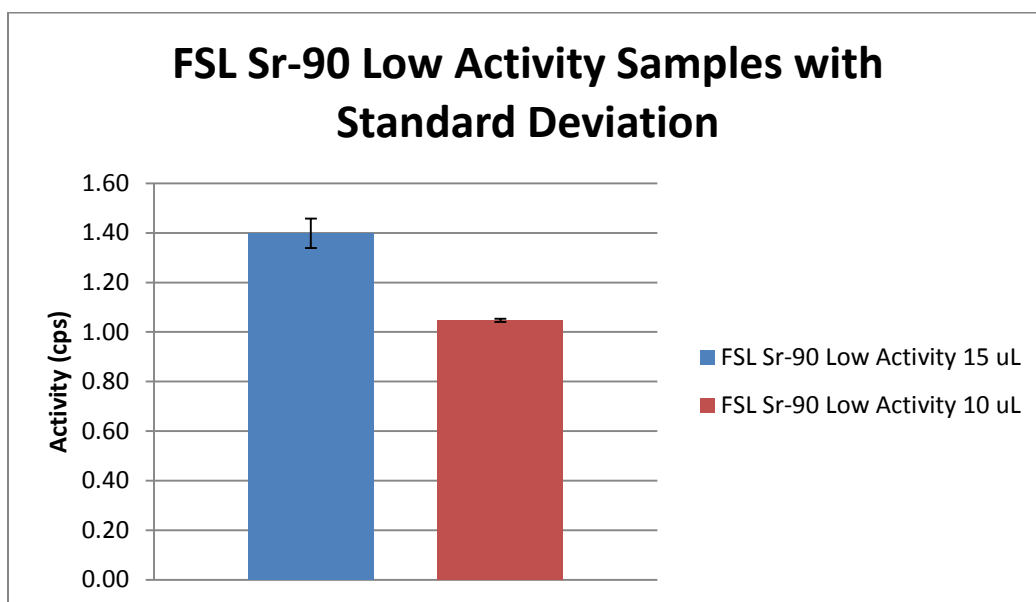


Figure 74 - Millipore Fluoropore Sr-90 Low Activity Samples with Standard Deviation Calculated

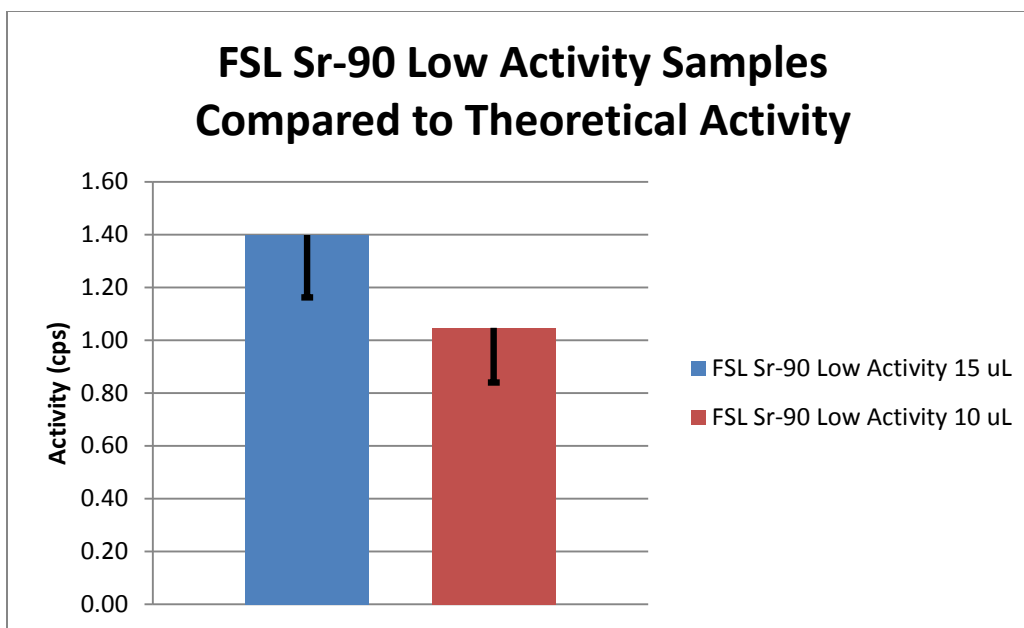


Figure 75 - Millipore Fluoropore Sr-90 Low Activity Samples with Theoretical Activity

In general, the measured activity of high activity samples tends to be less than the theoretical or calculated value based on the standard solution activity concentration, droplet volume and number of droplets. The percent difference ranged between 2.0% and 36.7% of the theoretical value. Interestingly, as the volume deposited into the filter decreased, the percent difference decreased as well. Therefore the greatest differences were in those filters treated with 15 μ L solution droplets. The glass fiber filters did not behave significantly differently, statistically, than membrane filters.

By comparison, the samples created using the low activity solution tended to yield count rates greater than the theoretical value. The percent difference of the measured value from the theoretical value ranged from 12.8% to 85.6%. In this case, as the volume of the droplets decreased, the percent difference increased. Therefore, the filters treated with

droplets of 5 μL of solution were least accurate. This trend was recognized across all filter types. There was no appreciable difference in this regard between the membrane filters and the glass fiber filters.

Discussion

The two parameters which seem to matter the most during this study were (1) the total of activity deposited on the filter and (2) whether alpha spectroscopy was to be performed. These two parameters had the strongest effect on the resulting data. It goes without saying that whenever possible (within reason) one should choose the strongest source possible for best statistics. The activity used in the high activity samples are a reasonable starting place. It is not suggested that calibration sources contain less than 1 Bq as was used in the filters in this study. As noted in in Section 4.3 “Am-241 Analysis”, analyzing filters by alpha spectroscopy may not be sufficient, especially when the medium is not a thin membrane filter. For glass fiber or cellulose filters a large source of error and uncertainty is introduced by burial effects and losses as deposited material migrates deep into the fibers. Additionally, it is important to consider counting geometry when choosing a filter to detector setup. Filters should be smaller than the active area of the detector. This will allow a greater fraction of the activity to be counted during an analysis. In this experiment, the filters were larger than the active area of the detector and therefore, a collection efficiency for this geometry was obtained from literature.

Overall, samples treated with Sr-90 and Cs-137 did not vary significantly from what was expected in terms of measured activity, resolution and FWHM when taking error and uncertainty of the measurement into account. Samples treated with an alpha emitter should,

in the field, be considered for rough assessment via scalar counts or alpha spectroscopy. Final analysis should involve the dissolution of the filter and other analyses which require wet chemistry.

In terms of ruggedness and usefulness of a filter, the glass fiber filters performed the best. These filters withstood a fair amount of handling, including the use of double sided tape without destruction. Solutions do not tend to bleed through these filters easily, which is important not only for contamination control but also to ensure that all of the calculated materials remain in the filter and thereby reducing another potential source of error (i.e. loss of sample). However, when attempting to create a standard that has minimal material attenuation and a tendency to hold material in the place it is set, membrane filters are the best fit. It is suggested that tape not be used if the filters are to be mounted to some surface for analysis, especially for filters such as the Pall 60301 filters. These filters tended to crumble easily.

Chapter 5 Error Sources

Systematic Errors

In procedures carried out by others, when the radioactive materials are deposited by pipetting, it is accomplished using mechanized tools ((IAEA), (Ceccatelli, De Felice and Fazio), and (McFarland)). These tools reduce errors introduced by inconsistent pressure applied to the pipette plunger and location where the droplets are placed. In this procedure, an attempt was made minimize placement errors by using a jig to pipette a reproducible pattern of droplets. However, this does not remove all uncertainty in droplet location. First, the pipette tips are slightly smaller than the holes drilled into the jig (approximately 0.05 mm) to allow the tip to move in and out of the holes easily.

Second, the behavior of filter media varies in the presence of water. As noted during the process with colored dye, glass fiber filters simply allow the liquid to bead and then absorb it. Membrane filters such as the Pall 60301 filters immediately disperse the materials in all directions. Other membrane filters such as the Millipore Fluoropore filters react to moisture by curling up forming a concave shape similar to Pringles crisps while the droplets slide across the surface. This may be overcome by mounting the filters to the work surface using double sided tape, carefully securing the edges. However, the surface of this filter was so smooth that even when secured to a surface the droplets moved about freely as they were released from the pipette. Therefore, these droplets had a tendency to roll out of place and into one another, forming larger droplets or sliding off the filter entirely. Although much care was taken to

ensure each filter had 19 droplets, some residual material may have remained on the surface from previous droplets which had rolled off.

The intrinsic error of the pipette quoted by the manufacturer (VWR International) could introduce an error of 0.6 – 1.0% in accuracy and 0.3 – 1.5% in precision when using the 2-20 μL pipettor. This error could result in activity losses (or gains) of up to 0.5 Bq/filter. Furthermore, most of the liquid standards used to produce the filters were created using these pipettors. In fact, only the low activity Am-241 solution was used as prepared. After performing an assessment of the pipettor directly it was found to over-dispense liquid in each of the volume settings used for this work. On average the 15 μL setting released 18 μL , the 10 μL setting release 13 μL , and the 5 μL setting released 8.5 μL . Therefore, all theoretical calculations were adjusted to reflect this change.

The stock solutions used in this work were not certified by an outside source and could, therefore, have significant uncertainty associated with their activity. One could gain a reasonable estimate of the solution error by consulting vendor product catalogs of radionuclide solutions. The Eckert & Zeigler product catalog, for example, provides two types of solutions; those whose activity is certified by the National Institute of Standards and Technology (NIST) to be accurate within 3 – 5% of the stated value and those with nominal activity of $\pm 15\%$ of the stated value. No NIST certificate was available for any of the stock solutions used therefore it is reasonable to err toward the high uncertainty value of $\pm 15\%$ error introduced by the standard solution.

Breakthrough losses could be another source of error. The place to best study this is to consider the Fluoropore filters treated with Cs-137; given that the filters were created from

within a planchet and the counting efficiency of the NaI(Tl) detector used. The filters were counted alone, inside of the petri dish. The planchet was then counted separately. A representative spectrum is below, Figure 76 is the spectrum of a low activity/high volume (1.7 Bq/ml of Cs-137 standard in 15 μ L droplets for 0.48 Bq) filter. Note that there is no net activity from Cs-137 in the spectrum.

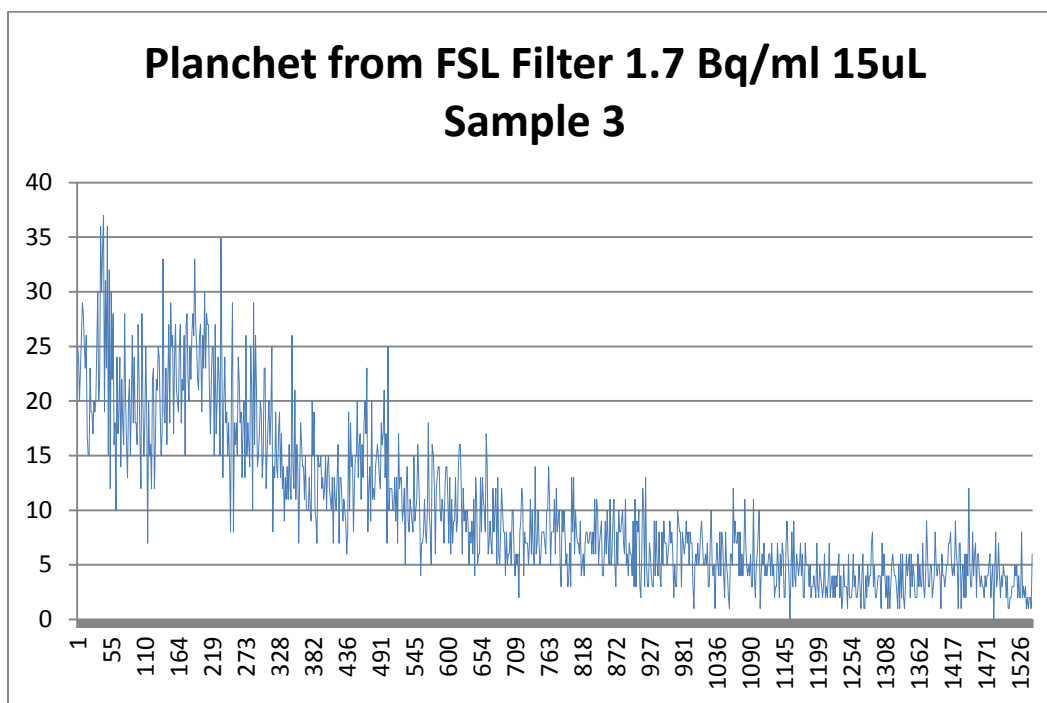


Figure 76 - Spectrum of planchet used to mount a FSL low activity filter treated with Cs-137.

Other Errors

Other errors introduced into the study are human errors. Creating the stock solutions required a fair amount of manipulation of materials (use of graduated cylinders, pipettors, and transfer solutions) which all present opportunities for making an error. Furthermore, over the course of this study over 200 filters were created with varying amounts of liquid upon each.

This provided a minimum of 3,800 chances of depressing the pipettor plunger too hard (or too soft), not placing the pipette tip completely in fluid, etc. Lastly, analyzing over 120 spectra by hand can lend itself to some transcription errors. This was mitigated by several checks built into the numerous spreadsheets created to manage these data. Though the data have been validated, there are a sizeable number of variables and values which must be tracked and managed which means there will inevitably be some remaining errors.

Chapter 6 Conclusion

Air filter analysis is incredibly complex and vulnerable to the effects of environmental factors. Reducing the error and uncertainty in one part of the process, such as the calibration of the counting system using filter standards, can greatly impact the downrange effects on calculations related to public and worker safety.

Overall, the process of creating of filter standards is challenging. The precision required to create a reliable standard compels the processor to apply tight controls of the process from standard solutions to storage. Wherever possible, the processor should standardize and mechanize the application of standard solution to the filters. Furthermore, the standard solution used should be certified to reduce errors.

However, even when the process is well controlled, a filter created in a laboratory may not well approximate a filter collected in the field. It is challenging to replicate the effects of dust loading and the impaction of radiative materials into the filter media. Users of the standard must take this into account when analyzing.

The particular challenging situation is creating standards for alpha emitting radionuclides. While standards for gamma and beta emitters may easily be covered by mylar to protect it from loss and cross contamination, this is not effective for alpha emitters. Aside from protecting from physical loss of materials, loss may occur due to burial in the filter media.

Chapter 7 Future Work

There are a number of items which could be explored should it be desired to continue this work. First, future work should focus on removing sources of error or quantifying/anticipating error. One place to begin in this process is to simply purchase NIST certified liquid standards. Repeating this experiment using a certified source could remove as much as 10% of the error in the calculated activity value. Another option is to remove the possibility of mechanical and human error involved in the pipetting process. Future work could take advantage of available automated systems used to pipette liquids in large batches. Last, to further reduce error or uncertainty the samples could be created in replicate sets of at least five filters. In some cases, especially when analyzing low activity Am-241 samples, the statistics are poor with only three samples to use determine averages and standard deviation.

Future work could focus on performing this study using other counting techniques and tools such as High Purity Germanium detectors or scalars. One may also choose to analyze different types of air filters. Once the variables are well characterized and controlled for, environmental factors present during real sampling may be simulated. Effects of dust loading or precipitation, for example could also be studied with these filter standards creating a new type of standard – one that is based on the environment, instrumentation, and type of radionuclide.

Bibliography

- Burnett, Bill and Larry Burchfield. "Sample Preparation for Alpha Spectroscopy." n.d. Canberra. 10 October 2010 <<http://www.canberra.com/literature/954.asp>>.
- Cabot, George. Health Physics Society. 13 June 2005. 10 October 2010 <<http://www.hps.org/publicinformation/ate/q4547.html>>.
- Ceccatelli, A., P. De Felice and A. Fazio. "Development of Simulated Air Filters for Gamma-Ray Spectrometry Proficiency Testing." Applied Radiation and Isotopes (2010): 1240-1246.
- Hoover, Mark D. "Filtration." Maiello, Mark L. and Mark D. Hoover. Radioactive Air Sampling Methods. Boca Raton: CRC Press, 2011. 157-181.
- IAEA, International Atomic Energy Agency. ALMERA Proficiency Test: Determination of Gamma Emitting Radionuclides in Simulated Air Filters IAEA-CU-2009-04. Technical Summary Report. Vienna: International Atomic Energy Agency, 2010.
- Kelly, Lyndsey Renee. Optimization of the Microprecipitation Procedure for Nuclear Forensics Applications. Master's Thesis. Las Vegas: Univeristy of Nevada, Las Vegas, 2009.
- Knoll, Glenn F. Radiation Detection and Measurement. Hoboken: John Wiley & Sons, Inc., 2000.
- Marlette, Guy. "Handbook for the Department of Energy's Mixed Analyte Performance Evaluation Program (MAPEP)." 28 August 2010. Mixed Analyte Performance Evaluation Program (MAPEP). 13 August 2010 <<http://www.inl.gov/resl/mapep/>>.
- McFarland, Robert C. "Geometric Considerations in the Calibration of Germanium Detectors for Filter-Paper Counting." Radioactivity & Radiochemistry 2.1 (1991): 55 - 59.
- Mishima, Jofu and David Pinkston. Airborne Release Fractions/Rates and Respirable Fractions for Nonreactor Nuclear Facilities. Handbook. Washington DC: The United States Department of Energy, 1994.
- O'Haver, Tom. A Pragmatic Introduction to Signal Processing - Smoothing. 9 April 2015. March 2015 <<http://terpconnect.umd.edu/~toh/spectrum/Smoothing.html>>.
- Shaw, P.G. "Rapid Determination of Pu Content on Filters and Smears Using Alpha Liquid Scintillation." Ross, Harley, John E. Noakes and Jim D. Spaulding. Liquid Scintillation Counting and Organic Scintillators. Chelsea: Lewis Publishers, Inc., 1991. 729.
- VWR International. VWR Signature(TM) Ergonomic High Performance Single-Channel Variable Volume Pipettors. 2015. 18 April 2015 <us.vwr.com/store/catalog/product.jsp?product_id=4698601>.

Curriculum Vitae

Graduate College
University of Nevada, Las Vegas

Rajah Marie Mena

Degrees: Bachelor of Science, Health Physics, 2006
University of Nevada, Las Vegas

Thesis Title: Optimization of the Development Process for Air Sampling Filter Standards

Thesis Examination Committee

Chairperson, Ralf Sudowe, Ph.D.

Committee Member, Steen Madsen, Ph.D.

Committee Member, Carson Riland, Ph.D.

Graduate Faculty Representative, Vernon Hodge, Ph.D.